DIGITAL MODELS FOR MANAGING URBAN HEATING NETWORKS

2026

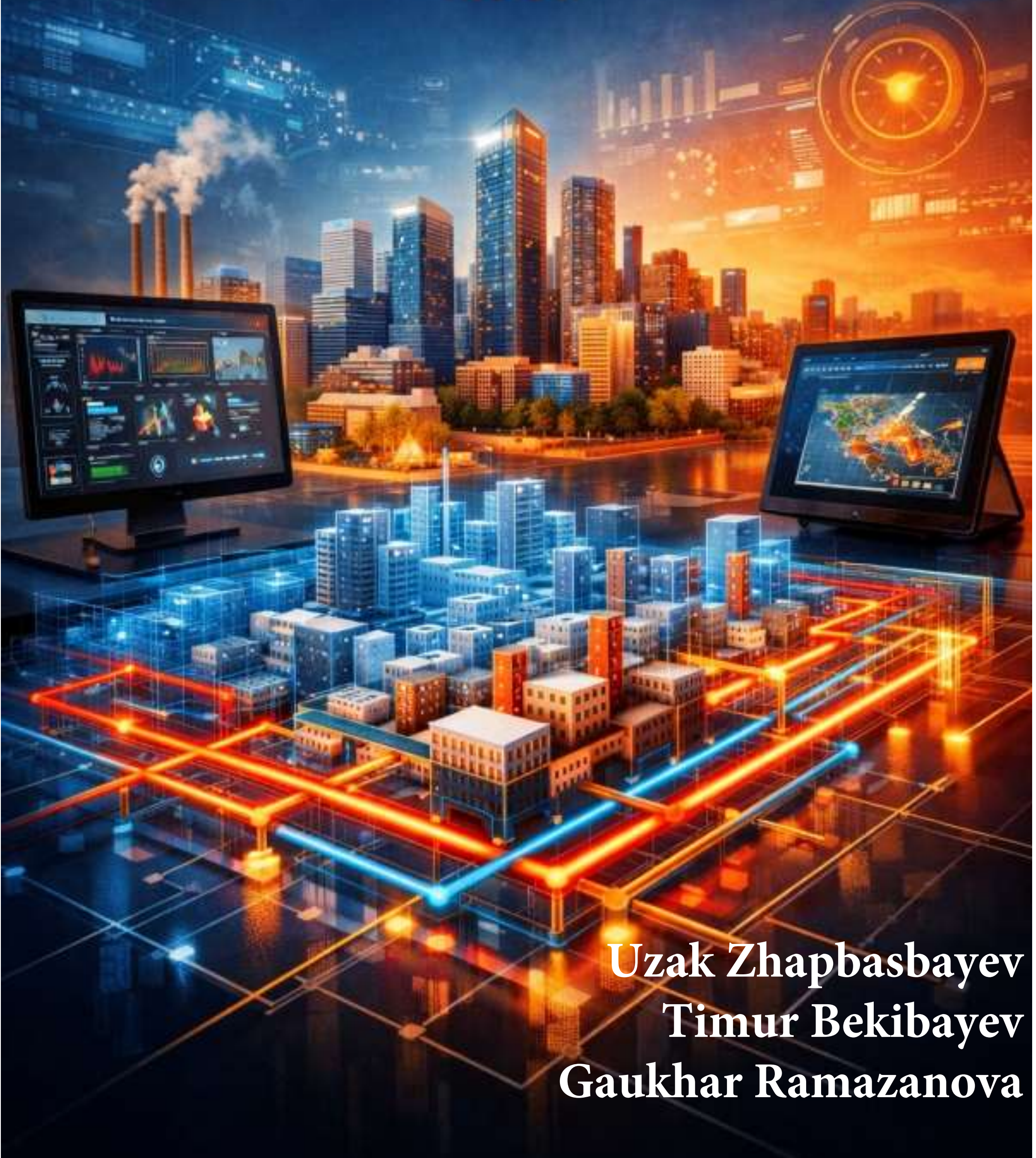

Uzak Zhapbasbayev
Timur Bekibayev
Gaukhar Ramazanova

DIGITAL MODELS FOR MANAGING URBAN HEATING NETWORKS

A research Monograph submitted in fulfillment of the requirements for the scientific project

ISBN

979-8-89695-350-0

DOI

https://doi.org/10.5281/zenodo.18866115

March / 2026

USA

Date: 05.03.2026

Liberty Publishing House
Water Street Corridor New York, NY 10038
www.libertyacademicbooks.com
+1 (314) 597-0372

adopted by Mariam Rasulan
ISBN: 979-8-89695-350-0

TABLE OF CONTENTS

CHAPTER III

CHAPTER IV

LIST OF ABBREVIATIONS AND SYMBOLS

The following abbreviations and designations are used in this monograph:

DB	database
DBMS	database management system
CHP	combined heat and power plant
CHS	central heating substation
GIS	geographic information system
HN	heating network
HS	heating system
HWS	hot water supply
IHS	individual heating substation
SP	software product
VS	ventilation system
δ	local heat loss coefficient
L	length, m
q	specific heat losses, kcal/(m·h)
C	specific heat capacity, kcal/(kg·°C)
ρ	density, kg/m^3
T	temperature, °C
Q	heat losses, kcal/h
G	network water flow rate, t/h
P	pressure, bar
D	diameter, m
ζ	local resistance coefficient
u	velocity, m/s
h	elevation, m
Indexes	
ab	aboveground
am	average monthly
ann	average annual
AH	air heater
c.w	cold water
h.w	hot water
ret	return pipeline
sec	pipeline section
sup	supply pipeline
under	underground

INTRODUCTION

In recent years, countries and regions worldwide have shown a growing trend toward developing clean, low-carbon, safe, and efficient energy sectors. As a key infrastructure of modern cities, central heat supply systems provide stable, reliable, and high-quality heat supply. However, their energy consumption and associated emissions have raised widespread concern. To meet energy-saving and emission-reduction policy requirements, as well as user preferences, accurate modeling and optimization of central heating supply systems are of critical importance.

With the advancement of digital technologies and computational power, digital twin technology has emerged, based on real-time big data processing. By integrating sensor data and historical operational data, digital twin models offer enhanced performance and accuracy, reflecting the entire life cycle of the corresponding physical object in real time.

A digital twin is a software-based model of a physical process. At a minimum, this technology includes the unique identification of the actual asset. It provides a digital representation of a tangible entity, such as a car engine, the structure of a solar farm, or even an entire city. A digital twin can simulate various processes that physical assets may undergo and predict their performance under those conditions.

A digital twin is a simple algorithm that predicts how a product or process will perform based on real-world data. These applications incorporate the internet of things, artificial intelligence, and data analytics to improve outcomes. Given sufficient information, a digital twin can recommend solutions that are more likely to be suitable for each individual, taking into account their unique medical history and statistical data. Intelligent digital twin components are connected to physical objects through sensors that collect data on operating conditions and real-time status. These components form a cloud-based system that gathers and analyzes all sensor data and compares it with industry data.

As digital twin architectures for heating networks (HNs) gradually become more complex due to multi-source configurations and looped topologies, the hydraulic characteristics of large-scale HNs are often suboptimal, leading to high pumping costs. From the perspective of real-time model parameter updating, the identification of hydraulic resistance is a key parameter of the mechanistic model and can be adopted as an effective approach for modeling HNs.

In addition to transmission and distribution modeling, it is essential to develop a heat load forecasting model for substations when building a digital twin platform in order to achieve efficient planning. Deep learning models demonstrate superior performance in identifying complex linear and nonlinear patterns in time-series data and in constructing highly accurate heat load forecasts by considering multiple factors, including temperature, humidity, wind speed, and others. By integrating deep learning with optimization algorithms to adjust the weights between the two models and enhance predictive capability, hybrid models show excellent performance in solving complex load forecasting problems. In practical applications, both accuracy and computational efficiency must be considered for heat load forecasting.

In [1], a comprehensive review of modeling approaches and the associated software tools related to district-level HNs is presented. This review complements earlier studies [2–4] by focusing on models that account for interactions between thermal systems at the district scale and by evaluating the capabilities of available software tools alongside the modeling approaches employed. New models and tools addressing these district-level interactions are analyzed, and their capabilities are assessed. They are categorized into the following areas: HNs and the urban microclimate, as related to energy demand.

The spread of central heating supply technology is closely linked to improvements in design and control techniques [5]. Holistic modeling of central HNs is one of the most promising tools (see Figure 1). It is aimed at both sizing new installations and optimizing existing ones, while significantly reducing the time, cost, and complexity of field testing.

Here, [5] presents the application of innovative modeling procedures to a real system, namely the HN of the University of Parma campus, with a total length of about 2 km, 12 connected buildings, and a total heating demand of 11.2 MW. The results show that the modeling tool provides a detailed representation of the actual system behavior and enables a comprehensive analysis of the evolution of the thermodynamic parameters of the heat carrier. In [6], the results of an analysis of a municipal energy system are presented, highlighting the role of the HN. The analysis demonstrates that the HN can play an important role in the transformation of the municipal energy system.

In studies [7–27], various approaches to modeling HNs have been proposed. In [7], the pressure at booster stations of a heating system with multiple heat sources is calculated. Reference [8] presents the hydraulic state of the HN with multiple heat sources. In [9], neural networks are used to forecast the supply temperatures of the secondary network for the heating system. The dynamics of temperature variation in the HN of Næstved (Denmark) are analyzed in [10], while [11] examines technologies implemented in "smart" HNs. A thermohydrodynamic model of large-scale HNs aimed at analyzing primary energy-saving potential is proposed in [12]. In [13], a comparative study of the performance characteristics and energy consumption of various heat sources is conducted.

For central heating systems in China, the main challenges are systematized in [14], and possible solutions are proposed. Based on a simulation model, [15] investigates optimized dispatching of an intelligent heating system. In [16], the results of modeling the large-scale utilization of waste heat in urban HNs are presented. Reference [17] examines flow control under a constant–variable scheme and analyzes energy consumption in heating systems with indirect connections. Studies [18] and [19] are devoted, respectively, to the main problems and solutions in the control of space-heating systems in Northern China and to the analysis of the operation of a multi-source HN in the city of Jinan.

The implementation of a small-scale fourth-generation heating system is demonstrated in [20]. In [21, 22], approaches to optimizing component reliability and assessing the availability of HNs are proposed. Hydraulic optimization of HNs with multiple heat sources is addressed in [23]. In [24, 25], the reliability and availability of repairable HNs under varying external conditions are evaluated, and pathways for improving network layouts and pipe sizing in low-energy heating systems serving low-energy buildings are identified. In [26, 27], the results of modeling the operation of heating systems and assessing their reliability are presented, including the application of graph theory methods.

Various optimization problems of urban heating systems are addressed in studies [28–37]. Optimal configuration planning based on mixed-integer linear programming is presented in [28], while optimization of energy-saving operations in an urban heating system is discussed in [29]. Network flexibility of urban heating systems is examined in [30]. Online hydraulic calculation and operational optimization of industrial steam HNs, accounting for heat losses in pipes, are carried out in [31]. Study [32] focuses on energy management systems for microgrids. Optimized network partitioning for the operation of large-scale urban heating systems is investigated in studies [33–38].

The monograph is devoted to the development of the software product (SP) incorporating elements of artificial intelligence for modeling and optimizing the operation of urban HNs. The SP is intended to support engineering calculations, analyze the operating modes of heating infrastructure, and support decision-making related to its development and operation.

The monograph presents the results of developing the SP DB structure, which includes tables for storing information about urban HN assets and historical measured data. Tables were created to describe buildings, their connections to the HN, parameters of heat substations, as well as to store data on temperature, pressure, heat carrier flow rate, and electricity consumption. The developed structure enables scalability of the solution to different cities, supports engineering calculations, and facilitates analysis of network operating modes.

A basic computational framework was created through the development of mathematical models and intelligent modules of the SP. Mathematical models and algorithms were presented for topological analysis of the HN, calculation of flow and temperature distribution accounting for heat losses, and the corresponding software modules were implemented. A commissioning calculation module was developed, allowing the determination of the actual distribution of the heat carrier across network sections and the selection of optimal operating modes of the valves based on specified thermal loads. The verification calculation module is designed to assess the compliance of current operating modes with regulatory requirements under given settings of control devices. A temperature distribution model in the network, accounting for standard heat losses, was implemented, enabling calculations under various seasonal conditions. The commissioning and verification calculation modules provide flexibility in analyzing both design and actual operating modes of the heating system.

The results of digitizing and inputting the parameters of the HN section in Almaty are presented. The SP DB was populated with parameters of the HN nodes, pipeline sections, and buildings, including their types and characteristics. Geographic coordinates of all objects were also entered, ensuring their correct display on the map and enabling spatially referenced calculations. The collected data serve as a basis for performing full-scale thermo-hydraulic calculations and analyzing the operating modes of both distribution and main sections of the city's HN. The commissioning calculation shows a stable pressure drop along the network section from start to end. The uniform pressure drop confirms the correctness of the operating parameters and the absence of significant local hydraulic losses. The verification calculation was carried out to assess the current condition of the network and to check its compliance with design and regulatory requirements.

The developed software components have been integrated with the program DB and are prepared for further functionality expansion.

The monograph presents the structure of the program's user interface, providing convenient and intuitive interaction with elements of the urban HN. The interface is divided into four main areas: the menu panel, the toolbar, the status bar, and the main workspace. Specialized graphical interface elements have been implemented for inputting and editing network parameters and configurations. Users can add and configure pipeline sections, network nodes (thermal chambers, CHPs, sources and consumers, pump stations, etc.), modify their parameters and types, and utilize map layers to simplify visual perception. Functions for saving, undoing changes, and editing internal object parameters have been implemented, significantly facilitating the process of modeling and updating the digital twin.

Functionality for exporting the results of thermo-hydraulic and commissioning calculations to MS Word and MS Excel formats has been developed and implemented. The SP provides automatic report generation while preserving structure and formatting, including parameter tables, calculation results, descriptive sections, headings, and captions. The interface allows users to flexibly manage data, visualize calculations, and efficiently prepare reporting documentation. The created interface elements ensure connectivity between the HN model and its visual representation, enhancing clarity and ease of use.

The results of creating the GIS, serving as the basis for forming a digital twin of the urban HN, are presented. Tools have been developed for converting the positions of HN elements from one coordinate system to another, as well as for linking buildings and other city objects to network elements. Imported objects are converted into the structure of the SP DB and automatically associated with the nearest HN elements. The developed SP provides visualization, storage, and interaction of spatial and technical data necessary for modeling and analyzing heating operations at the city scale.

CHAPTER 1

DIGITAL MODEL OF THE HEATING NETWORK

.

Uzak Zhapbasbayev[1]
Timur Bekibayev[2]
Gaukhar Ramazanova[3]

---

[1] Laboratory "Modeling in Energy", Satbayev University, 22 Satpaev Street, 050013 Almaty, Kazakhstan, ORCID ID: 0000-0001-5973-5149 .

[2] Laboratory "Modeling in Energy", Satbayev University, 22 Satpaev Street, 050013 Almaty, Kazakhstan. Email: timur_bekibaev@mail.ru, ORCID ID: https://orcid.org/0000-0001-7030-0015

[3] Laboratory "Modeling in Energy", Satbayev University, 22 Satpaev Street, 050013 Almaty, Kazakhstan. Email: Email: gaukhar.ri@gmail.com, ORCID ID: https://orcid.org/0000-0002-8689-9293.

1.1 Creation of the overall database structure. Definition of relationships between entities. Data normalization

The SP DB has a relational data model and is implemented using the MySQL DBMS. The overall structure of the SP DB was designed with scalability in mind.

The relationship schema of the main SP objects is shown in Figure 1.1. Direct elements of the city's HN are shown in blue, city objects in orange, and HN subscribers in green.

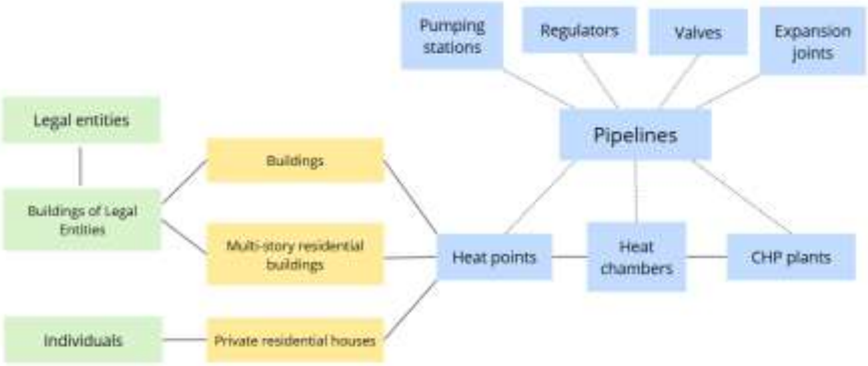

Figure 1.1. Scheme of relationships between the main objects

HN subscribers are divided into two groups: individuals and legal entities. Legal entities are associated with administrative objects at different addresses. For example, a company may have several facilities in the city: headquarters, warehouse, workshop, retail store No. 1, retail store No. 2, and so on. Each subscriber object in the SP DB corresponds to its thermal loads (loads on the heating system, ventilation system, and hot water supply system).

Subscribers are connected to the city's HN through building objects (residential, administrative, social, and industrial buildings). Each building object has separate input and output parameters necessary for calculations and analyzing the efficiency of the HN, such as the designed temperature profile, building height, degree of building heating, and so on.

Elements of the city's HN are connected to building objects through the heat substation object. HN elements (such as pipelines, pump stations, heat substations, valves, various regulators, thermal chambers, boiler houses, and CHPs) directly control the operation of the heating system and have separate objects in the SP DB.

It should be noted that some city objects (pump stations, CHPs, boiler houses) are considered in the SP simultaneously as subscribers, buildings, and HN elements, and, consequently, have separate entities in the SP DB. For example, Pump Station No. 2 in Pavlodar has separate parameters both as a subscriber object (considering it as a legal entity), as a building object (considering the station as a separate building in the city), and as a HN object (considering its parameters that directly control the heating system operation).

Thus, the following entities were defined in the SP DB, containing information and parameters of the corresponding objects:

- "Corporates" – legal entities;
- "Consumers" – consumers (individuals or objects of legal entities);
- "Buildings" – various buildings connected to the heating system;
- "HeatPoints" – heat substations;
- "PumpStations" – pump stations;
- "Regulators" – regulators;
- "Valves" – valves;
- "Segments" – pipeline sections;
- "Nodes" – HN nodes;
- "HeatSources" – heat sources (CHPs, boiler houses).

The parameters of legal entity objects were combined into the "Consumers" entity. The "Consumers" entity is related to "Corporates" (companies) via a many-to-one relationship. If a specific subscriber is an individual, their parameters are not linked to the "Corporates" entity.

The "Nodes" entity contains parameters common to HN nodes. The entities "HeatPoints", "PumpStations", "Regulators", "Valves", and "HeatSources" are linked to the "Nodes" entity via a one-to-one relationship.

The "Consumers" entity is related to the "Buildings" entity via a many-to-one relationship, since a specific consumer can only be located in one building, while a building can contain multiple consumers. The "Buildings" entity is related to the "HeatPoints" entity via a many-to-many relationship, as in some cases one building can be connected to multiple heat substations, while heat substations can serve either a single building (IHS) or several buildings at once (CHS).

Heat substations, pump stations, thermal chambers, valves, regulators, pipe branching points, and heat source stations are all considered nodes of the HN. Therefore, the "Nodes" entity is related to the "Segments" entity via a one-to-two relationship, since each pipeline section corresponds to a specific start and end node.

The following entities were defined for the correct rendering of system DB objects on the map of the SP interface:

- "MapPoints" – points with geographic and local coordinates;
- "MapLines" – sequences of points describing a polyline;
- "MapShapes" – sequences of points describing a two-dimensional shape.

The "MapPoints" entity is related to the "MapLines" and "MapShapes" entities via a many-to-many relationship, since different points can belong to different shapes and lines. The location of HN nodes is described by a single point, so the "Nodes" entity is related to the "MapPoints" entity via a one-to-one relationship. Pipeline sections are represented by a polyline, so the "Segments" entity is related to the "MapLines" entity via a one-to-one relationship. Building outlines on the map are described by a two-dimensional shape, so the "Buildings" entity is related to the "MapShapes" entity via a one-to-one relationship.

Data normalization was carried out to reduce data redundancy in the SP DB. As part of data normalization, the following new entities were introduced:

Pump units of pump stations and heat source objects were extracted into a separate entity, "Pumps", which is related to the "PumpStations" and "HeatSources" entities via a many-to-one relationship;

Pump rotor objects were extracted into a separate entity, "RotorTypes", which is related to the "Pumps" entity via a one-to-many relationship;

Pump motor objects were extracted into a separate entity, "MotorTypes", which is related to the "Pumps" entity via a one-to-many relationship;

Boiler units of heat source objects were extracted into a separate entity, "Boilers", which is related to the "HeatSources" entity via a many-to-one relationship;

Certain valve parameters were extracted into a separate entity, "ValveTypes", which is related to the "Valves" entity via a one-to-many relationship;

Certain pipeline section parameters related to pipe insulation were extracted into a separate entity, "InsulationTypes", which is related to the "Segments" entity via a one-to-many relationship;

Certain parameters of multi-apartment residential buildings were extracted into a separate entity, "ApartmentBuildings", which is related to the "Buildings" entity via a one-to-one relationship.

It should be noted that HN elements can have fixed parameters (set during installation) and adjustable parameters, which may change depending on the heating mode. To normalize data in the SP DB, the entity "Modes" (heat supply modes) was created, and each HN element received additional entities:

Subscriber mode parameters were extracted into a separate entity, "ConsumersInModes", which is related to the "Consumers" entity via a many-to-one relationship and to the "Modes" entity via a one-to-one relationship;

Mode parameters of multi-apartment residential buildings were extracted into a separate entity, "ApartmentBuildingsInModes", which is related to the "ApartmentBuildings" entity via a many-to-one relationship and to the "Modes" entity via a one-to-one relationship;

Heat substation mode parameters were extracted into a separate entity, "HeatPointsInModes", which is related to the "HeatPoints" entity via a many-to-one relationship and to the "Modes" entity via a one-to-one relationship;

Pump station mode parameters were extracted into a separate entity, "PumpStationsInModes", which is related to the "PumpStations" entity via a many-to-one relationship and to the "Modes" entity via a one-to-one relationship;

Regulator mode parameters were extracted into a separate entity, "RegulatorsInModes", which is related to the "Regulators" entity via a many-to-one relationship and to the "Modes" entity via a one-to-one relationship;

Valve mode parameters were extracted into a separate entity, "ValvesInModes", which is related to the "Valves" entity via a many-to-one relationship and to the "Modes" entity via a one-to-one relationship;

Heat source mode parameters were extracted into a separate entity, "HeatSourcesInModes", which is related to the "HeatSources" entity via a many-to-one relationship and to the "Modes" entity via a one-to-one relationship;

Pump unit mode parameters were extracted into a separate entity, "PumpsInModes", which is related to the "Pumps" entity via a many-to-one relationship and to the "Modes" entity via a one-to-one relationship;

Boiler unit mode parameters were extracted into a separate entity, "BoilersInModes", which is related to the "Boilers" entity via a many-to-one relationship and to the "Modes" entity via a one-to-one relationship.

Heat supply modes were grouped and assigned to different SP users. The entities "ModeGroups" (mode groups) and "Users" were created, which are related to the "Modes" entity via a one-to-many relationship.

Figure 1.2 shows the relationship schema of the SP DB entities. Entities containing subscriber information and/or fixed parameters are shown in green, entities containing city building information and/or fixed parameters in orange, entities containing HN elements' information and/or fixed parameters in blue, entities containing mode parameters and data related to heat supply modes in yellow, and cartographic data in gray. The relationship types between entities are denoted as "1-1", "1-∞", "∞-1", and "∞-∞", corresponding to one-to-one, one-to-many, many-to-one, and many-to-many, respectively.

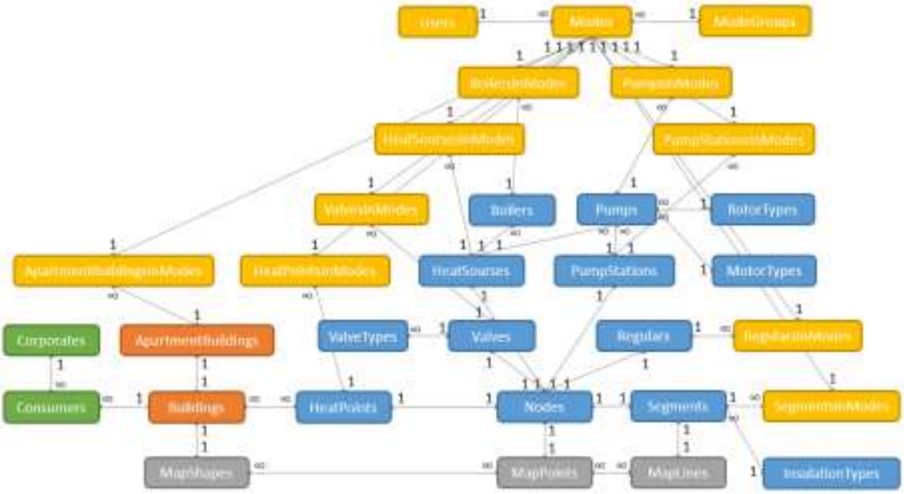

Figure 1.2. Relationship schema of the SP DB entities

1.2 Definition of database tables and their fields for heating network elements (pipelines, individual heating substations, central heating substations, combined heat and power plants, pump stations, valves, bypasses, regulators)

The designed entities of the SP were implemented as corresponding tables in the MySQL DBMS. Below is a description of the tables for elements of the HN.

The Segments table contains the constant parameters of a pipeline section between two nodes of the HN. The table includes the following fields:

–Pipeline section identifier (primary key);

–Identifier of the first node (foreign key to the Nodes table);

–Identifier of the second node (foreign key to the Nodes table);

–Identifier of the line on the map (foreign key to the MapLines table);

- Length of the section;
- Thermal conductivity of the surrounding soil;
- Number of supply pipes;
- Inner diameter of the supply pipe;
- Identifier of the supply pipe insulation type (foreign key to the InsulationTypes table);
- Condition coefficient of the supply pipe insulation;
- Roughness of the inner wall of the supply pipe;
- Wall thickness of the supply pipe;
- Total local resistance of the supply pipe;
- Number of return pipes;
- Inner diameter of the return pipe;
- Identifier of the return pipe insulation type (foreign key to the InsulationTypes table);
- Condition coefficient of the return pipe insulation;
- Roughness of the inner wall of the return pipe;
- Wall thickness of the return pipe;
- Total local resistance of the return pipe.

The SegmentsInModes table contains the operational parameters of the pipeline section between two nodes of the HN. The table includes the following fields:

- Pipeline section identifier (foreign key to the Segments table);
- Mode identifier (foreign key to the Modes table);
- Openness of the supply pipe (yes/no);
- Heat carrier loss in the supply pipe;
- Openness of the return pipe (yes/no);
- Heat carrier loss in the return pipe.

The Nodes table contains the general constant parameters of the HN nodes. The table includes the following fields:

- Node identifier (primary key);
- Node name;
- Identifier of the point on the map (foreign key to the MapPoints table);
- Elevation of the ground level;
- Elevation of the pipeline axis;
- Position of the label on the map;
- Presence of a bypass between the supply and return pipes.

The HeatPoints table contains the constant parameters of heating substations (IHS and CHS). The table includes the following fields:

- Heating substation identifier (primary key);
- Node identifier (foreign key to the Nodes table);
- Type of connection for the HS;
- Type of connection for the HWS;
- Type of connection for the VS;
- Type of regulation for the HS;
- Type of regulation for the HWS;
- Presence of a circulation line for the HWS;
- Presence of a control valve for the VS;
- Design outdoor air temperature for the HS;
- Design outdoor air temperature for the VS;
- Thermal load of the HS;
- Thermal load of the HWS;
- Thermal load of the VS;
- Design temperature at the supply pipe;

- Design temperature at the HS inlet;
- Design temperature at the HS outlet;
- Design indoor air temperature for the HS;
- Design indoor air temperature for the VS;
- Maximum pressure in the return pipe;
- Hot water temperature;
- Cold water temperature;
- Maximum pressure in the HWS;
- Design available head in the HS (dependent HS);
- Number of heat exchanger sections in the HS (independent HS);
- Head loss in the first section of the heat exchanger (independent HS);
- Number of parallel groups (independent HS);
- Design water temperature at the heat exchanger outlet (independent HS);
- Design water temperature at the consumer outlet (independent HS);
- Design available head in the VS;
- Head loss in the HWS system (open water intake);
- Number of heat exchanger sections at the first stage (closed water intake);
- Number of parallel heat exchanger groups at the first stage (closed water intake);
- Head loss in the first section of the heat exchanger at the first stage (closed water intake);
- Number of heat exchanger sections at the second stage (closed water intake);

- Number of parallel heat exchanger groups at the second stage (closed water intake);
- Head loss in the first section of the heat exchanger at the second stage (closed water intake).

The HeatPointsInModes table contains mode parameters of heating substations (IHS and CHS). The table includes the following fields:

- Heating substation ID (foreign key to the HeatPoints table);
- Node ID (foreign key to the Modes table);
- Load variation coefficient for the heating system (HS);
- Load variation coefficient for hot water supply (HWS);
- Load variation coefficient for the ventilation system (VS);
- Flow capacity coefficient of the HS regulator;
- Maximum flow rate in the HS;
- Required indoor air temperature;
- KVS of the HWS regulator;
- Balance coefficient for HWS;
- Installed elevator number;
- Diameter of the installed elevator nozzle;
- Set temperature of cold water (for closed water intake);
- Pump head in the HWS circuit;
- Parameters of the throttle rings in the supply pipe;
- Parameters of the throttle rings in the return pipe;
- Parameters of the throttle rings in the HWS;
- Parameters of the throttle rings in the HWS circulation line;
- Parameters of the throttle rings in the VS.

The PumpStations table contains the permanent parameters of a pump station in the HN. The table includes the following fields:

- Pump station ID (primary key);
- Node ID (foreign key to the Nodes table);
- Pumping direction relative to the HN;
- Location on the pipeline (on the supply or return pipeline);
- Minimum allowable pressure at the station inlet;
- Maximum allowable pressure in the pump;
- Maximum allowable pressure at the station outlet;
- Number of VFDs available in the station;
- Presence of a pressure regulator at the station outlet.

The PumpStationsInModes table contains the mode parameters of the pump station in the HN. The table includes the following fields:

- Pump station ID (foreign key to the PumpStations table);
- Mode ID (foreign key to the Modes table);
- Outlet pressure (if specified, pump unit modes are ignored);
- Pressure loss on the pressure regulator.

The Valves table contains the permanent parameters of a valve node. The table includes the following fields:

- Valve node ID (primary key);
- Node ID (foreign key to the Nodes table);
- Type of valve on the supply pipeline (foreign key to the ValveTypes table);
- Type of valve on the return pipeline (foreign key to the ValveTypes table).

The ValvesInModes table contains the mode parameters of the valve node. The table includes the following fields:

- Valve node ID (foreign key to the Valves table);
- Mode ID (foreign key to the Modes table);
- Valve opening coefficient.

The Regulators table contains the permanent parameters of a regulator node. The table includes the following fields:

- Regulator node ID (primary key);
- Node ID (foreign key to the Nodes table);
- Throttling method;
- Location on the pipeline (on the supply or return pipeline);
- Bypass pipe diameter;
- Bypass pipe length;
- Bypass pipe roughness.

The RegulatorsInModes table contains the mode parameters of the regulator node. The table includes the following fields:

- Regulator node ID (foreign key to the Regulators table);
- Mode ID (foreign key to the Modes table);
- Controlled pressure differential;
- Controlled outlet pressure;
- Controlled inlet pressure;
- Controlled water flow;
- Controlled water temperature.

The HeatSources table contains the permanent parameters of a heat source node (CHPs, boiler houses). The table includes the following fields:

- Source node ID (primary key);
- Node ID (foreign key to the Nodes table);
- Maximum make-up water flow;
- Installed thermal capacity;
- Minimum allowable pressure at the node inlet;
- Maximum allowable pressure in the pump;

- Maximum allowable pressure at the node outlet;
- Number of VFDs available at the node;
- Presence of a pressure regulator at the node outlet.

The HeatSourcesInModes table contains the mode parameters of a heat source node (CHPs, boiler houses). The table includes the following fields:

- Source node ID (foreign key to the HeatSources table);
- Mode ID (foreign key to the Modes table);
- Network make-up operation (yes/no);
- Outlet water temperature (if specified, boiler modes are ignored);
- Outlet pressure (if specified, pump unit modes are ignored);
- Pressure loss on the pressure regulator.

The Boilers table contains the permanent parameters of steam boilers. The table includes the following fields:

- Steam boiler ID (primary key);
- Boiler number;
- Source node ID (foreign key to the HeatSources table);
- Ratio of heat carried by steam to fuel combustion heat;
- Specific steam production;
- Specific fuel consumption per unit of steam production;
- Boiler position number in the boiler house.

The BoilersInModes table contains the mode parameters of steam boilers. The table includes the following fields:

- Steam boiler ID (foreign key to the Boilers table);
- Mode ID (foreign key to the Modes table);
- Status (on/off);
- Fuel consumption.

The Pumps table contains the permanent parameters of pump units that circulate water in the HN. The table includes the following fields:

- Pump unit ID (primary key);
- Pump unit number;
- Purpose (mainline or booster);
- Rotor type ID (foreign key to the RotorTypes table);
- Motor type ID (foreign key to the MotorTypes table);
- Type of containing node (pump station or heat source node);
- Node ID (foreign key to the PumpStations or HeatSources table);
- Pump unit position number in the schematic;
- VFD capability (yes/no).

The PumpsInModes table contains the operational parameters of pump units circulating water in the HN. The table includes the following fields:

- Pump unit ID (foreign key to the Pumps table);
- Mode ID (foreign key to the Modes table);
- Status (on/off);
- Rotor rotation frequency (when operating with VFD).

The RotorTypes table contains the permanent parameters of centrifugal pump rotor types. The table includes the following fields:

- Rotor type ID (primary key);
- Rotor type name;
- Impeller diameter;
- Impeller blade width;
- Minimum allowable operating water flow;
- Maximum allowable operating water flow;

- Coefficients #1, #2, #3 for head vs. flow dependence;
- Coefficients #1, #2, #3 for efficiency vs. flow dependence;
- Coefficient #1 of the dependence of the cavitation reserve on the water flow rate;
- Coefficient #2 of the dependence of the cavitation reserve on the water flow rate;
- Nominal rotor speed;
- Specific speed coefficient.

The MotorTypes table contains the permanent parameters of pump motor types. The table includes the following fields:

- Motor type ID (primary key);
- Motor type name;
- Rated power;
- Voltage;
- Efficiency at rated load;
- Synchronous speed;
- Slip;
- Minimum allowable rotation frequency.

The InsulationTypes table contains the permanent parameters of pipeline insulation types. The table includes the following fields:

- Insulation type ID (primary key);
- Insulation type name;
- Insulation layer thickness;
- Insulation material name;
- Thermal conductivity at 0 °C;
- Coefficient for calculating thermal conductivity at other temperatures.

1.3 Definition of database tables and their fields for city objects (residential buildings, enterprises, social facilities, etc.)

To store data on city buildings, the Buildings, ApartmentBuildings, ApartmentBuildingsInModes, CityRoads, and CityZones tables were created in the SP DB. The table descriptions are provided below.

The Buildings table contains constant parameters of city buildings. The table includes the following fields:

- Building ID (primary key);
- Identifier of the geometric shape on the map (foreign key to the MapShapes table);
- Building name;
- Building number (as part of the address);
- Street or district name (as part of the address);
- Building type;
- Number of floors in the building;
- Building height;
- Identifier of the object in the OpenStreetMap DB (if imported from an OSM file).

The CityRoads table contains constant parameters of city streets/roads. The table includes the following fields:

- Street/Road ID (primary key);
- Identifier of the line on the map (foreign key to the MapLines table);
- Street name;
- Previous street name (optional);
- Street/Road type;
- Identifier of the object in the OpenStreetMap DB (if imported from an OSM file).

The CityZones table contains constant parameters of city zones (parks, water areas, industrial zones, etc.). The table includes the following fields:

- Street/Road ID (primary key);
- Identifier of the geometric shape on the map (foreign key to the MapShapes table);
- Zone name;
- Zone type;
- Identifier of the object in the OpenStreetMap DB (if imported from an OSM file).

The ApartmentBuildings table contains constant parameters of multi-apartment buildings connected to the heating system. The table includes the following fields:

- Apartment building ID (primary key);
- Building ID (foreign key to the Buildings table);
- Number of the general building heat meter;
- Number of heat energy metering points for individuals;
- Number of residents;
- Total area.

The ApartmentBuildingsInModes table contains operational parameters of Apartment buildings. The table includes the following fields:

- Apartment building ID (foreign key to the ApartmentBuildings table);
- Mode ID (foreign key to the Modes table);
- Load adjustment coefficient for the HS;
- Load adjustment coefficient for the HWS;
- Load adjustment coefficient for the VS.

Figure 1.3 shows the scheme of the relationships of tables for city objects with some other tables in the SP DB. Tables containing only operational parameters are shown in yellow; tables containing constant parameters of city elements are shown in orange; tables related to subscribers that are physical or legal entities (in this case, only the Consumers table) are shown in green; tables containing technical parameters of HN elements (in this case, only the HeatPoints table) are shown in blue; and tables defining the location and geometric dimensions of elements are shown in gray.

The Buildings table is linked to the HeatPoints table by a one-to-many relationship, since in some cases a single building may be connected to several connection points in the HN (for example, different entrances of the building connected to different connection points). Similarly, the Buildings table is linked to the Consumers table by a one-to-many relationship, since a single building may contain several consumers. Therefore, the HeatPoints and Consumers tables include a building identifier field to reference the corresponding record in the Buildings table.

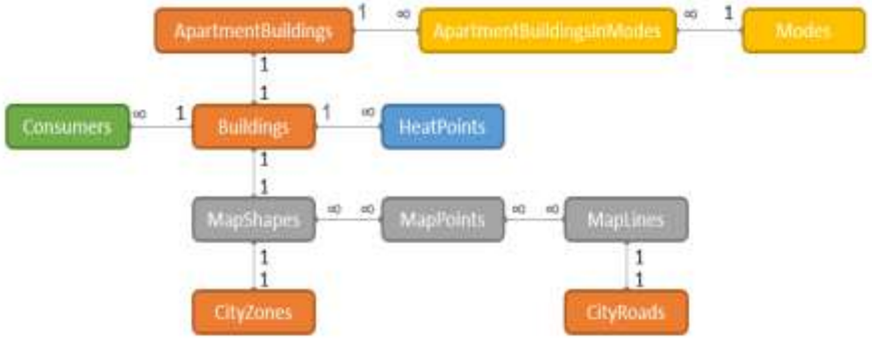

Figure 1.3. Diagram of relationships between tables for city objects and other DB tables

The constant parameters of buildings classified as apartment residential buildings were stored in a separate table, ApartmentBuildings (rather than in the Buildings table), in order to avoid empty fields for apartment buildings in records of other building types (social, commercial, administrative buildings, etc.). This approach provides more compact and logical data storage. Since each record in the ApartmentBuildingsInModes table contains the operating parameters of one specific apartment building under one specific heating mode, the ApartmentBuildingsInModes table is related to the ApartmentBuildings and Modes tables by a "many-to-one" relationship.

1.4 Definition of database tables and their fields for historical measured data (values of temperature, pressure, heat carrier flow rate, electricity consumption, etc.)

In the MySQL DBMS, DB tables and their fields were defined for historical measured data (values of temperature, pressure, heat carrier flow rate, electricity consumption, etc.) for the purpose of subsequent data input. The Sensors, SensorReadings, SensorTypes, and SensorChanges tables were created in the SP DB. The table descriptions are given below.

The Sensors table contains the technical parameters and locations of sensors (including flow meters) in the city heating system. The following fields were included in the table:

- Sensor identifier (primary key);
- Type of measurement (heat carrier temperature, pipe pressure, etc.);
- Identifier of the measured node of the heating system (foreign key to the Nodes table);
- Identifier of the reference node of the heating system (foreign key to the Nodes table);
- Type of the measured pipe (supply or return pipe);
- Identifier of the measured pump (foreign key to the Pumps table);
- Measurement side (at the outlet or at the inlet of the object);
- Sensor type (foreign key to the SensorTypes table).

If a sensor measures the values of a HN node, then the identifier of the measured HN node is specified in its record in the Sensors table, while the identifier of the measured pump remains empty. If the sensor measures pump values, the opposite applies. If the measurement direction is important (for example, the heat carrier flow in a specific direction at a branching node of the HN), the identifier of the guiding HN node (the next node in the given direction) must be specified; otherwise, this field should remain empty. If the value of a variable may differ at the inlet and outlet of the HN object (for example, pressure at the pump inlet and outlet), the corresponding field "measurement side" must be specified.

It is known that the accuracy of heat carrier temperature measurements depends on the sensor installation type: contact sensors placed in immersion pockets inside the pipe provide high measurement accuracy, whereas clamp-on sensors mounted on the external surface of the pipe have reduced accuracy and are mainly used for auxiliary monitoring. It is also known that diaphragm and vortex flow meters for heat carriers have significantly higher measurement errors than ultrasonic or electromagnetic ones. Since historical measured data will be used in the SP for solving inverse problems (for which the accuracy of the measured HN operating parameters is taken into account), it was decided that each stored measurement of a HN sensor must be associated with its sensor type.

The SensorTypes table contains the technical parameters of sensor types. The following fields were included in the table:

- Sensor type identifier (primary key);
- Measurement method;
- Allowable measurement error;
- Upper measurement range limit;
- Lower measurement range limit.

The SensorReadings table contains historical measured values of sensors at HN facilities. The following fields were included in the table:

- Measurement date;
- Sensor identifier (foreign key to the Sensors table);
- Measured value.

It is known that during long-term operation of the HN, sensors may be replaced. New sensors may have significantly different measurement accuracy. To correctly account for the accuracy of different historical periods of measured data, the SensorChanges table was created.

The SensorChanges table contains the history of sensor/flow meter replacements at HN facilities. The following fields were included in the table:

- Replacement date;
- Sensor/flow meter identifier (foreign key to the Sensors table);
- Identifier of the replaced sensor type (foreign key to the SensorTypes table).

Figure 1.4 shows the schema of relationships between tables for historical measured data and several other tables of the SP DB.

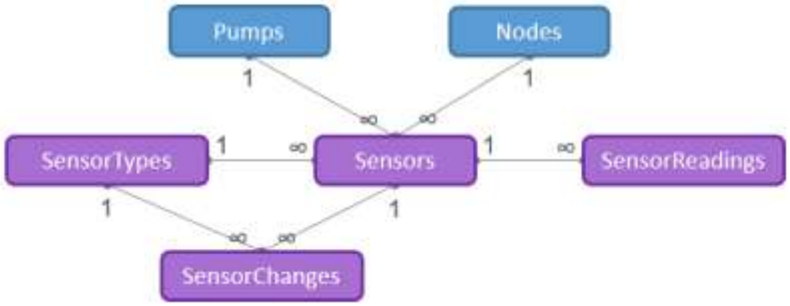

Figure 1.4. Diagram of table relationships for historical measured data with other DB tables

The tables highlighted in purple represent the newly created tables containing sensor parameters and their historical measured readings, while the tables highlighted in blue correspond to elements of the heating system. Since a single HN node or a pump in a HN pumping station may be equipped with several different sensors, the Nodes and Pumps tables have a one-to-many relationship with the Sensors table. A similar one-to-many relationship exists between the SensorTypes and Sensors tables, as different sensors may belong to the same sensor type. The SensorTypes and Sensors tables can be linked to each other through the SensorChanges table by a many-to-many relationship. As many historical measurements of HN operation may correspond to the same sensor, the SensorReadings table is related to the Sensors table by a many-to-one relationship.

Using the table relationships implemented in this way (Figure 1.4), any segment of historical HN measurements stored in the SensorReadings table can be associated with the corresponding HN objects, their measurement type, and accuracy level.

CHAPTER 2

CREATION OF A BASIC CALCULATION COMPLEX

.

Uzak Zhapbasbayev
Timur Bekibayev
Gaukhar Ramazanova

2.1 Development of algorithms for solving topological problems of the heating network (search for connected objects along and against the flow direction, path finding, loop detection)

In developing algorithms to solve topological problems of the HN, the structure of the HN was represented as a graph. The vertices of the graph are the following nodes of the HN: sources (CHPs, boiler points), consumers (IHS, CHS), pump stations, pipeline branching points, and points of diameter change. Additionally, when a main thermal chamber is considered a generalized consumer, this node also serves as a vertex in the graph for topological tasks. The edges of the graph are the sections of pipes connecting the aforementioned types of nodes.

Based on the graph, an overall adjacency matrix between the nodes is constructed. The directed adjacency matrix is determined using the overall adjacency matrix and the depth-first search algorithm, where the starting node is the HN source. For any two nodes in the HN, the directed adjacency matrix stores the value 1 if the heat carrier flows directly from the first node to the second; -1 if the heat carrier flows directly from the second node to the first; and 0 if the heat carrier does not directly flow between these two nodes.

The functions for finding connected objects in the direction of flow and against the direction of flow were implemented using the breadth-first search algorithm and the directed adjacency matrix. The input parameter is the HN node selected by the user. The output parameters define the set of HN nodes to which the heat carrier arrives from the specified node (calculation in the direction of flow) or from which the heat carrier arrives (calculation against the direction of flow). Figure 2.1 shows the interface of the System, displaying highlighted nodes of the HN connected in the direction of flow.

The functions for finding connected flow objects were implemented using the breadth-first search algorithm and the overall adjacency matrix. The input parameters are the starting and ending nodes of the HN chosen by the user. The output parameters define the set of routes, each containing an ordered list of nodes and sections of pipes in the HN along the path from the starting node to the ending node.

The function for detecting loops in the HN was implemented using the depth-first search algorithm and the overall adjacency matrix. Loops in the network were identified if, during depth-first search search among the neighboring nodes of the current node, previously visited vertices were found that did not include their parent vertex. Thus, the function for detecting loops in the HN was reduced to the problem of identifying cycles in the graph. The heat carrier source was used as the starting vertex in depth-first search. The output parameters consist of a set of routes, each of which contains an ordered list of nodes and sections of the HN pipeline from the loop node back to itself.

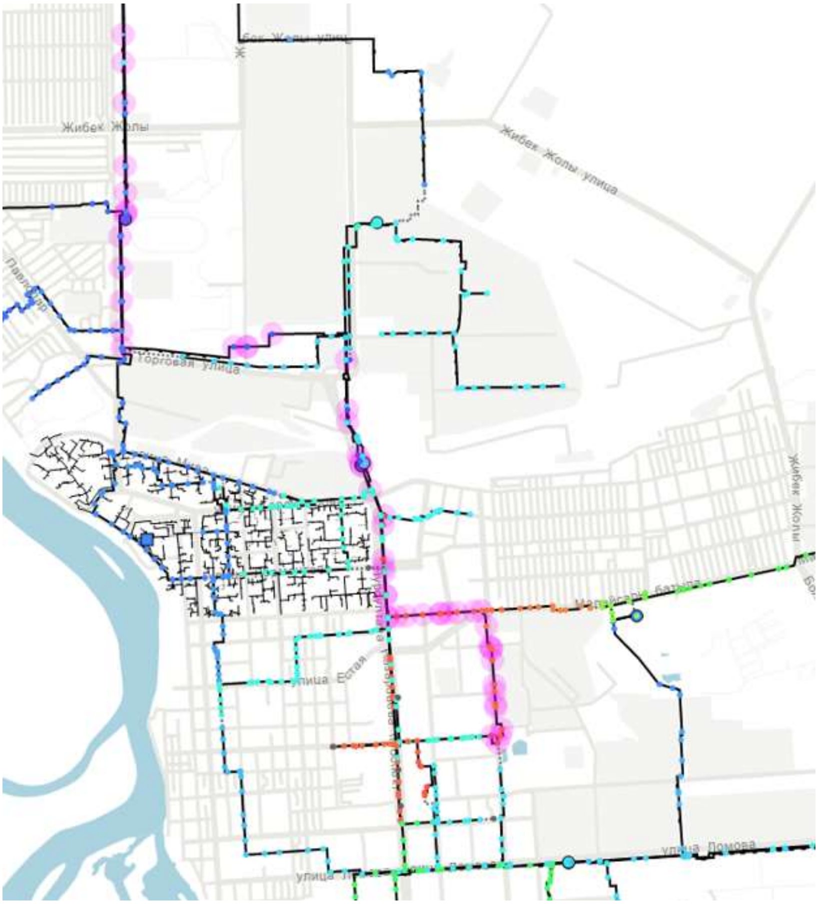

Figure 2.1. Highlighting objects connected in the direction of flow

In the programming implementation of the breadth-first search algorithm, a "queue" data structure was used. The programming implementation of the depth-first search algorithm utilized recursion to identify subsequent neighboring nodes. The program code for solving topological problems in the HN was written in C# and implemented as a separate SP module.

2.2 Creation of a basic calculation complex by constructing mathematical models and developing intelligent software product modules

In the SP, a mathematical model for the distribution of the heat carrier flow for any configuration of the HN was formulated, and an algorithm for its numerical solution was developed. In the development of the numerical solution algorithm and its software implementation, a modified loop current method [8]-[12] was used.

A pipeline network is considered that consists of m nodes and n pipe sections connecting these nodes. The network may have any number of branches, loopings, and closed loops. Let the vector $\vec{q} = (q_1, q_2, \dots, q_n)$ denote the network water flow rates in the pipe sections, the vector $\vec{h} = (h_1, h_2, \dots, h_3)$ denote the head losses in the pipe sections, and the vector $\vec{P} = (P_1, P_2, \dots, P_3)$ denote the pressures at the nodes of the HN, where some values P_j are known (pump unit pressures). Each pipe section is assigned its own conditional positive direction, which is chosen arbitrarily. If the i-th pipe section between nodes A and B has a conditional positive direction, then A → B. If $q_i < 0$ and $h_i < 0$, this means that the network water flows in the direction B → A.

Kirchhoff's laws are formulated for the network under consideration. Loops of the HN are closed paths along which one can pass without repeating any pipe section. A pipe section of the HN that is not included in other loops is called a chord. Let there be a system of independent loops, i.e., a system of loops each of which contains at least one chord [12]. It should be noted that a system of independent loops can be selected in several ways. Let each loop have its own conditional orientation (traversal of nodes clockwise or counterclockwise), which is chosen arbitrarily. As is known, the number c of loops in a system of independent loops is determined by Maxwell’s formula [12]:

$$c = n - m + 1$$

According to Kirchhoff’s first law, a mass balance must be satisfied at each i-th node of the HN, which ensures the principle of flow continuity.

Thus, the following relationships were used:

$$\sum_{i=1}^{r_j} q_i = Q_j^{out}, \qquad j = 1,2, \dots, m$$

where r_j is the number of pipe segments connected to the j-th node; Q_j^{out} is the external inflow at the j-th node. If $Q_j^{out} < 0$, then the corresponding node is a consumer; if $Q_j^{out} > 0$, then the corresponding node is a source; if $Q_j^{out} = 0$, then the j-th node is simply a branching point in the considered HN. At the same time, a zero balance of inflows must be maintained:

$$\sum_{j=1}^{m} Q_j^{out} = 0$$

According to Kirchhoff's second law, in any loop of an electrical network, the total change in potential difference must be zero. In relation to the HN, pressure drops were considered as the potential difference.

Thus, the following relationships were used:

$$\sum_{i=1}^{p_j} h_i = 0, \qquad j = 1,2, \dots, c$$

where p_j is the number of pipeline sections associated with the j-th independent loop of the HN.

The head loss in a pipe section was represented as the sum of the change in static head and the friction head losses. The friction head losses were determined in a generalized form using the Leibenzon formula [13–18], taking into account the flow direction.

Thus, for the i-th pipe section, the head loss was expressed as a function of the network water flow rate as follows:

$$h_i = s_i |q_i|^{1-\alpha} q_i - z_i, \qquad s_i = \frac{\beta \nu_i^{\alpha} L_i}{D_i^{5-\alpha}} > 0$$

where z_i, L_i, and D_i are the elevation difference, length, and internal diameter of the pipe in the i-th section, respectively; ν_i is the kinematic viscosity of water; and α and β are the Leibenzon coefficients, which depend on the flow regime in the pipeline and are listed in Table 1.

Thus, unlike electrical circuits, the value of h_i has a complex and nonlinear dependence on q_i.

Table 1. Leibenzon coefficients for different flow regimes

Flow regime	$\boldsymbol{Re}$ **range**	$\boldsymbol{\alpha}$	$\boldsymbol{\beta}$
Laminar regime	$Re \leq 2040$	1	4.15
Transitional regime	$2040 < Re \leq 2800$	-1.035	$12.5 \cdot 10^{-7}$
Turbulent regime. Hydraulically smooth zone	$2080 < Re \leq Re^{I}$	0.25	0.0246
Turbulent regime. Mixed friction zone	$Re^{I} < Re \leq Re^{II}$	0.1	$0.0166 \cdot \varepsilon^{0.15}$
Turbulent regime. Quadratic friction zone	$Re^{II} < Re$	0	$0.00909 \cdot \varepsilon^{0.25}$

The Reynolds number for the i-th pipe section of the HN [13, 18] was determined as follows:

$$Re_i = \frac{u_i D_i}{\nu_i} = \frac{4 q_i}{\pi \nu_i D_i}, \qquad Re_i^{I} = \frac{17.5}{\varepsilon_i}, \qquad Re_i^{II} = \frac{531}{\varepsilon_i}$$

where u_i is the average velocity across the pipe cross-section, and ε_i is the relative roughness of the pipe's internal surface.

The matrix $\bar{A}$ was defined as the connectivity matrix of the m nodes and n pipe sections of the HN, in which each element a_{ji} has the following value: 0 – if the i-th pipe section is not connected to the j-th node, 1 – if the j-th node is the starting node of the i-th section, −1 – if the j-th node is the ending node of the i-th section.

The matrix $\bar{A}$ uniquely describes the configuration of the HN under consideration. As is known (similarly to the properties of electrical circuits), the rank of the matrix $\bar{A}$ (the maximum number of its linearly independent rows or columns) is equal to $m - 1$. Next, the matrix A is considered – a reduced connectivity matrix of size $(m - 1) \cdot n$, containing only linearly independent rows. Such a matrix can be obtained from $\bar{A}$ by removing an arbitrary row. The matrix A also uniquely describes the configuration of the HN.

The matrix B was defined as the loop matrix of size $c \cdot n$, which uniquely fixes the chosen system of independent loops. Each element b_{ji} has the following value: 0 – if the i-th pipe section does not belong to the j-th loop, 1 – if the j-th loop contains the i-th section and its traversal coincides with the section's direction, −1 – if the j-th loop contains the i-th section and its traversal is opposite to the section's direction.

The following diagonal matrices were also introduced:

$$S = \begin{bmatrix} s_1 & \cdots & 0 \\ \vdots & \ddots & \vdots \\ 0 & \cdots & s_n \end{bmatrix}, \qquad Q = \begin{bmatrix} |q_1|^{1-\alpha} & \cdots & 0 \\ \vdots & \ddots & \vdots \\ 0 & \cdots & |q_n|^{1-\alpha} \end{bmatrix},$$

$$Z = \begin{bmatrix} z_1 & \cdots & 0 \\ \vdots & \ddots & \vdots \\ 0 & \cdots & z_n \end{bmatrix}$$

Taking into account the introduced matrices, the formulated relationships (2.1)–(2.3) for q_i and h_i were expressed in the following matrix form:

$$\begin{gathered} A\vec{q} = \vec{Q}^{out} \\ B\vec{h} = 0 \\ \vec{h} = SQ\vec{q} - Z \end{gathered} \tag{2.4}$$

where $\vec{Q}^{out} = (Q_1^{out}, Q_2^{out}, \dots, Q_{m-1}^{out})$ is the vector of inflows at the nodes of the HN. The values of the elements of the matrices A, B, Z, and the vector $\vec{Q}^{out}$ are known and given in advance. The first matrix equation consists of $m-1$ linearly independent equations of type (2.1), the second matrix equation consists of c equations of type (2.2), and the third matrix equation consists of n equations of type (2.3).

Thus, the system (2.4) contains $m-1+c+n=2n$ equations for n unknown q_i and n unknown h_i.

By eliminating the vector $\vec{h}$, the order of the system of equations (2.4) can be reduced from $2n$ to n:

$$\begin{aligned} A\vec{q} &= \vec{Q}^{out} \\ BSQ\vec{q} &= BZ \end{aligned} \tag{2.5}$$

The reduction of the order of the system of equations (2.5) can be achieved by decomposing the matrices A and B. For this purpose, the numbering of the pipe sections was arranged so that the first c numbers were assigned to the chords of the non-repeating independent loops. In addition, the loop numbers and their orientation (traversal direction) were made to correspond to the numbers and directions of the respective chords. After this decomposition, the following notations were introduced:

$$\begin{gathered} \vec{q} = \{q_\chi, q_\eta\}, \;\; \vec{q}_\chi = (q_1, q_2 \dots, q_c)^T, \\ \vec{q}_\eta = (q_{c+1}, q_{c+2}, \dots, q_n)^T \\ A = \{A_\chi, A_\eta\}, \qquad\qquad B = \{E, B_\eta\} \end{gathered} \tag{2.6}$$

where $\vec{q}_\chi$ and A_χ are the left-hand parts of the vector $\vec{q}$ and matrix A, respectively, whose elements/rows correspond to the first c pipe sections (chords); $\vec{q}_\eta, A_\eta$, and B_η are the right-hand parts of the vector $\vec{q}$ and matrices A and B, respectively, whose elements/rows correspond to the pipe sections numbered from $c+1$ to n; E is the right-hand part of the matrix B, composed of ones along the main diagonal.

With this decomposition of vectors and matrices, the vector $\vec{q}_\chi$ and the vector $\vec{Q}^{out}$ uniquely determine the vector $\vec{q}_\eta$:

$$\begin{gathered} A\vec{q} = A_\chi\vec{q}_\chi + A_\eta\vec{q}_\eta = \vec{Q}^{out} \\ \vec{q}_\eta = A_\eta^{-1}\left(\vec{Q}^{out} - A_\chi\vec{q}_\chi\right) \end{gathered} \tag{2.7}$$

Moreover, the matrix A_η^{-1} (the inverse matrix of A_η) always exists. This is because, when the chords are removed from the HN graph, the remaining pipe sections form a tree, and for a tree graph, its connectivity matrix without the last row necessarily has a nonzero determinant [19].

It can also be shown through straightforward matrix manipulations that there is a relationship between the parts of matrices A and B:

$$A_\chi + A_\eta B_\eta^T = 0 \tag{2.8}$$

Since the values of the elements of the matrices S and Q depend on the vector $\vec{q}$, the equations of the second group in system (2.5) are nonlinear (unlike the equations of an electrical circuit). Therefore, an iterative method of successive linearization of residuals [12] was used to solve the system of equations (2.5).

Numerical solution algorithm of the model

Let $f_A(\vec{q}) = A\vec{q} - Q$ and $f_B(\vec{q}) = BSQ\vec{q} - BZ$ be the residual vectors of the first and second groups of equations in system (2.5), respectively. Then these residual vectors are linearized for the subsequent approximate solution as follows:

$$\vec{q}^{(k+1)} = \vec{q}^{(k)} + \Delta\vec{q}^{(k)} \tag{2.9}$$

$$f_A(\vec{q}^{(k+1)}) = f_A(\vec{q}^{(k)} + \Delta\vec{q}^{(k)}) = f_A(\vec{q}^{(k)}) + A\Delta\vec{q}^{(k)}$$

$$\begin{aligned} f_B(\vec{q}^{(k+1)}) &= f_B(\vec{q}^{(k)} + \Delta\vec{q}^{(k)}) \\ &\approx f_B(\vec{q}^{(k)}) + 2BS^{(k)}Q^{(k)}\Delta\vec{q}^{(k)} \end{aligned} \tag{2.10}$$

where k is the iteration number; the matrices $S^{(k)}$ and $Q^{(k)}$ are determined taking into account the coefficients α and β, which are calculated according to Table 1 using the values of the vector $\vec{q}^{(k)}$. In the iteration process, $f_A(\vec{q}^{(k)})$ and $f_B(\vec{q}^{(k)})$ essentially represent the residual vectors of the system of equations (1.5) when the approximate solution $\vec{q}^{(k)}$ is substituted into them. The expression $f_A(\vec{q}^{(k)})$ is calculated exactly (not approximately as $f_B(\vec{q}^{(k)})$), since the first group of equations in system (2.5) is linear.

To ensure better convergence of the iterative process for solving system (2.5), all approximations $\vec{q}^{(k)}$ were chosen so as to strictly satisfy the first group of equations in system (2.5). For this purpose, an initial approximation was used that satisfies the following condition:

$$f_A(\vec{q}^{(0)}) = A\vec{q}^{(0)} - \vec{Q}^{out} = 0$$

Then, due to the condition $f_A(\vec{q}^{(k+1)}) - f_A(\vec{q}^{(k)}) = 0$ and expression (2.9), all subsequent increments $\Delta\vec{q}^{(k)} = \left(\Delta q_1^{(k)}, \Delta q_2^{(k)}, \ldots, \Delta q_n^{(k)}\right)^T$ will have zero balance at the nodes; in other words, $A\Delta\vec{q}^{(k)} = 0$. Taking into account expressions (2.7)–(2.8), the residual vector $\Delta\vec{q}_\eta^{(k)}$ was determined through $\Delta\vec{q}_\chi^{(k)}$ by inverting the matrix A_η:

$$\Delta\vec{q}_\eta^{(k)} = -\left(A_\eta^{-1}A_\chi\right)\Delta\vec{q}_\chi^{(k)} = B_\eta^T\Delta\vec{q}_\chi^{(k)}$$

For each k-th iteration, the corrections to the flow vector $\Delta\vec{q}^{(k)}$ were explicitly expressed through $\Delta\vec{q}_\chi^{(k)}$ as follows:

$$\Delta\vec{q}^{(k)} = \left\{\Delta\vec{q}_\chi^{(k)}, \Delta\vec{q}_\eta^{(k)}\right\} = \left\{E\Delta\vec{q}_\chi^{(k)}, B_\eta^T\Delta\vec{q}_\chi^{(k)}\right\} = B^T\Delta\vec{q}_\chi^{(k)}$$

Thus, thanks to the previously performed decomposition (2.6), only the corrections to the flows in the chords $\Delta\vec{q}_\chi^{(k)}$ were taken as independent variables. By equating the approximation (2.10) for the residual $f_B\left(\vec{q}^{(k+1)}\right)$ to zero and using the definition of the vector $f_B\left(\vec{q}^{(k)}\right)$, a system of equations for $\Delta\vec{q}_\chi^{(k)}$ of order c was obtained:

$$K^{(k)}\Delta\vec{q}_{\chi}^{(k)} = -\delta\vec{H}^{(k)}$$

$$K^{(k)} = 2BS^{(k)}Q^{(k)}B^{T}, \delta\vec{H}^{(k)} = BS^{(k)}Q^{(k)}\vec{q}_{\chi}^{(k)} - BZ$$

According to the definitions of the matrices B, S, and Q and expression (2.14), the element $\kappa_{r,t}^{(k)}$ of the matrix $K^{(k)}$ in the *r*-th row and *t*-th column is defined by the following expression:

$$\kappa_{r,t}^{(k)} = 2\sum_{i=1}^{n} b_{r,i}b_{t,i}s_i^{(k)}\left|q_i^{(k)}\right|^{1-\alpha_i^{(k)}}$$

where $b_{r,i}$ and $b_{t,i}$ are the elements of the matrix B in the *i*-th column and in the r-th and t-th rows, respectively, which, by definition, can take values of 0, 1, or -1 depending on the inclusion and direction of the corresponding pipe section in the HN loop.

It should be noted an important property of the matrix $K^{(k)}$ for the chosen system of independent loops:

$$\left|\kappa_{r,r}^{(k)}\right| > \sum_{t=1}^{t\le c, t\ne r} \left|\kappa_{r,t}^{(k)}\right|$$

This property is true for the following reasons: first, the *t*-th loop shares with the other loops the same number of common pipe sections as it does with the *r*-th loop. For a common section, the product $b_{r,i}b_{t,i}$ in expression (2.15) can take the value $b_{r,i}b_{t,i} = \pm 1$, and in the case $t = r$, it takes the value $b_{r,i}b_{r,i} = 1$. Therefore, the inequality (2.16) holds. Second, each independent *r*-th loop contains at least one chord that does not belong to any other loop, i.e., in expression (2.15) there is at least one nonzero additional term $s_i^{(k)}\left|q_i^{(k)}\right|^{1-\alpha_i^{(k)}}$, which makes the inequality (2.16) strict.

For real HNs, the number of loops *c* is usually large; therefore, in each *k*-th iteration, the system of linear algebraic equations derived from its matrix form (2.14) must be solved using iterative methods.

According to (2.16), the matrix $K^{(k)}$ has strict diagonal dominance, which ensures the convergence of iterative methods for solving the system of linear algebraic equations (2.14) to the exact solution $\Delta\vec{q}_\chi^{(k)}$, which exists and is unique for any values of the vector $\delta\vec{H}^{(k)}$.

The iterative process for numerically finding the vector q⃗ according to (2.9)–(2.10) continues until the convergence condition is satisfied:

$$\left|\vec{q}^{(k+1)} - \vec{q}^{(k)}\right| = \max_{1\le i\le n}\left|q_i^{(k+1)} - q_i^{(k)}\right| < \varepsilon$$

where ε is the allowable error of the water flow rates in the network sections.

Once the flow vector $\vec{q}$ is determined, the vector of head losses $\vec{h} = (h_1, h_2, \ldots, h_n)$ and the vector of pressures at the nodes $\vec{P} = (P_1, P_2, \ldots, P_m)$ are calculated. The elements of the vector $\vec{h}$ are determined using formula (2.3). The elements of the vector $\vec{P}$ are calculated using a depth-first search (graph traversal method) through the HN, starting from the nodes with specified initial pressures (pump units). During the traversal of nodes, the pressure values at the nodes are calculated according to the following formula:

$$P_b = P_a + y_{ab}\rho g h_{ab}$$

where a and b are the indices of the parent and child nodes of the network, respectively, during graph traversal; ρ is the density of the heat carrier (water); h_{ab} is the head loss of the HN section connecting nodes a and b; and y_{ab} is a value of ±1 depending on the conditional positive direction of the HN section: if the section has a conditional positive direction from node a to node b, then $y_{ab} = 1$; otherwise, $y_{ab} = -1$.

Thus, the algorithm for solving the problem of heat carrier flow distribution for any HN configuration includes the following steps:

1) Selection of a system of independent loops of the HN;

2) Calculation of the elements of matrices A and B;

3) Decomposition of vectors and matrices according to (1.6);

4) Set $k = 0$. Search $x^{(0)}$ satisfying condition (1.11);

5) Calculation of the elements of matrices $K^{(k)}$ and $\delta H^{(k)}$ using formula (1.14);

6) Calculation of $\varDelta\vec{q}_{\chi}^{(k)}$ by solving the system of linear algebraic equations of form (1.13);

7) Calculation of $\varDelta\vec{q}^{(k)}$ using formula (1.12);

8) Calculation of $\vec{q}^{(k+1)} = \vec{q}^{(k)} + \varDelta\vec{q}^{(k)}$;

9) Verification of condition (17). If it is not satisfied, set $k = k + 1$ and return to step 5;

10) Set $\vec{q} = \vec{q}^{(k+1)}$. Calculation of the vector $\vec{h}$ using formula (1.3);

11) Calculation of the vector $\vec{P}$ using depth-first search and formula (1.18).

The software code for solving the problem of heat carrier flow distribution for any configuration of the heat supply network was written in the C# programming language and implemented as a separate SP module.

2.3 Development of a mathematical model for temperature distribution in the heating network based on the heat exchange process with the environment

Problem statement

Figure 2.2 shows a schematic of the pipeline system of the HN. The nodes of the main pipeline are represented as points.

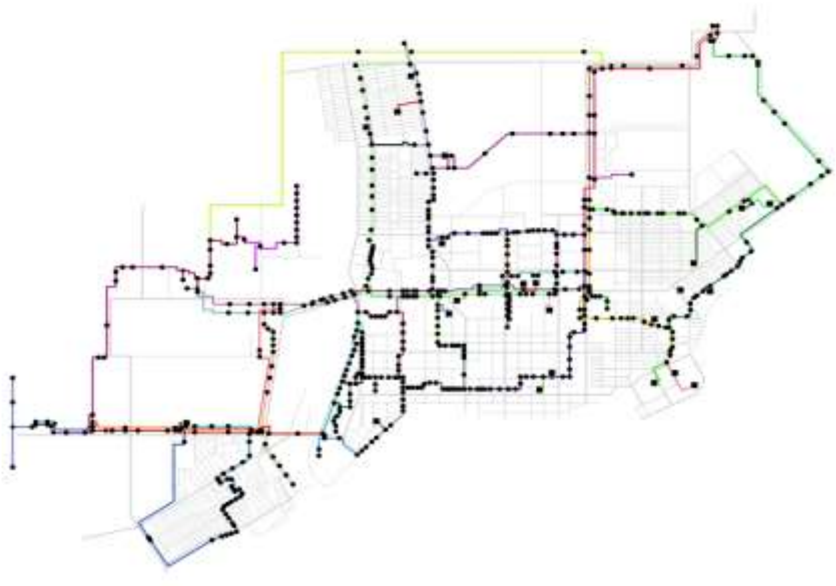

Figure 2.2. Schematic of the HN pipeline system

The temperature distribution along the length of a (supply or return) pipe section between the nodes of the HN is described by the following heat transfer equation:

$$u\frac{\partial T}{\partial x}+\frac{4K}{\rho D C_P}(T-T_{env})=0$$

where x is the coordinate along the length of the pipe section; T is the temperature of the heat carrier (water); ρ and C_P are the density and specific heat capacity of water; D is the internal diameter of the pipeline; u is the cross-section-averaged flow velocity, which is expressed in terms of the water flow rate q as $u=\frac{q}{0.25\pi D^2}$;

K is the heat transfer coefficient from the heat carrier flow to the surrounding environment; and T_{env} is the ambient temperature.

This equation has the following solution, known as the Shukhov’s formula:

$$T(x) = T_{env} + (T_0 - T_{env})e^{-\frac{\pi\rho K D x}{q c_P}}$$

The value of K is determined from the following relationship:

$$\frac{1}{K\pi D} = R = R_{in} + R_{ins} + R_{out}$$

where R is the total thermal resistance of the pipe; R_{in} is the thermal resistance from the heat carrier to the pipe wall; R_{ins} is the thermal resistance of the pipe insulation; and R_{out} is the thermal resistance from the outer surface of the pipe to the surrounding environment.

The value of R_{in} was determined using the Nusselt number Nu, which is expressed in terms of the Reynolds number Re and the Prandtl number Pr [13]:

$$R_{in} = \frac{1}{\lambda_w \pi Nu}, \qquad Nu = 0.021 \cdot (Re)^{0.8} \cdot (Pr)^{0.43}$$

$$Re = \frac{uD}{\nu}, \qquad Pr = \frac{\nu\rho C_P}{\lambda_w}$$

where λ_w is the thermal conductivity of water, and ν is the kinematic viscosity of water.

The value of R_{ins} was determined using the parameters of the pipe insulation:

$$R_{ins} = \frac{1}{2\pi\lambda_{ins}} \ln\frac{D_2}{D_1}$$

where D_1 and D_2 are the inner and outer diameters of the pipe insulation layer, and λ_{ins} is the thermal conductivity of the insulation layer.

The value of T_{env} in formula (2.20) and the value of R_{out} in relation (2.21) were determined depending on the type of pipeline installation (aboveground, underground without a channel, and underground in a channel). Typically, each HN section contains two pipes: a supply and a return pipe, each carrying heat carrier at different temperatures. Unlike underground installation, for aboveground pipelines, the influence of the temperature field of a parallel (neighboring) pipe on the considered pipe was not taken into account.

For aboveground pipeline installation, the outside air was considered as the surrounding environment, and the value of R_{out} was calculated using the following formula [14]:

$$T_{env} = T_{air}, \qquad R_{out} = \frac{1}{\alpha_{air} \pi D_2}, \qquad \alpha_{air} = 11.6 + \sqrt{w}$$

where α_{air} is the heat transfer coefficient from the outer surface of the pipe to the surrounding air; w is the wind speed; and T_{air} is the ambient air temperature.

For underground pipelines without a channel, the surrounding soil was considered as the environment, and the value of R_{out} was calculated using the following relationship, accounting for the mutual influence of the current and neighboring pipes [14]:

$$T_{env} = T_{gr}, \qquad \frac{T_{avg} - T_{gr}}{R_{out}} = \frac{(T_{avg} - T_{gr})\bar{R}_0 - (\bar{T}_{avg} - T_{gr})R_0}{R_0 \bar{R}_0 - R_{inf}^2}$$
$$R_{inf} = \frac{1}{2\pi\lambda_{gr}} \ln \sqrt{1 + \left(\frac{2H}{s}\right)^2} \qquad (2.25)$$

where T_{gr} is the soil temperature; T_{avg} and $\bar{T}_{avg}$ are the average temperatures of the considered and neighboring pipes, respectively; R_{inf} is the additional thermal resistance between the two pipes in the soil; λ_{gr} is the thermal conductivity of the surrounding soil; H is the burial depth of the pipeline to its axis; s is the distance between the axes of the considered and neighboring pipes; and R_0 and $\bar{R}_0$ are the total thermal resistances of the considered and neighboring pipes without accounting for the mutual influence of their temperature fields.

The values of R_0 and $\bar{R}_0$ are calculated using formula (2.21), where the corresponding values of R_{out} and $\bar{R}_{out}$ are equal to the soil thermal resistance R_{gr}, which is determined using the Forchheimer formula [13]:

$$R_{gr} = \frac{1}{2\pi\lambda_{gr}} \ln\left(\frac{2H}{D_2} + \sqrt{\left(\frac{2H}{D_2}\right)^2 - 1}\right)$$

For underground channel installation of the pipeline, he air inside the channel was considered as the surrounding environment. The value of R_{out} was calculated as the sum of the thermal resistances of the consecutive heat transfers within the channel:

$$\begin{gathered}
T_{env} = T_{air}^{ch}, \qquad R_{out} = R_{air}^{ch} + R_{wall}^{ch} + R_{gr}^{ch} \\
R_{air}^{ch} = \frac{1}{\alpha_{air}^{ch}\pi D_2}, \qquad R_{wall}^{ch} = \frac{1}{\alpha_{air}^{ch}\pi D_{ch}}, \\
D_{ch} = \frac{2d_{ch}h_{ch}}{d_{ch} + h_{ch}}, \qquad R_{gr}^{can} = \frac{\ln\left(3.5\,\frac{Hh_{ch}}{d_{ch}^2}\right)}{\lambda_{gr}\left(5.7 + \frac{d_{ch}}{2h_{ch}}\right)}
\end{gathered} \tag{2.26}$$

where $R_{air}^{ch}, R_{wall}^{ch}$, and R_{gr}^{ch} are the values of the corresponding thermal resistances: heat transfer from the surface of the insulated pipeline into the air space of the channel, heat transfer from the air in the channel to the ground, heat transfer of the ground around the channel; α_{air}^{ch} is the heat transfer coefficient of the air in the channel, which was taken as 8 W/(m^2·°C) according to [14]; D_{ch}, d_{ch} and h_{ch} are the equivalent diameter, width, and height of the duct; and T_{air}^{ch} is the temperature of the duct air, which was calculated based on the following relationship for thermal resistances:

$$\frac{T_{air}^{ch} - T_{avg}}{R_{ins} + R_{air}^{ch}} + \frac{T_{air}^{ch} - \bar{T}_{avg}}{\bar{R}_{ins} + \bar{R}_{air}^{ch}} + \frac{T_{air}^{ch} - T_{gr}}{R_{wall}^{ch} + R_{gr}^{ch}} = 0 \tag{2.27}$$

where $\bar{R}_{ins}$ and $\bar{R}_{air}^{ch}$ are the values of the corresponding thermal resistances (insulation layer and heat transfer from the pipe surface to the air in the channel), which were calculated using formulas (2.23) and (2.26) with respect to the parameters of the neighboring pipe.

As can be seen from formulas (2.25)–(2.27), calculating the temperature at the end of an underground pipe section requires the computed temperature of the water in the neighboring pipe, which in turn depends on the temperature in the considered pipe. Therefore, for underground installations, an iterative process is carried out to calculate the final temperature of the section until the required accuracy is achieved.

Thus, using the initial temperature T_0 at the inlet of the HN pipe section and the heat carrier flow rate q through this section, the corresponding outlet temperatures T_{end} were determined using formulas (2.20)–(2.27).

The temperature distribution throughout the HN was determined using a breadth-first search (graph traversal method), starting from the network nodes (CHPs, boiler houses) where outlet temperatures are specified. The traversal of the network nodes was performed along the positive flow direction ($q > 0$). During the traversal, the inlet temperature T_0 of subsequent HN sections (the temperature at the outlet of the initial node of the section) was calculated based on the heat energy balance:

$$T_0 = \frac{\sum_{i=1}^{n}(q_i \cdot (T_{end})_i)}{\sum_{i=1}^{n} q_i} - \Delta T$$

where n is the number of HN nodes from which flow enters the current node; q_i and $(T_{end})_i$ are the values of the water flow rate and the outlet temperature in the i-th pipe section entering the current node; and ΔT is the temperature loss at the current node. If the current node is a consumer in the heat supply system, then $\Delta T > 0$; otherwise, $\Delta T = 0$.

Figure 2.3 shows the calculated data for the distribution of temperature and piezometric head in the supply and return pipelines of the HN. Heat exchange with the environment leads to a decrease in the water temperature in the supply pipeline from 109.7 °C to 105 °C over a length of L = 9520 m (see Fig. 2.3). It can be seen that along the pipeline up to point L_1 = 5280 m, the hot water temperature distribution is almost linear; from this point, the temperature decreases until point L_2 = 7540 m. After that, the drop in hot water temperature stabilizes (see Fig. 2.3).

Figure 2.3 also shows the piezometric heads in the supply (red line) and return (blue line) pipelines. In the supply pipeline, the pressure decreases due to the withdrawal of hot water for heat supply to consumers, whereas in the return pipeline, the pressure increases due to the inflow of cooled water (see Fig. 2.3). The sharp drop in pressure at point L_3 = 7700 m in the return pipeline is associated with a local resistance at that location.

The software code for solving the problem of temperature distribution in the HN, based on the heat exchange with the environment, was written in C# and implemented as a separate SP software module.

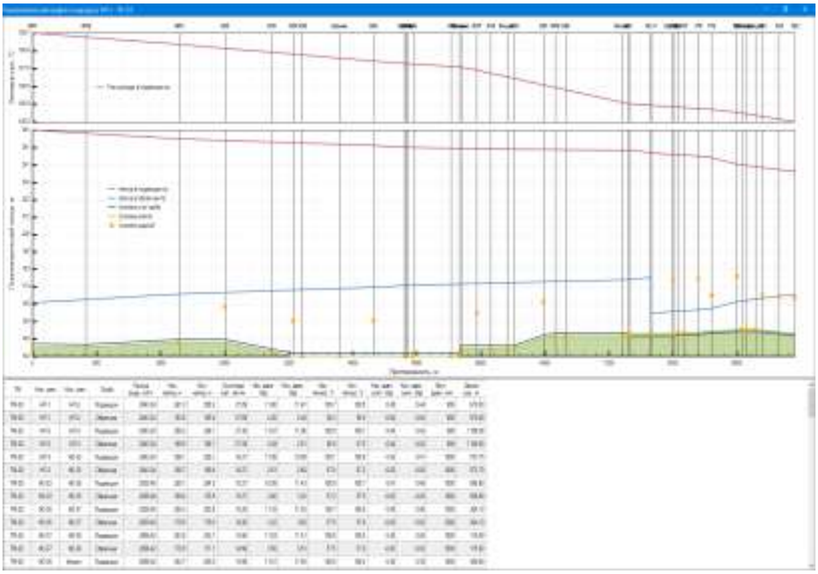

Figure 2.3. Temperature distribution in the supply and return main pipelines of the heating network

Determining heat losses from the distribution of heat through pipelines is one of the greatest challenges in modeling temperature distribution in the HN. This study presents the results of heat loss calculations depending on the type of pipeline installation in the HN. The temperature distribution throughout the HN was determined using a breadth-first search (graph traversal method), starting from network nodes (CHPs, boiler houses) where outlet temperatures are specified. The traversal of the network nodes was performed along the positive flow direction ($q > 0$). During the traversal, the inlet temperature T_0 of subsequent HN sections (the temperature at the outlet of the initial node of the section) was calculated based on the heat energy balance.

2.4 Development of a mathematical model for temperature distribution in the heating network based on standard heat losses

In the SP, a mathematical model was developed and software code was created to solve the problem of temperature distribution in the HN based on standard heat losses.

The algorithm for calculating standard heat loss values was implemented in accordance with the requirements of methodological guidelines for determining heat losses in water and steam HNs, approved by Order No. 59 dated 05.03.2013 of the First Vice Minister of Industry and New Technologies of the Republic of Kazakhstan: "Methodological Guidelines for Determining Fuel, Electricity, and Water Consumption for Heat Production by Heating Boilers of Municipal Heat and Power Enterprises of the RK".

The implemented function for calculating standard values of heat and HN water losses uses the following additional input data:

- The average monthly temperatures of the HN water in the supply and return pipelines;
- The temperature schedule of the operation of the heat source unit (CHP, boiler house);
- The average monthly soil temperatures;
- The average monthly temperatures of the incoming water.

The standard values of the average annual heat losses through insulation were determined using the following formula [41]:

$$Q_{und}^{ann} = \sum \beta q_{und} L\,, Q_{ab,sup}^{ann} = \sum \delta q_{ab,sup} L\,, Q_{ab,ret}^{ann} = \sum \delta q_{ab,ret} L \qquad (2.28)$$

where Q_{und}^{ann}, $Q_{ab,sup}^{ann}$, and $Q_{ab,ret}^{aan}$ are the standard average annual heat losses for sections with underground installation, and for the supply and return pipelines of aboveground sections, respectively; δ is the local heat loss coefficient, accounting for heat losses from fittings, supports, and compensators; L is the length of the HN section characterized by the same pipe diameter and type of installation; and q_{und}^{ann}, $q_{ab,sup}^{ann}$, and $q_{ab,ret}^{ann.}$ are the standard values of specific heat losses for underground and aboveground installation for each pipe diameter and installation type.

The standard values of specific heat losses for each pipeline diameter are determined by interpolation based on the appendices of the methodological guidelines for determining heat losses in water and steam HNs, approved by Order No. 59 dated 05.03.2013 of the First Vice Minister of Industry and New Technologies of the Republic of Kazakhstan.

The average monthly standard heat loss due to network water leakage Q_{leak}^{mon} is determined by the following formula [41]:

$$Q_{leak}^{mon} = a \cdot C \cdot V \cdot \rho \cdot \left(\frac{T_{sup}^{am} - T_{ret}^{am}}{2} - T_{c.w}^{am} \right) \cdot t \qquad (2.29)$$

where a is the normative value of leakage from the HN and local systems, taken as 0.25% of the total network volume; C is the specific heat capacity of water (heat carrier); V is the total volume of the HN; ρ is the density of the heat carrier; T_{sup}^{am} and T_{ret}^{am} are the average monthly temperatures in the supply and return pipelines, respectively; $T_{c.w}^{am}$ is the average monthly temperature of the water used for make-up of the heating system; t is the operating time of the heating system.

The temperature of the heat carrier at the end of a pipeline section T_{end}^{sec} is determined as follows:

$$T_{end}^{sec} = T_{start}^{sec} - \frac{Q + Q_{leak}^{mon}}{C\rho q_{sec}} \tag{2.30}$$

where T_{start}^{sec} is the initial temperature at the inlet of the pipeline section; Q is the normative heat loss of the section through insulation depending on the pipe type and installation method (Q_{sup}^{ann}, $Q_{ab,sup}^{ann}$, $Q_{ab,ret}^{ann}$); q_{sec} is the heat carrier flow rate in the pipeline section.

Thus, using the initial temperature T_{start}^{sec} at the inlet of the pipeline section of the HN and the heat carrier flow rate q through this section, the corresponding outlet temperatures T_{end}^{sec} were determined using formulas (2.20)–(2.27).

The temperature distribution throughout the entire HN was determined using a breadth-first search (graph traversal method), starting from the heat source nodes of the network (CHPs and boiler houses), for which the outlet temperatures were specified. The traversal of the HN nodes was performed along the positive direction of the heat carrier flow ($q > 0$). When bypassing the nodes of the HN, the temperature value $T_{start}^{next\,sec}$ at the input of subsequent sections of the HN (the temperature at the output of the initial node of the section) was calculated based on the balance of thermal energy:

$$T_{start}^{next\,sec} = \frac{\sum_{i=1}^{n}(q_i \cdot (T_{end}^{sec})_i)}{\sum_{i=1}^{n} q_i} - \Delta T \tag{2.31}$$

where n is the number of nodes in the HN from which the flow enters the current node; $q_i, (T_{end})_i$ are the water flow rates and final temperatures at the i-th pipe section entering the current node; ΔT is the temperature loss at the current node. If the current node is a consumer in the heating system, then $\Delta T > 0$, otherwise $\Delta T = 0$.

Based on the algorithm described above, a C# code was written to calculate the temperature distribution in the HN based on standard heat losses. This code is used as one of the options for calculating the HN temperature distribution in the commissioning and verification calculation modules, which are described in sections 2.5-2.8.

2.5 Creation of a commissioning calculation module for specified thermal loads of consumers

In the SP, a commissioning calculation module was implemented. The purpose of this calculation is to verify the available pressure at each consumer node and to select the adjustable resistance at the inlet and outlet of its HS. The input operating parameters of the HN for the commissioning calculation are as follows:

- Heat loads on the HS, VS, and HWS for all consumer nodes;
- Temperature at the outlet of the source nodes;
- Pressure at the inlet and outlet of the source nodes;
- Operating modes of pumping stations in the HN;
- Status of shut-off valves and control valves in intermediate nodes of the HN.

The commissioning calculation algorithm consists of the following steps:

1) Calculation of the design values of network water flow rates for consumer nodes;

2) Calculation of the distribution of heat carrier flows in the supply pipelines of the HN;

3) Calculation of the distribution of heat carrier flows in the return pipelines of the HN;

4) Calculation of the distribution of heat carrier temperatures in the supply pipelines of the HN based on the temperatures at the outlets of source nodes;

5) Calculation of the distribution of heat carrier temperatures in the return pipelines of the HN based on the temperatures at the outlets of consumer nodes;

6) Calculation of the pressure distribution in the supply pipelines of the HN based on the pressures at the outlets of source nodes;

7) Calculation of the pressure distribution in the return pipelines of the HN based on the pressures at the inlets of source nodes;

8) Verification of the available pressure at consumer nodes and calculation of the controllable resistance at the inlet and outlet of the HS.

For each consumer node, the calculated network water consumption was determined as the sum of the calculated flow rates for the heating system (G_{HS}^{calc}), ventilation system (G_{VS}^{calc}), and hot water supply system (G_{HWS}^{calc}). The formulas used to calculate these calculated flow rates are presented below.

Estimated consumption of network water for the HS connected according to the dependent scheme [42]:

$$G_{HS}^{calc} = \frac{Q_{HS}^{calc}}{C \cdot \left(T_{sup}^{calc} - T_{ret}^{calc}\right)} \tag{2.32}$$

where Q_{HS}^{calc} is the estimated heat load on the heating system; T_{sup}^{cals} and T_{ret}^{calc} are the water temperatures in the supply and return pipelines of the heating system, respectively, at the estimated outside air temperature for the design of the heating system.

Estimated consumption of network water for the HS connected according to the dependent scheme [42]:

$$G_{HS}^{calc} = \frac{Q_{HS}^{calc}}{C \cdot (T_{in}^{HE} - T_{out}^{HE})} \tag{2.33}$$

where T_{in}^{HE} and T_{out}^{HE} are the calculated temperatures of the heated heat carrier (secondary circuit) at the inlet and outlet of the heat exchanger, respectively.

The calculated heat carrier flow rate in the VS is given in [42]:

$$G_{VS}^{calc} = \frac{Q_{VS}^{calc}}{C \cdot \left(T_{sup}^{calc} - T_{AH}^{calc}\right)} \tag{2.34}$$

where Q_{VS}^{calc} is the calculated thermal load of the ventilation system; T_{AH}^{calc} is the calculated temperature of network water after the air heater of the ventilation system.

The calculated heat carrier flow rate for HWS in open heat supply systems [42]:

$$G_{HWS}^{calc} = \frac{\beta \cdot Q_{HWS}^{calc}}{C \cdot (T_{h.w} - T_{c.w})} \tag{2.35}$$

where Q_{HWS}^{calc} is the estimated heat load on the hot water supply system; $T_{h.w}$ and $T_{c.w}$ are the design temperatures of hot and cold water, respectively; β is the proportion of water taken for hot water supply from the supply pipeline ($\beta = \beta_{sup}$) or from the return pipeline ($\beta = \beta_{ret}$):

$$\beta_{sup} = \frac{T_{h.w} - T_{ret}^{calc}}{T_{sup}^{calc} - T_{ret}^{calc}}, \qquad \beta_{ret} = \frac{T_{sup}^{calc} - T_{h.w}}{T_{sup}^{calc} - T_{ret}^{calc}}$$

Estimated consumption of heat carrier (heating water) for the hot water supply system for closed heat supply systems with a parallel connection scheme of heaters for the hot water supply system [42]:

$$G_{HWS}^{calc} = \frac{Q_{HWS}^{calc}}{C \cdot \left(T_{sup}^{br} - T_{H,out}^{br}\right)} \tag{2.36}$$

where T_{sup}^{br} is the temperature of network water in the supply pipeline at the point of the temperature curve break; $T_{H,out}^{br}$ is the temperature of network water after the heater at the point of the temperature curve break (assumed to be 30 °C).

The calculation of the distribution of heat carrier flows through the heating system pipelines is implemented in accordance with the mathematical model described in section 2.2. For the supply network, the calculated flow rates of consumer nodes will be the external negative inflow, and for the return network, the external positive inflow. The external inflow value for a consumer node is defined as $G_{HS}^{calc} + G_{VS}^{calc} + G_{HWS}^{calc}$, i.e., it is the sum of the network water volumes, calculated using formulas (2.32)-(2.36), which are necessary to meet the specified heat load.

The calculation of the heat carrier temperature distribution along the supply and return pipelines of the HN is performed using one of two user options: either taking into account heat exchange processes with the environment (see Section 2.3) or taking into account standard heat losses (2.28)-(2.31) (see Section 2.4).

The pressure distribution across the entire HN is calculated using a depth-first search (graph traversal method), starting from the HN source nodes (CHPs, boiler houses), for which the supply/return pressure values are specified. When traversing the HN nodes, the pressure value at the end of the pipe section P_{end}^{sec} is calculated using the Darcy-Weisbach equation, taking into account losses due to local resistance and static pressure drop:

$$\begin{gathered} P_{end}^{sec} = P_{start}^{sec} - \Delta P_{hydr}^{sec} + \Delta P_{stat}^{sec}, \\ P_{start}^{next.sec} = P_{end}^{sec} + \Delta P^{node} \end{gathered} \tag{2.37}$$

$$\begin{gathered} \Delta P_{hydr}^{sec} = \left(\lambda \frac{L}{D} + \sum \zeta\right) \frac{u^2}{2} \rho, \\ \Delta P_{stat}^{sec} = \rho g (h_{start} - h_{end}) \end{gathered} \tag{2.38}$$

where P_{start}^{sec} is the pressure at the beginning of the pipe section; λ is the coefficient of linear hydraulic losses along the length; L is the length of the pipe section; D is the internal diameter of the pipe section; $\sum \zeta$ is the sum of the local resistance coefficients; u is the average flow velocity of the heat carrier over the section; ρ is the density of the heat carrier; h_{start} and h_{end} are the pipe elevation marks at the beginning and at the end of the pipe section; $P_{start}^{\text{next sec}}$ is the pressure at the beginning of the next adjacent pipe section; ΔP^{node} is the pressure drop across the HN node: at gate valve nodes $\Delta P^{node} < 0$, at operating pumping stations $\Delta P^{node} > 0$, in other cases $\Delta P^{node} = 0$.

The verification of the available pressure at consumer nodes is carried out according to the following criteria:

The pressure at the inlet of the HS (P_{in}^{HS}) must not exceed the maximum allowable pressure (P_{in}^{max}) for the internal heating elements within the building;

The pressure at the outlet of the HS (P_{out}^{HS}) must not be lower than the minimum allowable static pressure (P_{out}^{min}), which depends on the building height (otherwise, the upper floors will remain without circulation or air will be entrained into the building HS);

The pressure difference between the inlet and outlet of the building HS (ΔP^{HS}) is known and depends on the heat carrier flow rate through the HS.

Let P_{sup} and P_{ret} be the pressure values found in the supply and return pipelines of the consumer node, respectively; ΔP is the pressure loss on valves or regulators in the supply pipeline at the inlet of the consumer node HS; ΔP_{ret} is the pressure loss on valves or regulators in the return pipeline at the outlet of the HS consumer node. Then, the above-described verification reduces to solving the following system of inequalities for the variables ΔP_{sup} and ΔP_{ret}:

$$\begin{cases} P_{in}^{HS} = P_{sup} - \Delta P_{suo} \leq P_{in}^{max} \\ P_{out}^{HS} = P_{ret} + \Delta P_{ret} \geq P_{out}^{min} \\ P_{in}^{HS} - P_{out}^{HS} = \Delta P^{HS} \end{cases} \tag{2.39}$$

$$P_{out}^{min} = \rho g h_{\text{bldg}},$$

$$\Delta P^{HS} = \rho g s_{in}^{HS} \cdot \left(G_{in}^{calc,HS}\right)^2,$$

$$G_{in}^{calc,HS} = \frac{Q_{HS}^{calc}}{C \cdot \left(T_{in}^{calc,HS} - T_{ret}^{calc}\right)} \tag{2.40}$$

where h_{bldg} is the height of the consumer building; s_{inside}^{HS} is the hydraulic resistance coefficient of the HS inside the consumer building; $G_{inside}^{calc.HS}$ is the network water flow rate inside the HS; $T_{in}^{calc,HS}$ is the temperature of water in the supply pipeline inside the heating system at the calculated outdoor air temperature for heating design.

If, for a particular consumer node, there exists a solution to system (2.39) such that $\Delta P_{sup} > 0$ and ΔP_{ret} > 0, this indicates that the consumer is adjustable; otherwise, the consumer is problematic (i.e., adjusting it requires changing the operational parameters of the HN).

For consumer nodes that are adjustable, the coefficients of the established hydraulic resistance at the HS inlet (s_{in}^{HS}) and at the HS outlet (s_{out}^{HS}) are calculated based on the following relationships:

$$\begin{gathered} \Delta P_{sup} = \rho g s_{in}^{HS} \cdot \left(G_{HS}^{calc}\right)^2, \\ \Delta P_{ret} = \rho g s_{out}^{HS} \cdot \left(G_{HS}^{calc}\right)^2 \end{gathered} \tag{2.41}$$

Based on the above algorithm, a C# program code was developed for the commissioning calculation module. This module is implemented as one of the calculation types that can be run in the SP. To run this type of calculation, the HN operating mode must be selected in the SP interface (its operational parameters can be edited if necessary), then in the top toolbar of the mode, select the "Commissioning Calculation" option from the calculation type dropdown menu (see Fig. 2.4) and click the "Compute" button.

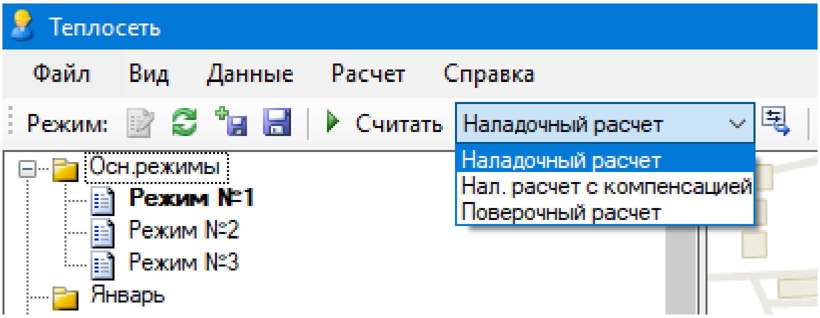

Figure 2.4. Starting the commissioning calculation

After performing the commissioning calculation, the results are displayed on the HN map and in tabular form when any HN element is selected (see Fig. 2.5). The SP user has the ability to:

– View a colored map of the HN relative to the selected output data of the calculation at nodes and pipes (pressure, available pressure, temperature or heat carrier flow rate, etc.). The coloring is performed using a transitional palette [blue - light blue - green - yellow - orange -

red]. Blue corresponds to the minimum value, red to the maximum, and transitional colors from blue to red indicate intermediate values. Figure 2.5 shows an example of the implemented SP interface, which displays a colored map based on the calculated actual heat load.

– View a colored map of the HN for the failure rate of HN facilities based on the user-selected criteria (insufficient available pressure, exceeding the maximum permissible pressure in the pipe, etc.). HN facilities that do not have an emergency value are colored green; otherwise, the facility should be colored red;

– Select a specific element of the HN and view its calculated values in a tabular format in the right-hand panel of the "Calculation Results" tab.

– Select the start and end nodes of the HN to plot graphs of calculated piezometric data along the selected pipeline route (see Fig. 2.6).

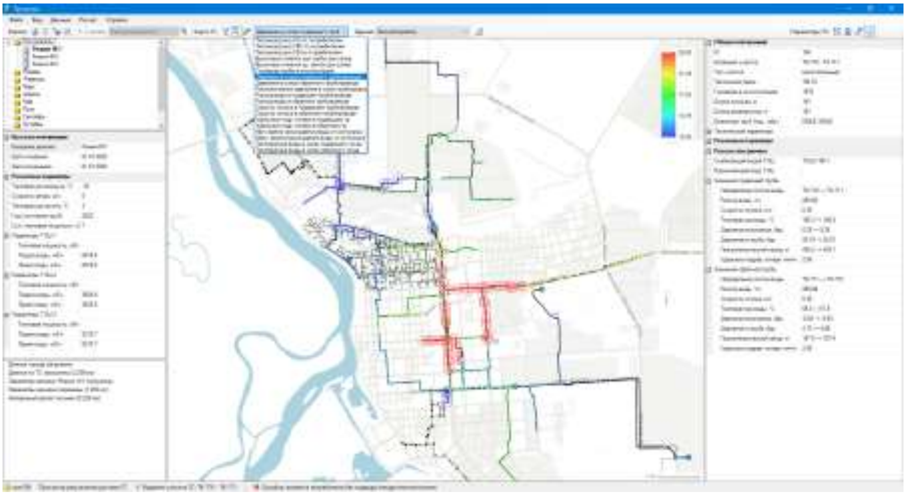

Figure 2.5. Displaying the results of the commissioning calculation in the main program window

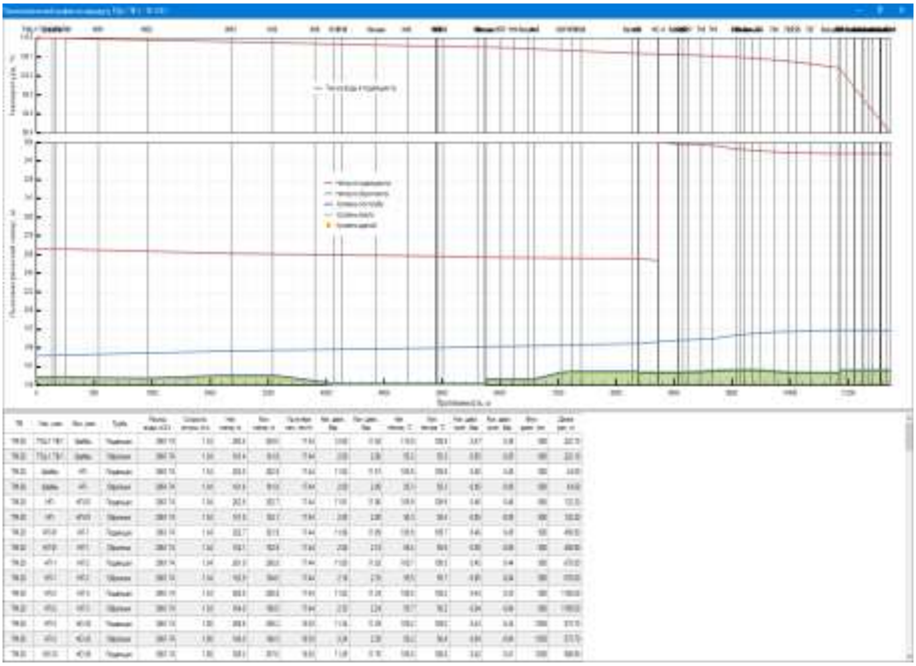

Figure 2.6. Window displaying the piezometric graph after the commissioning calculation for a given node route

2.6 Creation of a verification calculation module based on the specified installation parameters of gate valve and orifice plate settings at the consumer end

A verification calculation module was implemented in the SP, the purpose of which is to calculate the received thermal power for consumer nodes. The following data are the input mode parameters of the HN for the verification calculation:

- Established hydraulic resistances in consumer nodes (resistance of washers, control valves, etc.);
- Temperature at the outlet of source nodes;
- Pressure at the inlet and outlet of source nodes;
- Operating modes of pumping stations in the HN;
- Status of valves and control valves in intermediate nodes of the HN.

A verification calculation is the inverse of an commissioning calculation. A verification calculation can be used for a previously setup HN in which the hydraulic balance has been changed (removing a washer from a consumer, shutting off a pump in a pumping station, etc.). In this case, the verification calculation will show how a particular change in the hydraulic balance of the HN affected the resulting heat loads of the consumer nodes. Unlike a commissioning calculation, a verification calculation determines the correct heat carrier flow rates through the consumer nodes (and, consequently, the heat output they receive) based on the hydraulic characteristics of the HN.

The verification calculation algorithm consists of the following steps:

1) Calculation of the heat carrier flow distribution along the combined HN graph: jointly supply networks pass through the return network;

2) Calculation of the heat carrier temperature distribution along the combined HN graph based on the outlet temperature of the source nodes;

3) Calculation of the pressure distribution along the combined HN graph based on the outlet pressure of the source nodes;

4) Calculation of the received thermal power at the consumer nodes.

Figure 2.7 illustrates the construction of the calculated HN graph of a single network type (see Fig. 2.7a) into a combined supply and return network graph (see Fig. 2.7b). Vertices corresponding to source nodes are labeled with the letter И. Vertices corresponding to consumer nodes are labeled with the letter П. In the combined graph, the number of vertices and edges doubles (copies for the HN nodes and pipeline sections for both supply and return networks), and additional edges are added for consumer nodes (П1п-П1о, П2п-П2о, …). The supply network edges in Fig. 2.7 are shown in red, the return network edges in blue, and the internal edges for consumer nodes are shown in purple with a dashed line.

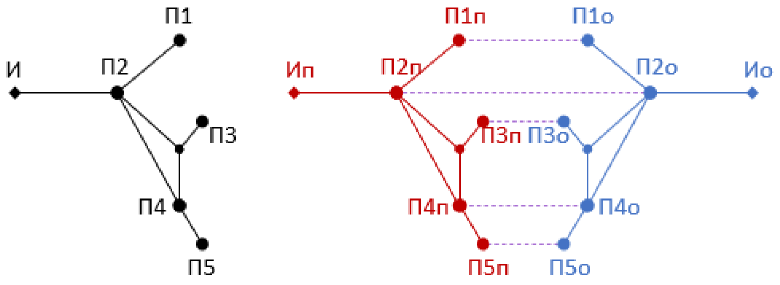

a) b)

Figure 2.7. HN calculation graph: a) graph of a single network type (either supply or return network); b) combined graph of the supply and return networks.

As in the main graph edges, pressure and temperature losses also occur in the internal edges of the consumer nodes depending on the heat carrier rate through the consumer node's heating system, i.e., as the heat carrier flows through the internal heating system pipes from the node's entry point from the supply network to the node's exit point into the return network.

The traversal of the graph and the calculation of the distribution of pressure, flows, and heat carrier temperatures over the combined HN graph in the verification calculation are performed using the same formulas (2.31) and (2.37) as in the commissioning calculation, but the source and sink vertices differ in the graphs used.

In the commissioning calculation using the supply network graph (see Fig. 2.7a), the vertices corresponding to source nodes ("И") serve as sources, while the vertices corresponding to consumer nodes ("П1", "П2", …) serve as sinks. In the commissioning calculation using the return network graph (see Fig. 2.7a), the roles of sources and sinks are reversed. In the combined graph (see Fig. 2.7b) for the verification calculation, the vertices corresponding to consumer nodes ("П1п", "П2п", …, "П1о", "П2о", …) are intermediate vertices without external inflow; the source vertex is "Ип" (the outlet of the source node via the supply pipeline), and the sink vertex is "Ио" (the inlet to the source node via the return pipeline). In the combined graph (see Fig. 2.7b), the source vertices are assigned the pressure and temperature values of the source nodes in the supply pipeline, while for the sink vertices, only the pressure of the source nodes in the return pipeline is assigned.

When traversing the graph to calculate flows and pressures in relation to the internal edges of consumer nodes, relation (2.38) takes the following form:

$$\Delta P_{hydr}^{sec} = \Delta P_{sup} + \Delta P^{HS} + \Delta P_{ret}, \qquad \Delta P_{stat}^{sec} = 0 \tag{2.42}$$

where the pressure losses ΔP_{sup}, ΔP^{HS}, and ΔP_{ret} are calculated using formulas (2.40) and (2.41), in which the flow rates through the consumer node are not determined in advance (as in the commissioning calculation) but are calculated within the edges of the combined graph (П1п-П1о, П2п-П2о, …; Fig. 2.7b) according to the flow distribution algorithm described in Section 2.2.

After calculating the flow distributions, the heat carrier temperature and the pressure in the combined HN graph, the values of the received thermal power in the consumer nodes for the HS, VS, and HWS are calculated using relations (2.32)-(2.36), in which the sought-after values will be the variables Q_{HS}, Q_{VS}, Q_{HWS} (and not Q_{HS}^{calc}, Q_{VS}^{calc}, Q_{HWS}^{calc}), and the corresponding values found in the verification calculation will be used as the values of the calculated flow rates (G_{HS}^{calc}, G_{VS}^{calc}, G_{HWS}^{calc}) and the calculated temperature (T_{sup}^{calc}) in the supply pipe.

Based on the above algorithm, a C# program code was developed for the verification calculation module. This module is implemented as one of the calculation types that can be run in the SP. To run this type of calculation, the HN operating mode must be selected in the SP interface (its operational parameters can be edited if necessary), then in the top toolbar of the mode, select the "Verification Calculation" option from the calculation type dropdown menu and click the "Compute" button. After performing the verification calculation, the SP user has access to the same actions for viewing results as in the commissioning calculation.

2.7 Modification of the commissioning calculation module to account for heat loss compensation due to an increase in the heat carrier flow rate

In the SP, the mathematical model of the commissioning calculation was implemented, and the commissioning calculation module was modified to allow for accounting of heat loss compensation by increasing the heat carrier flow rate.

In determining the network water flow rates at consumer nodes (2.32)–(2.36), the calculated temperature value in the supply pipeline (T_{sup}^{calc}) is used. However, as is known, the temperature at the inlet of the supply pipeline (T_{sup}) at a given consumer node can differ significantly from its specified calculated value ($T_{sup} < T_{sup}^{calc}$) due to heat losses of the heat carrier along the pipeline route, which results in the thermal power received by the consumer node being lower than the specified thermal load.

The function G of the flow rate required to ensure the necessary thermal load in the HS, VS, and HWS at the consumer nodes is introduced. The function G depends on the supply pipeline temperature T_{sup} as follows:

$$G(T_{sup}) = G_{HS}(T_{sup}) + G_{VS}(T_{sup}) + G_{HWS}(T_{sup})$$

where G_{HS}, G_{VS}, and G_{HWS} are the functions of the network water flow rate corresponding to the HS, VS, and HWS at the consumer nodes with constant values of the required thermal loads Q_{HS}^{calc}, Q_{VS}^{calc}, and Q_{HWS}^{calc}, respectively.

The functions G_{HS}, G_{VS}, and G_{HWS} are given by formulas (2.32)–(2.36), in which the temperature T_{sup} is used as the argument of the function instead of the calculated temperature values T_{sup}^{calc}.

In turn, the values of T_{sup} at the inlet of the consumer nodes depend on the heat carrier flow velocities in the supply pipelines: the greater the increase of the vector $\boldsymbol{G} = \{G_1, G_2, \dots\}$ compared to the vector $\{G(T_{sup,1}^{calc}), G(T_{sup,2}^{calc}), \dots\}$, the higher the flow velocity throughout the HN, and the lower the heat losses of the heat carrier to the external environment. Thus, for the HN as a whole, the vectors $\boldsymbol{G} = \{G_1, G_2, \dots\}$ and $\boldsymbol{T}_{sup} = \{T_{sup,1}, T_{sup,2}, \dots\}$ are interdependent: the direct dependence is defined by the function $G = G(T_{sup})$, while the inverse dependence is complex and is determined through the problem of flow and temperature distribution of the heat carrier over all sections of the supply network pipelines. In this regard, the process of determining the increase in heat carrier flow rate in the modified module is iterative in nature.

Below is the commissioning calculation algorithm that accounts for the compensation of heat losses by increasing the heat carrier flow rate, in which the recalculation of the required increase $\boldsymbol{G} = \{G_1, G_2, \ldots\}$ is performed using the under-relaxation method to ensure the stability of the iterative process:

1) Calculation of the flow rate for each consumer node as the initial approximation:

$$G^{(k)} = G^{(0)} = G\left(T_{sup}^{calc}\right), \qquad k = 0$$

2) Calculation of the flow distribution in the supply network of the HN considering the current values of the heat carrier flow rate $G^{(k)}$ for each consumer node;

3) Calculation of the temperature distribution in the supply network of the HN: the value of $T_{sup}^{(k)}$ is determined for each consumer node;

4) Recalculation of the heat carrier flow rate for each consumer node:

$$G^{(k+1)} = \alpha \cdot G\left(T_{sup}^{(k)}\right) + (1 - \alpha) \cdot G^{(k)}$$

where α is the relaxation coefficient. A value in the range $0.1 \leq \alpha \leq 0.3$ can be used.

5) Convergence check for each consumer node:

$$\left|G^{(k+1)} - G^{(k)}\right| \leq \varepsilon$$

where ε is the allowable error of the heat carrier flow rate.

If the convergence condition is satisfied for all nodes, proceed to step 6; otherwise, increase the iteration number ($k = k + 1$) and return to step 2.

6) Calculation of the heat carrier flow distribution in the return pipelines of the HN;

7) Calculation of the heat carrier temperature distribution in the return pipelines of the HN based on the outlet temperature from the consumer nodes;

8) Calculation of the pressure distribution in the supply pipelines of the HN based on the outlet pressure of the source nodes;

9) Calculation of the pressure distribution in the return pipelines of the HN based on the inlet pressures of the source nodes;

10) Check of the available pressure at the consumer nodes and calculation of the controllable resistance at the inlet and outlet of the HS.

In the above-described algorithm, the required increase of the flow rate through the consumer nodes is performed iteratively in steps 2–5. In the remaining steps 6–10, the calculation of the other HN parameters is carried out; in these steps, the calculations are performed in the same way as in a standard commissioning calculation.

As shown by the conducted calculations, with $\varepsilon = 10^{-3}$ and $\alpha = 0.2$, the iterative process in steps 2–5 of the algorithm converges steadily within 10–15 iterations.

Based on the above-described algorithm, a program code in C# was developed for the commissioning calculation module, taking into account the compensation of heat losses by increasing the heat carrier rate. This module is implemented as one of the types of calculations that can be run in the SP. To start this type of calculation, the HN operating mode must be selected in the SP interface (if necessary, its operating parameters can be edited), and in the calculation type drop-down menu on the top toolbar, the option "Commissioning Calculation with Compensation" should be chosen, then click the "Calculate" button. After the calculation is completed, the SP user can perform the same actions to view the results as for a standard commissioning calculation.

2.8 Modification of calculation modules considering various types of connection and control of the heating system, hot water supply, and ventilation system at the consumer end

In the SP, part of the work was carried out to modify the calculation modules, taking into account various types of connection and control of the HS, HWS, and VS at the consumer end. The objective of this section is to achieve more accurate and realistic modeling of the operation of consumer nodes and their impact on the HN.

Technical material was collected on various types of heating units and facilities for introducing the HN into buildings. Different methods of heat supply for the HS, VS, and HWS were considered for various types of urban buildings (modern residential complexes, Soviet-era apartment buildings, private-sector houses, various administrative buildings, etc.). Based on the conducted analysis, such parameters of the HS, VS, and HWS for consumer nodes were selected that can significantly affect a more detailed calculation of pressure drop, temperature variation, and the provision of thermal flow rate at consumer nodes. The main such parameters and their selected value options, which will be taken into account in HN calculations, are listed below.

Type of HS connection:

- Independent;
- Elevator-based;
- Direct;
- With a pump on the bypass between the supply and return pipelines;
- With a pump on the supply pipeline;
- With a pump on the return pipeline;
- HS not present.

HS control method:

- No control;
- Based on a specified heat carrier flow rate;

- According to the temperature schedule;
- Based on pressure in the return pipeline;
- Using orifice plates on the return pipeline.

Type of HWS connection:

- Open water draw-off;
- Parallel heaters;
- Series heaters;
- Two-stage series heaters;
- Two-stage mixed heaters;
- HWS not present.

HWS control method:

- No control;
- Based on a specified temperature;
- With draw-off from the supply pipeline;
- With draw-off from the return pipeline;
- Based on return temperature (for open HWS draw-off).

Type of VS connection:

- Before connection of the HS network;
- After connection of the HS network;
- VS not present.

Thus, using the selected parameters, practically any complex operation scheme of the consumer node (a heating substation or a HN building entry node) can be described. Figure 2.8 shows examples of different consumer node schemes and their descriptions according to the selected HS, HWS, and VS operating parameters. Figure 2.9 shows how the consumer node type parameters are displayed in the SP interface, with the ability to edit and save them in the DB.

At present, the calculation modules of the SP implement various dependencies between the network water flow rate and the received heat output for the case of independent HS connection (see Fig. 2.8b) and other types of HS connections (see Fig. 2.8a), as well as for the case of open HWS draw-off (see Fig. 2.8a) and other types of HWS connections (see Fig. 2.8c). In the future, it is planned to account in more detail for the operational characteristics of different consumer node schemes when calculating pressure and temperature losses of the heat carrier as it passes through the node.

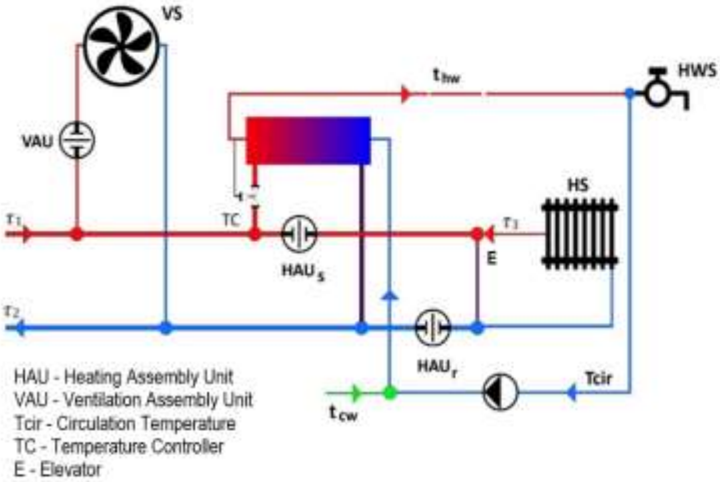

a)

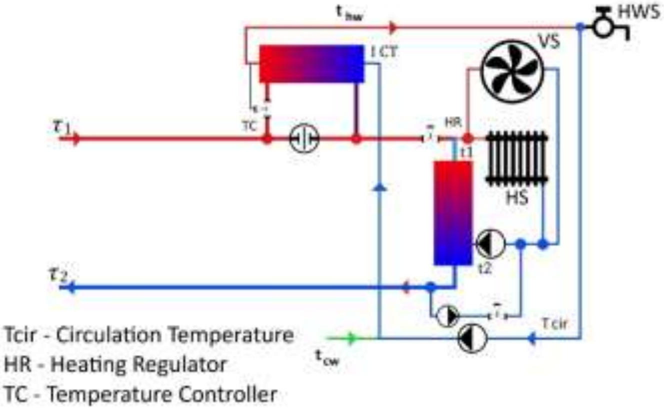

b)

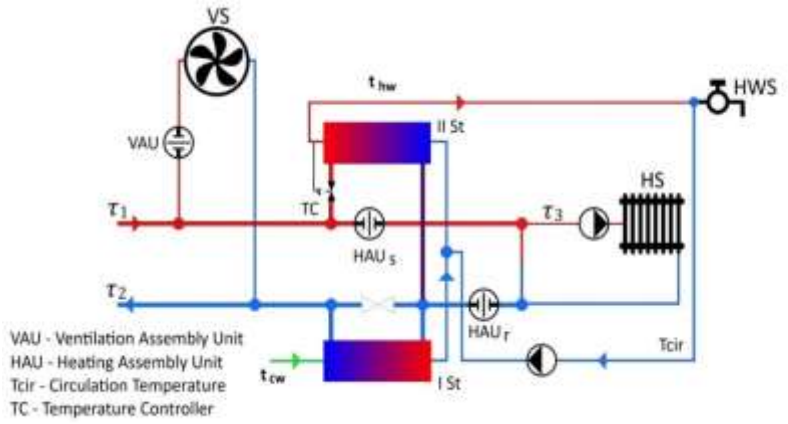

c)

Figure 2.8. Examples of consumer node schemes and their description by parameters in the SP DB: a) Elevator-based HS connection, parallel HWS connection, VS connection before the HS network; b) Independent HS connection, series HWS connection, VS connection within the HS network; c) HS connection with a pump on the supply pipeline, two-stage mixed HWS heaters connection, VS connection before the HS network.

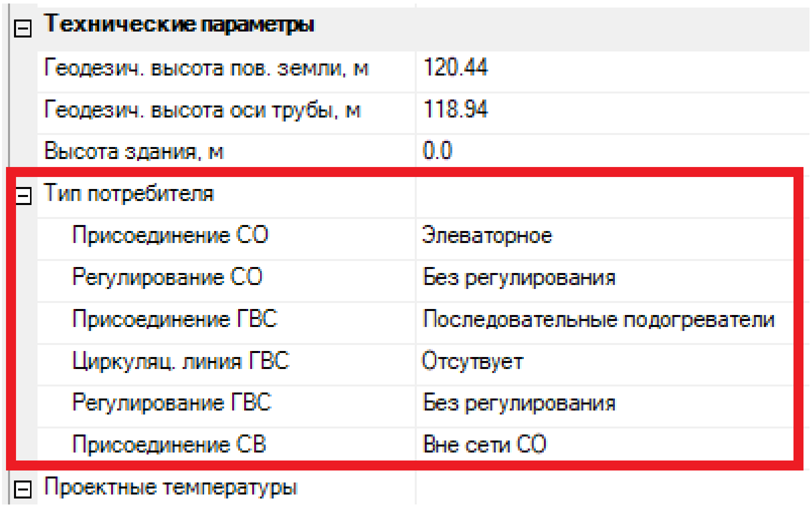

⊟ **Технические параметры**	
Геодезич. высота пов. земли, м	120.44
Геодезич. высота оси трубы, м	118.94
Высота здания, м	0.0
⊟ Тип потребителя	
Присоединение СО	Элеваторное
Регулирование СО	Без регулирования
Присоединение ГВС	Последовательные подогреватели
Циркуляц. линия ГВС	Отсутствует
Регулирование ГВС	Без регулирования
Присоединение СВ	Вне сети СО
⊟ Проектные температуры	

Figure 2.9. Viewing and editing consumer node type parameters

2.9 Results of heating network calculations

To verify the developed mathematical model and the numerical solution algorithm for heat carrier flow distribution, a specialized software suite was created, enabling hydraulic calculations of HNs of various configurations. The existing HN, including nodes, pipelines, and pump stations (PS), was selected as the object of study.

Commissioning Calculation

The commissioning calculation was carried out to determine the actual distribution of heat carrier flows across all sections of the network and to select the optimal operating modes of the control valves. The pressure at the outlet of the pump station was set taking into account the total calculated head losses and the pressure required by the end consumers (see Table 2). As a result of the calculation, the actual flow rates and pressure drops in each network section were obtained, and sections with insufficient or excessive pressure were identified.

The commissioning calculation was carried out to determine the actual distribution of heat carrier flows across all sections of the network and to select the optimal operating modes of control valves. The pressure at the outlet of the pump station was set taking into account the total calculated head losses and the pressure required by the end consumers (see Table 2). As a result of the calculation, the actual flow rates and pressure drops in each network section were obtained, and sections with insufficient or excessive pressure were identified.

Table 2. Initial parameters for the commissioning calculation

Heat pipeline	Outlet temperature, °C	Outlet pressure, bar	Inlet pressure, bar
TM-1	110	8	2

Figure 2.10 shows the HN scheme with the distribution of water flow in the supply pipeline and the available pressure at building inlets. The heat carrier flow is distributed unevenly, which is typical for networks with a branched structure and a large number of consumers. The highest flows are observed in the central sections of the network, shown in red and orange. The pressure at building inlets remains within standard values, ensuring stable heat supply to consumers.

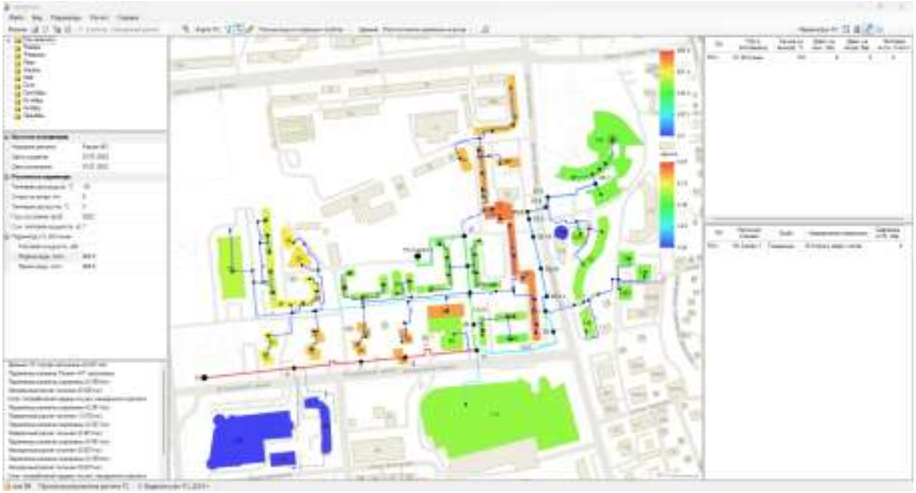

Figure 2.10. Results of the commissioning calculation displaying the water flow rate in the supply pipeline and the available pressure at the inlet in the buildings

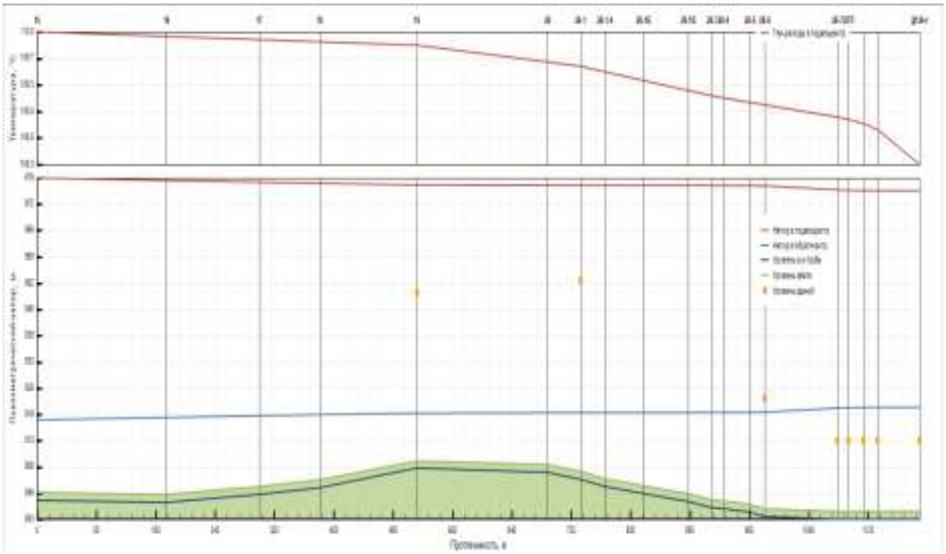

Figure 2.11. Piezometric diagram for the section UT-15 – D124-g

The piezometric diagram (Fig. 2.11) illustrates the variation of piezometric heads along the length of the considered HN main section. The diagram shows a steady decrease in head from the beginning to the end of the section, which corresponds to normal hydraulic operating conditions of the network. The head drop is uniform and does not exhibit abrupt changes, confirming the correctness of the selected initial parameters and the absence of significant local hydraulic losses.

Commissioning calculation with compensation

The commissioning calculation with compensation was carried out to identify measures capable of eliminating the network operation deviations detected in the previous commissioning calculation. To assess the effectiveness of the measures for compensating deviations in the operation of the heat supply system, a commissioning calculation with compensation was performed and compared with the baseline commissioning calculation. The comparative analysis is presented in Figure 2.12 and Table 2 below.

a b

Figure 2.12. Comparison of results: a – commissioning calculation, b – commissioning calculation with compensation

Table 3. Results of the commissioning calculation and the commissioning calculation with compensation

Operating parameters	Type of calculation	
	commissioning	commissioning with compensation
Water flow in the supply network, t/h	668.6	681.9
Received water consumption at the node, t/h	12.8	13.1
Water temperature (supply pipe), °C	108.3	108.3
Pressure at the node (supply pipe), bar	8.16	8.14
Piezometric head (supply pipe), m	975.9	975.7
Water temperature (return pipe), °C	70	70
Pressure at the node (return pipe), bar	2.79	2.8
Piezometric head (return pipe), m	921.1	921.2

The results showed that the compensatory measures allowed an increase in the total heat carrier flow in the supply network and improved consumption at the nodes. Changes in pressure and piezometric head were minor and remained within permissible limits, indicating the effective adjustment of the compensatory measures.

Verification calculation

A verification calculation was conducted to assess the current state of the network and verify its compliance with design and regulatory requirements without additional regulatory intervention. The pump station outlet pressure was set at 5 bar (see Table 4).

The results of the verification calculation, compared with the commissioning calculation for the HN section in question, are presented in Table 4 and Figures 2.13 and 2.14.

Table 4. Initial parameters for the verification calculation

Heat pipeline	Outlet temperature, °C	Outlet pressure, bar	Inlet pressure, bar
TM-1	110	5	2

The verification calculation showed a significant reduction in the heat carrier flow rates and pressures at the nodes compared to the commissioning mode (see Table 5). This highlights the importance of regular monitoring and the implementation of commissioning and compensatory measures to maintain efficient network operation.

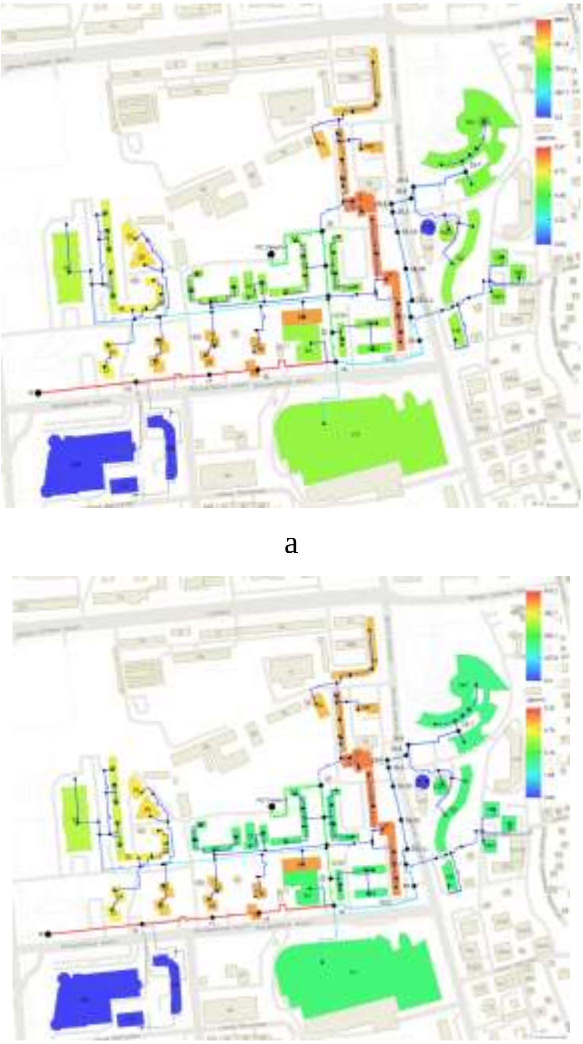

a

b

Figure 2.13. Comparison of results: (a) commissioning calculation and (b) verification calculation

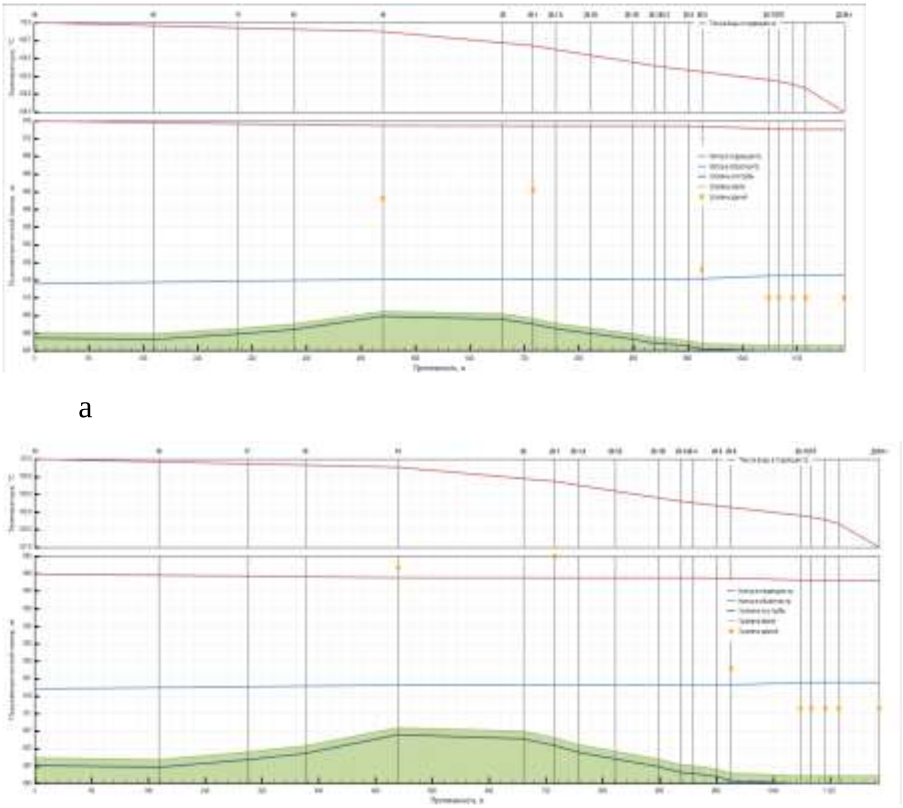

a

b

Figure 2.14. Piezometric diagrams: (a) commissioning calculation, (b) verification calculation

Table 5. Results of commissioning and verification calculations

Operating parameters	Type of calculation	
	Commissioning	Verification
Water flow rate to the supply network, t/h	668.6	510.2
Received water consumption per unit, t/h	12.8	9
Water temperature (supply pipeline),°C	108.3	107.6
Pressure at the node (supply pipeline), bar	8.16	5.3
Piezometric head (supply pipeline), m	975.9	946.7
Water temperature (return pipeline), °C	70	70
Pressure at the node (return pipeline), bar	2.79	2.64
Piezometric head (return pipeline), m	921.1	919.6

Analysis of network sensitivity to changes in hydraulic parameters

Sensitivity analysis is a study of how the final calculation results change when the input parameters are varied (see Table 6). In the context of modeling the distribution of heat carrier flows in a heat supply network, it helps to identify which input parameters have the most significant impact on the hydraulic operating conditions of the network in order to: (1) determine the most influential parameters affecting the accuracy and stability of network operation; (2) assess the robustness and reliability of the model; and (3) formulate recommendations for the selection and control of input data for calculations.

Table 6. Input parameters

Heat pipeline	Outlet temperature, °C	Outlet pressure, bar	Inlet pressure, bar
TM-1	90-130	8	2

The analysis of the change in pressure in the nodes and the piezometric head with varying temperature was carried out in the commissioning calculation mode, the results are given in Table 7.

Table 7. Results of varying the heat carrier temperature

Heat carrier tempera-ture, °C	Received water consump-tion, t/h	Water tempera-ture (supply pipeline), °C	Pressure at the node (supply pipeline), bar	Piezo-metric head (supply pipeline), m	Water tempera-ture (return pipeline), °C	Pressure at the node (return pipeline), bar	Piezomet-ric head (return pipeline), m
90	20.7	89.2	7.62	970.4	70	3.32	926.5
95	17.5	94	7.86	972.9	70	3.08	924.1
100	15.4	98.8	8	974.3	70	2.94	922.7
105	13.9	103.5	8.09	975.2	70	2.85	921.7
110	12.8	108.3	8.16	975.9	70	2.79	921.1
115	11.9	113	8.2	976.3	70	2.74	920.6
120	11.1	117.7	8.23	976.7	70	2.71	920.3
125	10.5	122.5	8.26	976.9	70	2.68	920
130	10	127.2	8.28	977.2	70	2.66	919.8

Figure 2.15 clearly shows that as the water temperature increases, the pressure in the supply line (feed pipe) rises slightly, while in the return line it decreases. The piezometric head behaves similarly. This

natural behavior is associated with a change in the density of water with increasing temperature (as the temperature increases, the density decreases, the hydraulic resistance changes somewhat, and the pressure and head differences are adjusted).

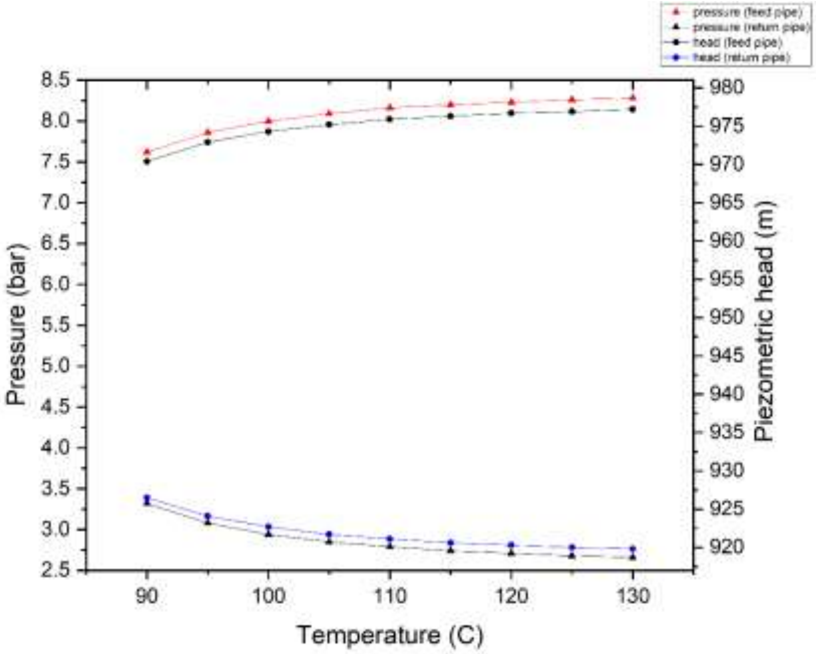

Figure 2.15. Change in pressure in nodes and piezometric head with varying water temperature

Calculation of emergency mode

To simulate an emergency mode, the pipeline section 26-7 – CHS (central heating substation) – was closed, and commissioning calculations were performed before and after the section was closed. The results of changes in heat carrier flow rates in the supply pipeline are shown in Figure 2.16, and the change in piezometric head is shown in Figure 2.17.

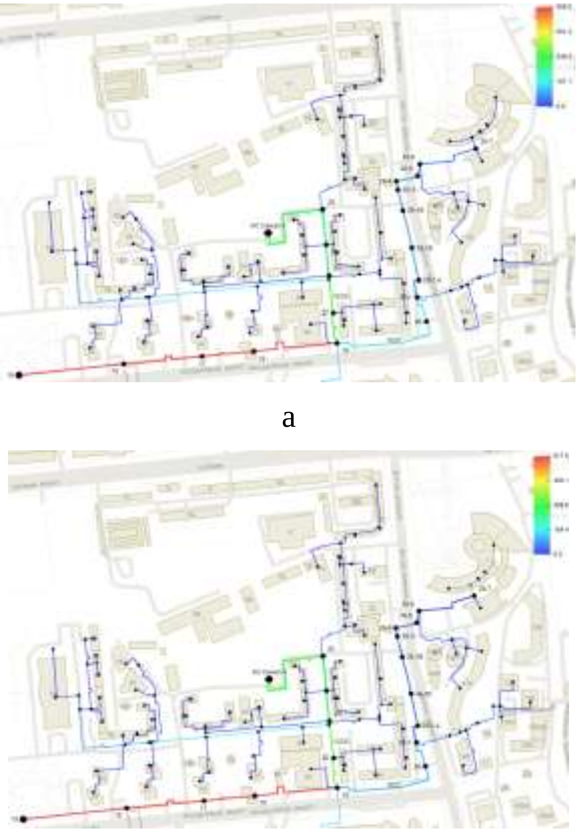

a

b

Figure 2.16. Calculation of water flow in the supply pipeline:

a – before the accident, b – after the accident

After the emergency, the heat carrier flow in the section sharply decreased from 63.81 t/h to 12.76 t/h (Figure 2.16), corresponding to a reduction of approximately 80% and indicating a significant limitation of heat carrier supply to the consumers connected to this section (see Table 8). The pressure after the emergency in node 26-6 increased slightly (from 8.21 bar to 8.25 bar), while in node 26-7 it rose from 8.18 bar to 8.32 bar. The piezometric head also increased after the emergency (from 976.1–977.1 m to 977.5 m), as clearly seen in the piezometric diagrams (Figure 2.16), reflecting the redistribution of hydraulic parameters and the reduction of load in the section (see Table 8).

Specific hydraulic losses decreased from 110.34 mm/m to 4.41 mm/m, indicating a significant reduction in flow velocity and an almost complete elimination of hydraulic resistance in the closed section (see Table 8).

Table 8. Calculation results for the section Node 26-6 – Node 26-7

No.	Node	Water flow, t/h	Water temperature, °C	Pipe pressure, bar	Piezometric head, m	Specific hydraulic losses, mm/m
Before the emergency						
1	26-6	63.81	109.0	8.21	977.1	110.34
2	26-7		108.9	8.18	976.1	110.34
After the emergency						
1	26-6	12.76	108.2	8.25	977.5	4.41
2	26-7		107.4	8.32	977.5	4.41

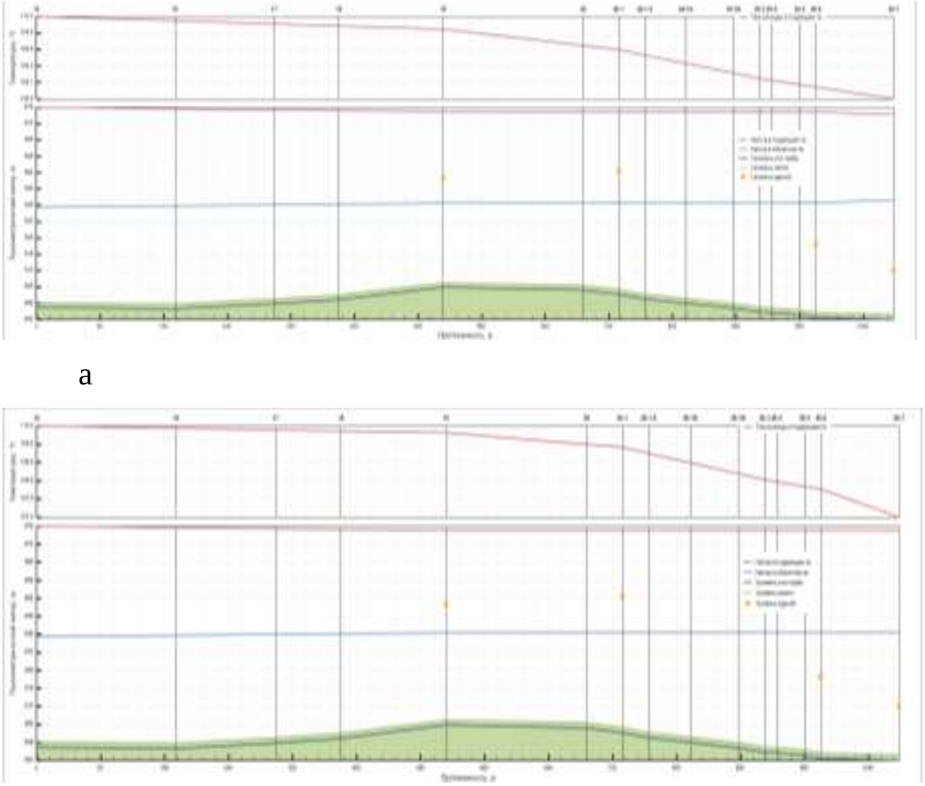

a

b

Figure 2.17. Piezometric diagrams: (a) before the emergency, (b) after the emergency

The network demonstrated significant sensitivity to the closure of this section, manifested by a sharp decrease in flow and substantial redistribution of flows. The heat carrier temperature changed very little (from 109 to 108.2°C), indicating that the temperature regime was practically unaffected by the emergency in the short term (see Table 8).

Recommendations based on the results of the emergency calculation:

1. It is necessary to provide for the possibility of flow redistribution through alternative routes (e.g., by creating additional bypasses or loop connections) to minimize the negative consequences of emergencies.

2. It is recommended to promptly switch flows and open additional valves or gate valves if an accident has already occurred in order to partially restore heat carrier circulation.

3. Install automated monitoring systems capable of quickly signaling sharp changes in network parameters (pressure and flow) to minimize the impact of emergency situations.

CHAPTER 3

DEVELOPMENT OF THE USER INTERFACE OF THE SOFTWARE PRODUCT

.

Uzak Zhapbasbayev
Timur Bekibayev
Gaukhar Ramazanova

3.1 Creation of interface objects (windows, panels, tables, charts, maps) for input and output of information

The user interface of the SP was developed using Microsoft .NET technology in C#.

The window user interface was divided into four areas (Figure 3.1):

1) Standard menu bar: a narrow horizontal strip at the top of the window containing various menu commands;

2) Standard toolbar: a narrow horizontal strip below the menu bar, containing various auxiliary buttons;

3) Status bar: a narrow strip at the bottom of the window displaying various information about the application status;

4) Main workspace: occupying the remaining area between the toolbar and the status bar.

The main workspace of the SP was implemented in a tile-based structure. Only five types of tile elements are used:

1) Object tree (top-left element in Figure 3.1). This element contains a list of objects that can have hierarchical relationships. The object tree has a white background, and tree objects themselves can have specific icons. Examples of such elements include lists of network operation modes, types of pumps and rotors, etc.

2) Modes table (middle-left element in Figure 3.1). This element contains a list of objects, each with multiple fields. The table generally has a white background. Some rows may be highlighted in specific colors. Examples include tables of heat loads for thermal chambers and central heat points, tables of simulation results for the heating system, tariff tables, etc.

3) Parameters panel (right element in Figure 3.1). This element contains a single object with multiple parameters. The panel itself has a gray background. Fields whose values can be modified have a white background; otherwise, they have a gray background. Examples of such elements include: the CHP parameter panel, the operating mode initial parameter panel, and the pump station parameter panel.

4) Console panel (bottom-left element in Figure 3.1). This element displays some intermediate information to the user. The console panel has a white background with text in different colors depending on the message importance. Examples include the modeling process console, the actual data loading console, etc.

5) Graphical element (central element in Figure 3.1). This element stores information that can be presented graphically. Examples include various functional dependency graphs, HN maps, pump operation diagrams in the pump station or CHP, etc.

The aspect ratio of tile-based structure elements were implemented with the ability to be adjusted using vertical and horizontal splitters. When the size of a graphical element changes, its graphical content is automatically scaled and redrawn to fit the new size. When the size of other tile objects changes, vertical and/or horizontal scroll bars may appear if the content does not fit within the element. The size ratios of tile elements also adapt to different window sizes and screen resolutions.

Thus, the SP has a scalable interface. In addition, the interface can be customized by the user.

The results of thermo-hydraulic calculations are displayed in a separate window (see Figure 3.2). This allows users to compare different results and, when multiple monitors are available, to move some windows to separate displays, making the SP interface more informative. If there are multiple simulation result states or multiple solution options, the results are displayed in the results window as separate tabs. Each tab contains the name of the state or option.

The number of buttons in the main workspace has been minimized. Action buttons are located on the toolbar and are displayed as icons and/or labels. The main workspace is intended for input, output, and editing of information. Only three types of buttons are allowed in the main workspace for editing information:

1) Pencil icon button: allows the user to start editing information, switching from read mode to edit mode;

2) Floppy disk icon button: allows the user to save information and return to read mode;

3) Undo arrow icon button: allows the user to cancel the completed editing and return to read mode.

Various data display actions in the main workspace can also be implemented through context menus.

The user can change the units of measurement for the following quantities using the settings depending on their preferences:

- Pressure: bar, kgf/cm^2, MPa, m water column;
- Heat carrier flow: t/h, t/2h, thousand t/day, million t/year, m^3/h;
- Heat consumption: kcal/h, MW;
- Length, location: km, m.

When abbreviating the names of various buttons, input/output fields, and columns, these elements have tooltips with more detailed descriptions.

When working with HN parameters or viewing calculation results, the user interface displays a map of the HN (see Figure 3.3). This map shows the connection structure of the network nodes. Pipeline sections between nodes can be displayed as straight or broken lines. Each type of node (CHP, pump station, CHS, branching points, and pipeline parameter change points) has a characteristic symbol (e.g., CHS may be displayed as squares). Also, for the convenience of spatial perception of HN objects in relation to city districts, the SP user can add various city streets to the HN map in the form of straight or broken lines.

The following capabilities have been implemented for the SP user when working with the HN map:

1) Zoom in/out on the map or move the view sideways or up/down on the HN map. Moreover, when the map is displayed at close range, their names should be displayed above the nodes of the HN;

2) Create new HN connection structures or edit existing structures stored in the SP DB;

3) Select HN objects (nodes or pipeline sections) to view their parameters;

4) Open/close pipeline sections for calculations;

5) View the colored map of the HN by the supply zones of the CHP after each closing/opening of pipe sections;

6) View a colored map of the HN relative to the selected output calculation value at nodes and pipes (pressure, available head, temperature, or heat carrier flow rate, etc.). Coloring is performed using a transitional palette [blue - light blue - green - yellow - orange - red]. Blue corresponds to the minimum value, red to the maximum, and transitional colors from blue to red represent intermediate values. Figure 3.4 shows an example of the implemented SP interface, displaying a colored map based on the calculated actual heat load.

7) View a colored map of the HN for the failure rate of HN facilities based on user-selected criteria (insufficient available head, exceeding the maximum permissible pressure in the pipe, etc.). HN facilities that do not have an emergency value are colored green; otherwise, the facility should be colored red;

8) Select start and end nodes of the HN to build piezometric diagrams along the selected pipeline route;

9) Select main thermal chambers or consumer nodes (IHS, CHS) to view or edit the heat load parameters of physical or legal entities. Figure 3.5 shows an example of the implemented SP interface, which displays a map with HN nodes and the parameters of consumers corresponding to them.

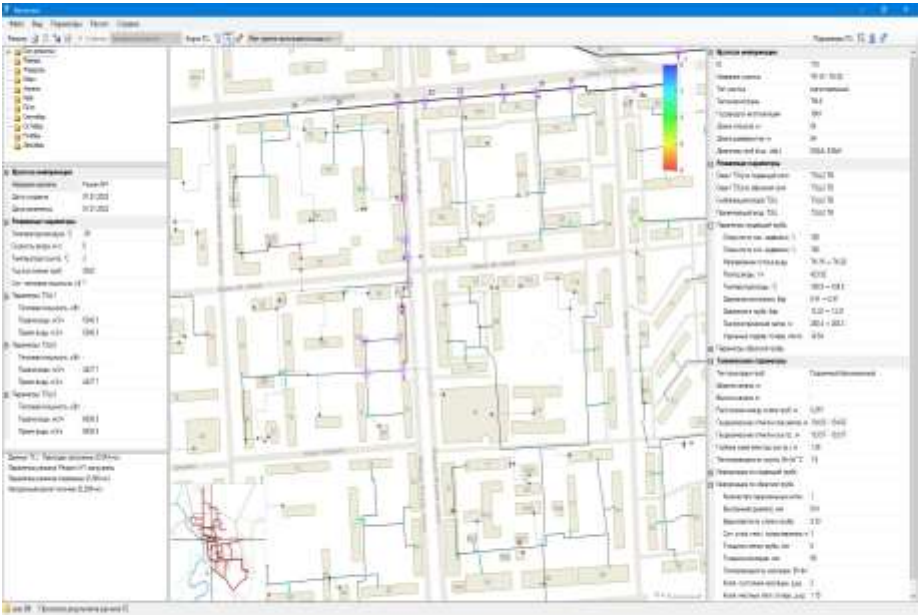

Figure 3.1. Panels of the main window of the SP

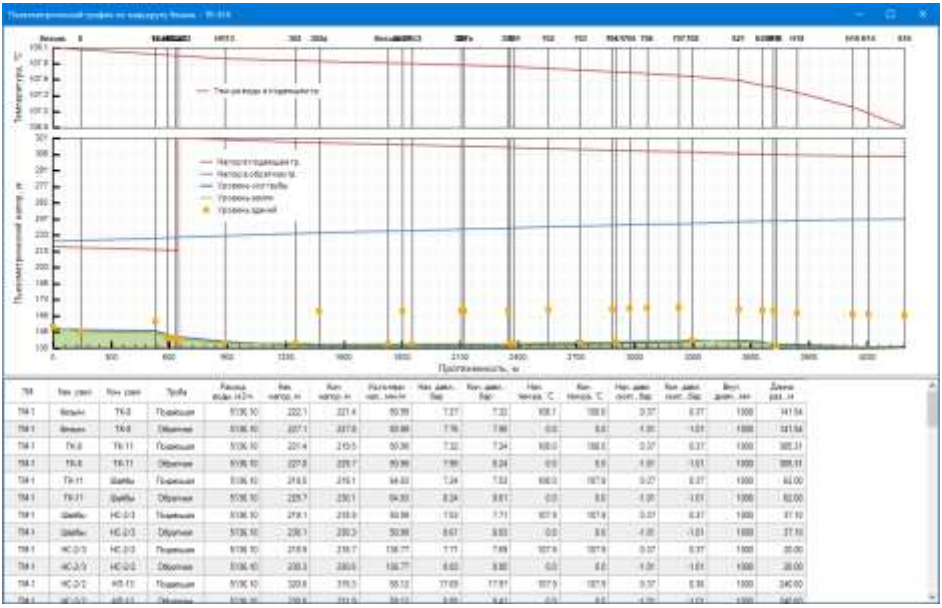

Figure 3.2. Window of results of thermohydraulic calculations

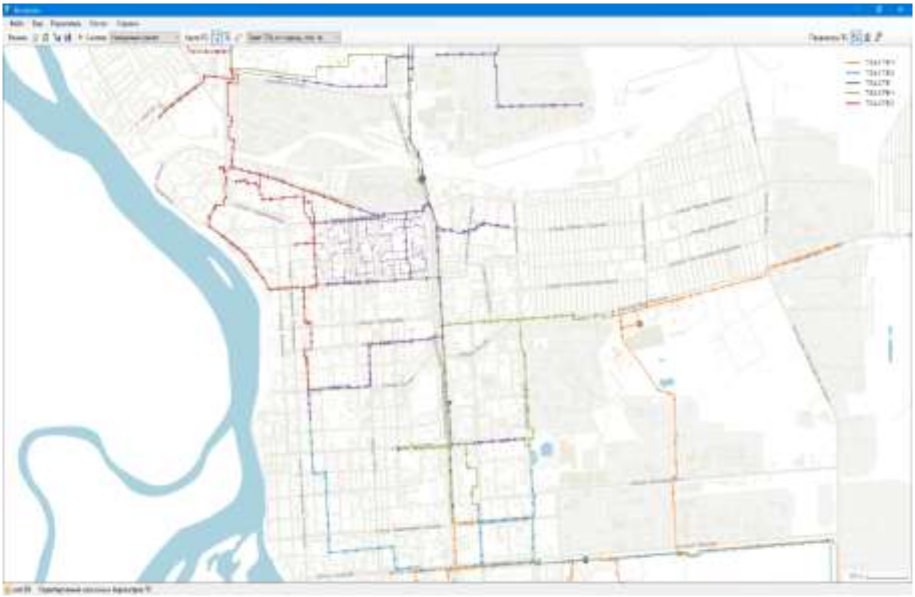

Figure 3.3. Map of heating networks

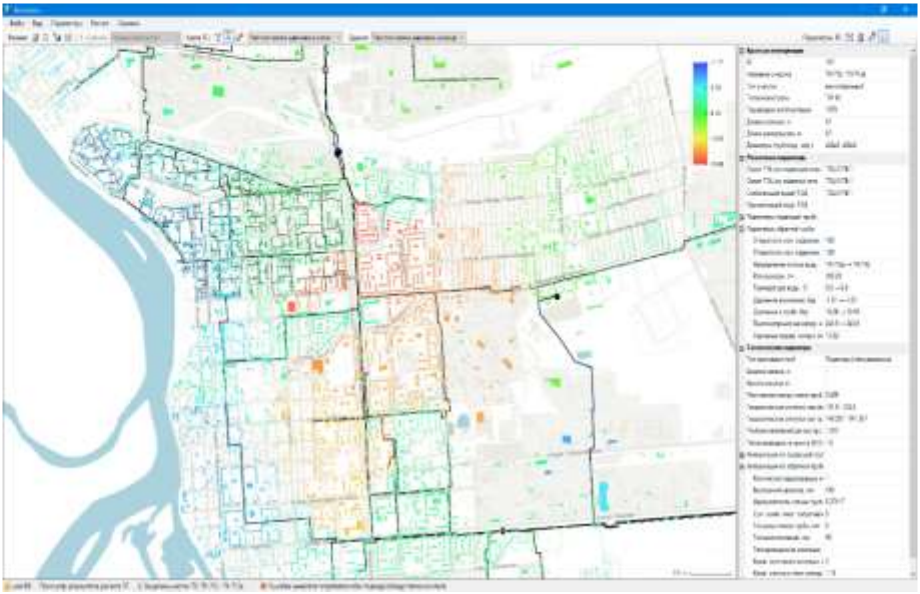

Figure 3.4. Colored map of the calculated heat load of buildings

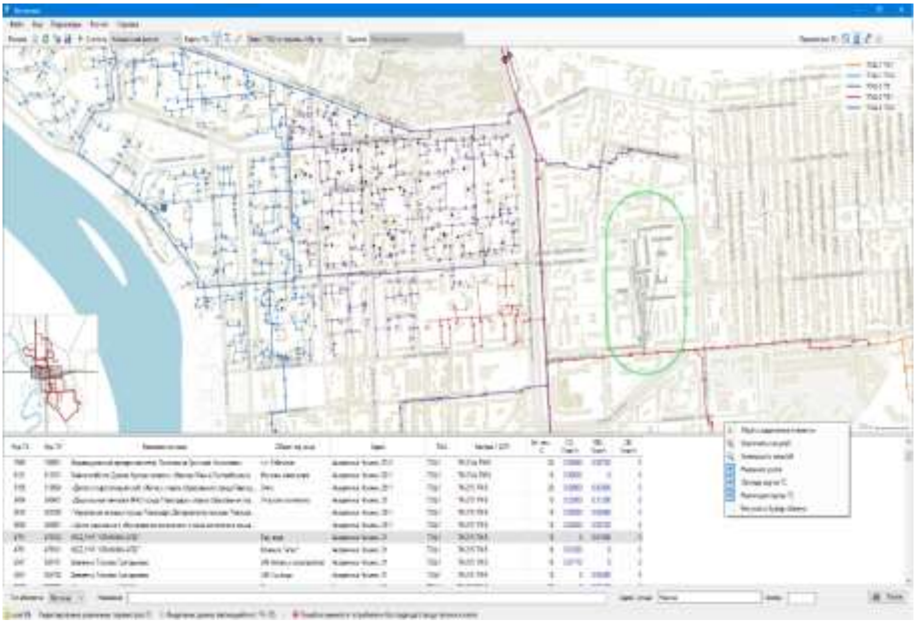

Figure 3.5. Viewing information on consumers connected to the selected heating chambers

Modifications to interface objects were made based on comments and recommendations from software users.

A "Flow velocity, m/s" column was added to the piezometric graph table to display the flow velocity values of the heat carrier in the supply and return pipes of the constructed pipeline section. Also, in the drop-down list in the tools of the upper panel, the possibility of coloring the HN according to the flow velocity values in pipe sections based on the calculation results was added (see Fig. 3.6).

Figure 3.6. Coloring of sections of HN pipes according to the flow velocity value

The procedure for drawing the names of city objects on the map has been complicated. The display of street names on curved sections of city roads has been corrected and complicated (see Fig. 3.7).

Figure 3.7. Displaying names for curved streets

The possibility of displaying the intersection of names for intersecting streets was eliminated by searching for the necessary position of street names on the road grid (see Figure 3.8). The search for the optimal position of street names was implemented based on the algorithm for finding the maximum matching in graphs. The algorithm for finding the position of the inscription of names and numbers for buildings of complex geometric shape has been complicated (see Fig. 3.9) according to the following criteria: the inscription is located in the widest part of the building, as close as possible to the center of mass of the building and without going beyond the boundaries of the building (if the size of the building's shape allows it).

Figure 3.8. Automatic placement of street names without intersections

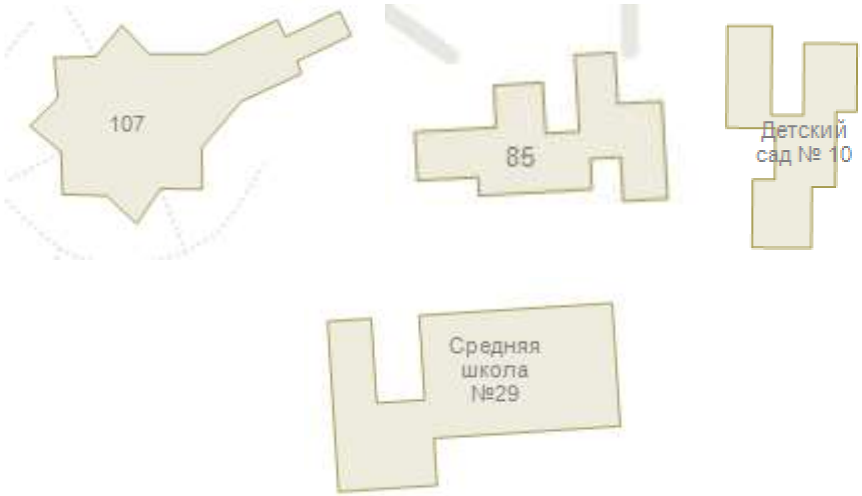

Figure 3.9. Displaying inscriptions on city buildings

As the SP was used on some users' computers, it became clear that the constant rendering of city objects when zooming on the HN map or when moving the view relative to the city area requires significant computing resources. Such rendering operations cause a noticeable delay in the response of the SP interface when working with the HN card. In this regard, work has been carried out to optimize the rendering process of city objects. For these purposes, it was decided to draw the display of the city for 9 scales, in which 10 pixels of the screen make up the real length. 800, 400, 200, 100, 50, 25, 12, 6 and 3 m. For each scale, the entire map of the city's features was drawn in advance (at the time of importing the city's data). Moreover, city objects are depicted differently for each scale (see paragraph 4.1 of the monograph). Each of the 9 huge images of the city maps was divided into separate tiles (square image fragments) measuring 3000 x 3000 pixels. The tile size was selected so that the length/width of the user's standard monitor did not exceed the tile size. Each tile has its own upper-left corner coordinate and size in the coordinate plane of the city. Now the process of dynamically drawing the city map has been reduced to drawing one or another part of the tile, depending on the location of the center point of the screen in the coordinate plane of the city. Using ready-made tiles to draw a city map has significantly reduced the load on the CPU, since there is no need to re-run the resource-intensive functions of drawing lines and geometric shapes, along with algorithms for correctly displaying house and street names.

Figure 3.10 shows the implemented principle of loading/unloading tiles into the user's computer's random access memory (RAM). The empty cells represent the tile coverage areas on the city map, the red rectangle represents the area of the city map displayed on the user's screen, the black dot represents the screen center position on the city map, and the blue cells represent the areas of the city map for which tiles have already been loaded into RAM. It is the portions of these tiles loaded into RAM that can be used for drawing.

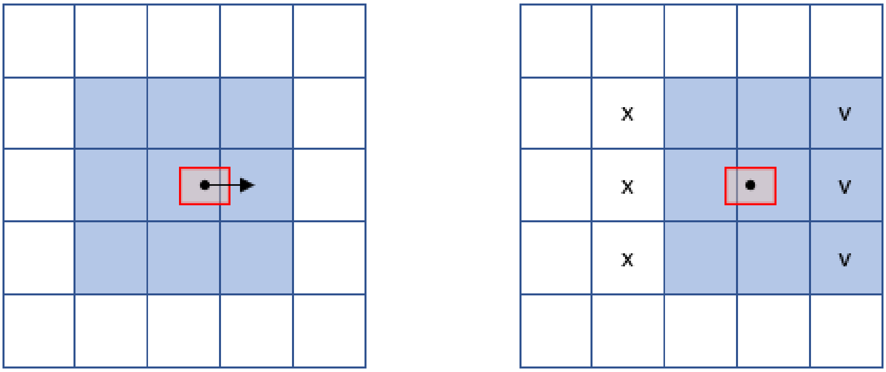

a) b)

Figure 3.10. Tiles of the city map in RAM and the position of the user's screen: a) before moving the screen; b) after moving the screen

A tile is stored in the computer's RAM, in the area of which the center of the screen is located, and its neighboring tiles (see Figure 3.10, a) - no more than 3 x 3 = 9 tiles in total. If, when the user moves the SP across the city map, the position of the center of the screen moves to the area of the neighboring tile (which is also stored in RAM), a parallel process is started that dynamically releases one part of the tiles from RAM (indicated by "x" in Fig. 3.10, b) and loads another part of the tiles into RAM (indicated by "v" in Fig. 3.10, b). This implemented storage method and mechanism for parallel loading/unloading of tiles from RAM allows for efficient rendering of the city map without lag.

3.2 Creation of tools for constructing or editing the heating network

The SP interface provides the user with the ability to manually construct or edit the HN. The required user actions when working with the implemented tools for building or editing the HN are described below.

To begin editing the HN, click "Data" -> "Edit Heating Network Configuration" in the top menu. After this action, the SP interface will switch from the HN calculation mode to the HN editing mode, which will display the HN map, toolbars, and HN parameters differently. The operating parameters of HN objects will not be displayed; in this mode, the SP user will only have access to edit the passport parameters of the HN (pipe diameters, pipeline installation methods, HN connection types at consumer nodes, installation or removal of control valves at main nodes, etc.).

In the HN editing mode, the top toolbar (see Fig. 3.11) will display buttons with the following functionality:

- Exit the HN editing mode ("General");
- Cancel the changes made to the HN ("General");
- Save the changes made to the HN ("General");
- Display object names ("HN Map");
- Color-code HN objects by type ("HN Map");
- Color-code HN objects by degree of modification ("HN Map");
- Hide/add the city map ("HN Map");
- Add a node or point ("Editing");
- Add a HN section ("Editing");
- Draw a HN section ("Editing");
- Cancel the creation of the previous HN object ("Editing");
- Restore a canceled HN object ("Editing").

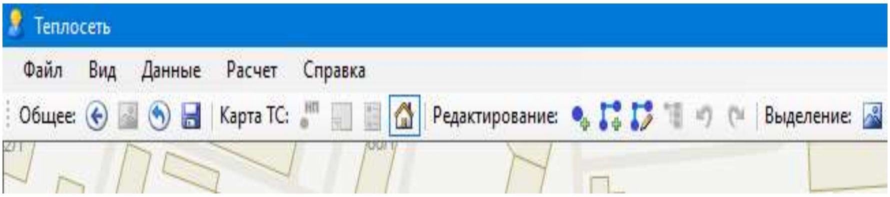

Figure 3.11. Tools for building or editing the heating network

Clicking the "Add Node or Point" button opens the auxiliary window shown in Fig. 3.12. Select "Heating network node" or "Pipeline turning point" as the object type. In the first case, the created object will be stored in the SP DB as the HN node, while in the second case, it will be stored as a point with a geographic position that can subsequently be used as an intermediate point in the geometry of a pipe section object. If the object type "Heating network node" is selected, the user must specify the node type (source, pump station, thermal chamber, branching node, pipe change node, central heat substation, consumer) and define its location on the city map. To specify the location of a point object, the user must select the coordinate type: geographic coordinates or one of the created local coordinate systems (described in more detail in Section 4.2 of the monograph). The corresponding coordinates can then be entered manually or selected by clicking on the HN map, in which case the coordinate fields are filled automatically. The specified location is displayed on the map as a black point. When the "OK" button is clicked, the entered point object of the HN is created and the object is drawn on the map of the HN. The user can edit the various passport parameters of the created node in the object parameters panel of the HN.

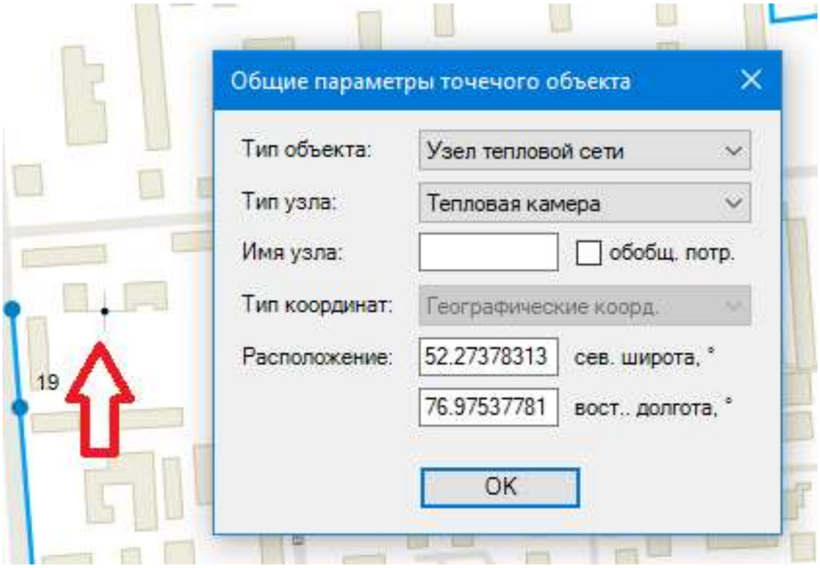

Общие параметры точечого объекта

Тип объекта: Узел тепловой сети

Тип узла: Тепловая камера

Имя узла: ☐ обобщ. потр.

Тип координат: Географические коорд.

Расположение: 52.27378313 сев. широта, °

76.97537781 вост.. долгота, °

Figure 3.12. Window for adding a point object of the heating network

When the "Add heating network section" button is clicked, the user creates a pipe section by selecting the start node, intermediate pipe turning points (optional), and then the end node. The used HN components and the pipe turning points must be created in advance. When clicking the "Draw heating network section" button, the user creates a sequence of points of the pipe section by clicking on the HN map, i.e. thereby the user draws the pipe section on the map while simultaneously creating its initial and final node. The user can edit various passport parameters of the created pipe section in the parameters panel of the HN object.

Pipeline sections of the HN can be created or edited by selecting a node on an existing part of the HN and opening the context menu with the right mouse button (see Figure 3.13). From this menu, the user can choose the commands "Connect to another node" or "Draw a branch". These operations also create a section of pipe in which the user-selected HN node will be the initial node (see Fig. 3.14). Also, using the context menu shown in Figure 3.13, for any selected node, the user can change its object type/location and delete the node. When a node is removed, its adjacent pipe sections are automatically removed.

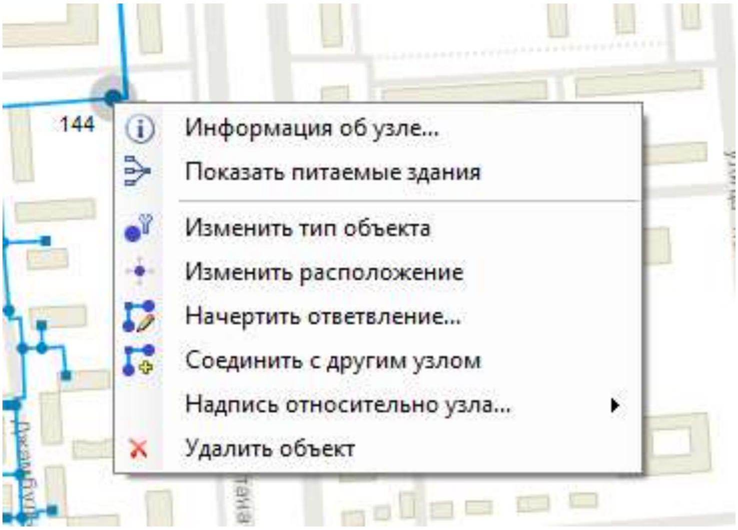

Figure 3.13. Context menu for editing the selected heating network node

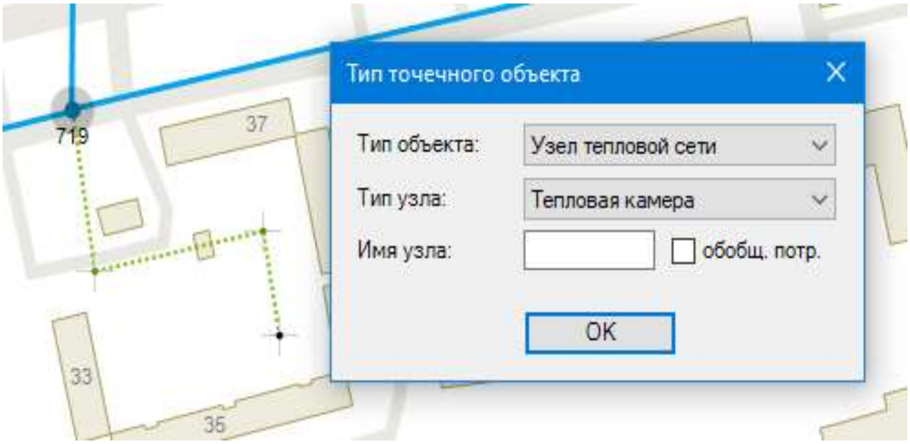

Тип объекта: Узел тепловой сети

Тип узла: Тепловая камера

Имя узла:

☐ обобщ. потр.

Figure 3.14. Construction of the heating network section using the "Draw branch" command

In the editing mode, the HN elements are color-coded as follows: newly created sections are displayed with a green dashed line; created but not yet saved pipeline sections and nodes are shown with a solid green line; network elements saved in the DB whose passport parameters have been modified are shown with a solid red line; and network elements saved in the DB whose parameters have not been changed are shown with a solid blue line. This display was made for the purpose of greater control over changes made to large HNs (see Fig. 3.15).

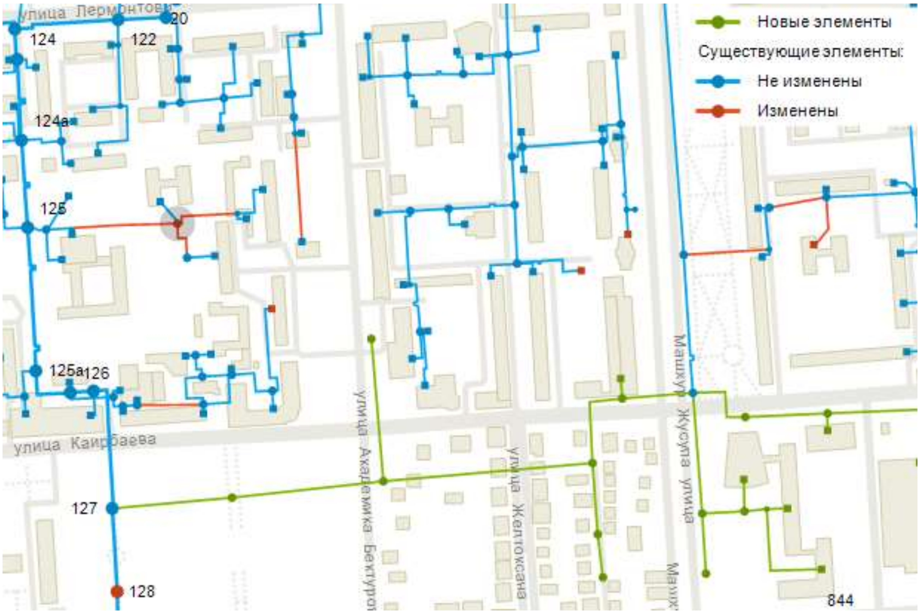

Figure 3.15. Coloring of created and existing heating network elements in edit mode

When the "Cancel heating network changes" button (↶) on the top toolbar is pressed, all newly created network elements are removed, and modified elements revert to their original parameters (their color changes back to blue). When the "Save HN changes" button (💾) is pressed, the newly created HN elements with their parameters, as well as the passport parameters of modified elements, are saved to the SP DB (the color of all elements becomes blue). Now it will be possible to undo the changes made only up to the current saved state of the HN.

The passport parameters of HN elements can be edited by the user in separate objects of the SP (see Section 3.5).

When the "Exit heating network editing mode" button (←) on the top toolbar is pressed, the process of interaction between the SP user and HN parameters switches to the calculation mode. In this mode, the user can modify only the mode parameters of the HN (opening/closing valves, pump station operating parameters, outlet temperature of the CHP, changes in consumer heat loads, etc.) and perform calculations for various HN operating modes. After exiting the HN editing mode, the SP user will have access to permanent parameters only in viewing mode.

3.3 Development of functionality for exporting calculation results into text format (MS Word) or into a table format (MS Excel)

The SP has implemented the ability to export calculation results to a text format (MS Word) or to a tabular format (MS Excel). To implement this feature, the Microsoft.Office.Interop.Excel and Microsoft.Office.Interop.Word libraries were used in the program code. The following is a description of the functionality of exporting to MS Word and MS Excel files.

After performing a calculation in the SP, the user can open a panel displaying the parameters of the selected HN node/section (which contains a calculation results tab) or open a table of the piezometric graph for the selected HN route. Right-clicking on these interface objects displays two commands: "Export to Excel file" and "Export to Word file." Figure 3.16 shows an example of exporting a table of the piezometric graph to an Excel file.

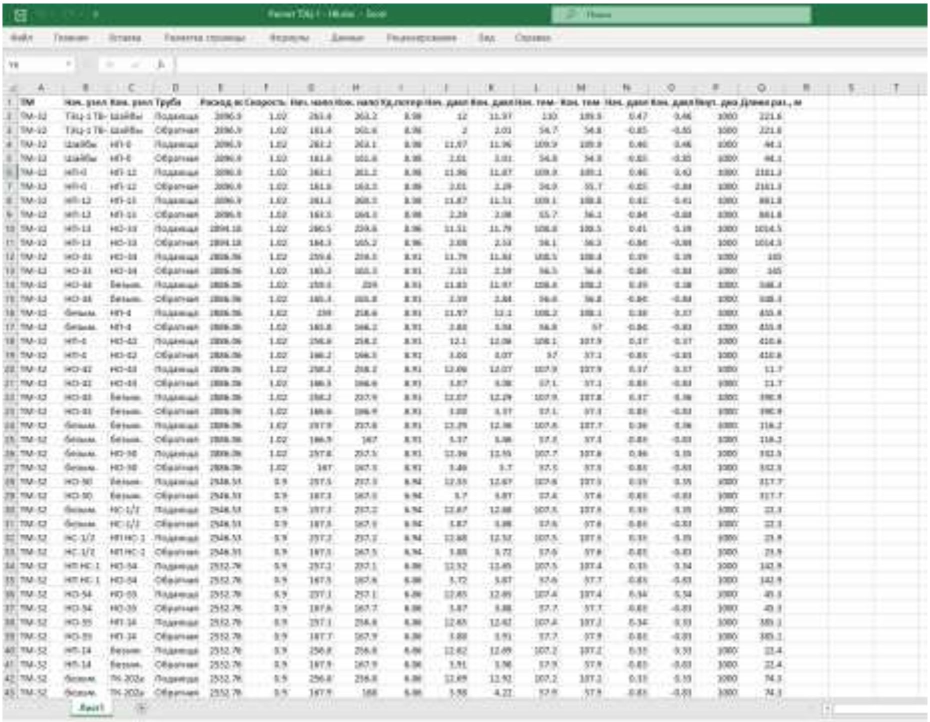

Figure 3.16. Exporting calculation results to an Excel file

Figure 3.17 shows an example of unloading the calculated parameters of a HN section into a Word file.

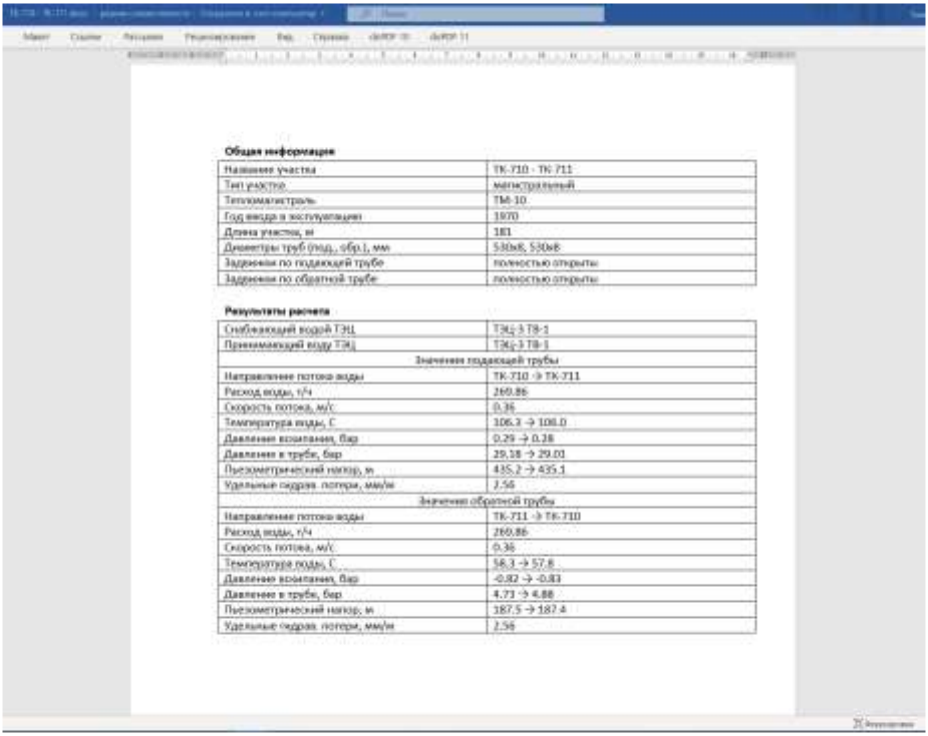

Общая информация

Название участка	ТК-710 - ТК-711
Тип участка	магистральный
Тепломагистраль	ТМ-10
Год ввода в эксплуатацию	1970
Длина участка, м	181
Диаметры труб (под., обр.), мм	530x8, 530x8
Задвижки по подающей трубе	полностью открыты
Задвижки по обратной трубе	полностью открыты

Результаты расчета

Снабжающий водой ТЭЦ	ТЭЦ-3 Т8-1
Принимающий воду ТЭЦ	ТЭЦ-3 Т8-1
Значения подающей трубы	
Направление потока воды	ТК-710 → ТК-711
Расход воды, т/ч	260.86
Скорость потока, м/с	0.36
Температура воды, С	106.3 → 106.0
Давление вскипания, бар	0.29 → 0.28
Давление в трубе, бар	29.18 → 29.01
Пьезометрический напор, м	435.2 → 435.1
Удельные гидрав. потери, мм/м	2.56
Значения обратной трубы	
Направление потока воды	ТК-711 → ТК-710
Расход воды, т/ч	260.86
Скорость потока, м/с	0.36
Температура воды, С	58.3 → 57.8
Давление вскипания, бар	-0.82 → -0.83
Давление в трубе, бар	4.73 → 4.88
Пьезометрический напор, м	187.5 → 187.4
Удельные гидрав. потери, мм/м	2.56

Figure 3.17. Exporting calculation results to a Word file

3.4. Creation of functionality for importing elements of the heating network

The SP has implemented functionality for importing elements of the HN from a separate file. The implemented import functionality includes the possibility of the following file downloads:

– "Uploading an AutoCAD file". This option allows the user to upload objects from two-dimensional drawings of the HN, including the geometry of the objects, their annotations, and text. The uploaded file must have the .dwg extension. To date, it is in DWG files that a large number of schemes for laying HNs in cities of Kazakhstan are stored.

– "Uploading the HeatingSystem file". This option allows the user to upload HN elements that were previously created in the SP and exported for storage in a separate file. These HeatingSystems files have the xml extension.

The functionality for importing elements of the HN is available in the HN editing mode. The listed commands are called from the menu on the top panel: "Data" → "Import heating network elements" → ... (see Fig. 3.18). When clicking the above import commands, the SP user must select the appropriate download file in the standard dialog box. If the "Import AutoCAD file" command was selected, the SP user must specify the coordinate system (see Figure 3.19), which is used for the geometric objects of the file, in addition to the downloaded file. The coordinate system is selected in a separate dialog box (for more information, see paragraph 4.2 of the monograph). Next, the HN elements will be loaded and displayed on the HN map. If the "Import AutoCAD file" command was selected, then all the uploaded nodes will have the "Thermal chamber" type, the passport parameters of the nodes and HN sections (except for the length values) will have default values.

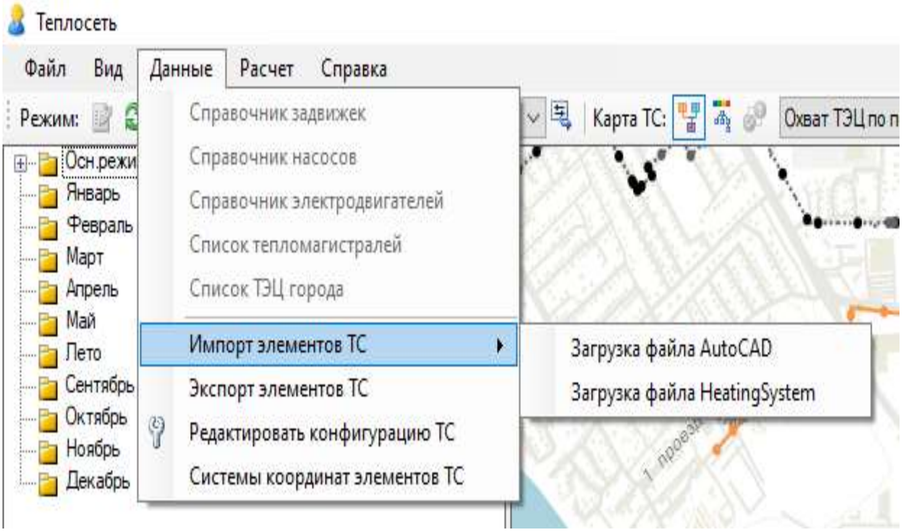

Figure 3.18. Calling import functions for heating network elements

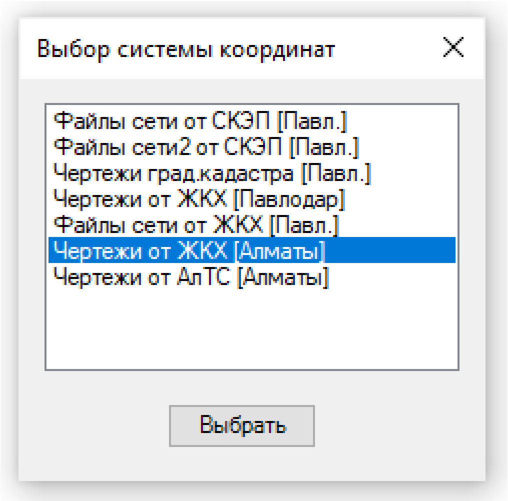

Figure 3.19. Selection of the coordinate system used in the imported file

In the future, the user can edit/supplement certain heating network elements and save them to the SP DB.

A special parser has been implemented that reads data from DWG files. The syntax of the data inside the following keywords describing the geometry of drawings was studied: *LINE*, *POLYLINE*, *LWPOLYLINE*, *ARC*, *SPLINEFIT*, *FITPOLYLINE*, *CIRCLE*, *POINT*, *INSERT*, *BLOCK*, *ENDBLK*. Based on the syntax rules of these keywords, the program code for the parser of the DWG file was written.

The functions of importing to a file and exporting HN elements from a file were implemented by serializing objects of classes and structures that relate to HN elements in the SP code. Class and structure objects are serialized using the standard *System.Xml.Serialization.XmlSerializer* class, which serializes program code objects into XML format.

3.5 Creation of a module for certification of heat supply system facilities

The SP implements a module for certification of heat supply system facilities: sections of main and distribution networks, HN nodes (CHP, heating points, CHS, etc.), heated buildings (apartment buildings, administrative and social buildings). The passport data of buildings includes technical information about the building, data about subscribers and their thermal loads.

Special tabs with passport data of nodes (see Figure 3.20) and HN sections (see Figure 3.21) were implemented in the property tables. An interface object was created and added for viewing and editing passport information about a user-selected city building (see Figure 3.22).

In the calculation mode, the passport data is available only for viewing. In the HN editing mode, the SP user has the opportunity to make changes there. When entering/changing the passport data of the HN objects, data validation functions were implemented. The data validation functions check the correctness of the variable type for the entered data (checking for an integer type, checking for a rational number type) and checking the correctness of the value for a specific type of measurement: for example, validation returns the error "Pressure value is too high" if the outlet pressure of the CHP is set to 900 bar. Validation of passport data also includes checking some parameters relative to others: for example, when changing the diameter of the supply/return pipe, the capacity of the new pipe sizes of the pipeline channel is automatically checked in the case of its channel laying; when the design temperature at the inlet of the HS for the consumer node changes, its correctness is automatically checked relative to the design temperatures in the supply pipe and the outlet of the HS.

The SP user has the opportunity to work with the passport data of heat supply facilities in this way: by clicking the right mouse button on the corresponding object on the HN map, select the command "Information about the building ...", "Information about the node ...", "Information about the site ...".

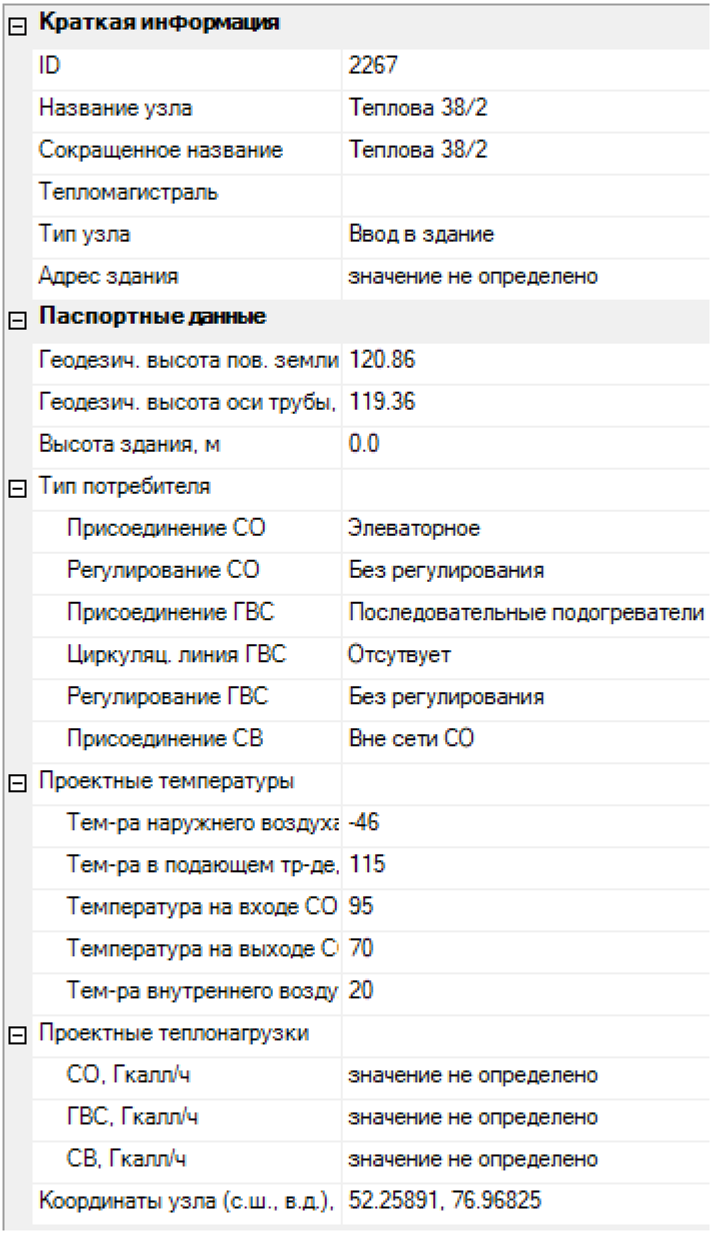

⊟ **Краткая информация**	
ID	2267
Название узла	Теплова 38/2
Сокращенное название	Теплова 38/2
Тепломагистраль	
Тип узла	Ввод в здание
Адрес здания	значение не определено
⊟ **Паспортные данные**	
Геодезич. высота пов. земли	120.86
Геодезич. высота оси трубы,	119.36
Высота здания, м	0.0
⊟ Тип потребителя	
Присоединение СО	Элеваторное
Регулирование СО	Без регулирования
Присоединение ГВС	Последовательные подогреватели
Циркуляц. линия ГВС	Отсутвует
Регулирование ГВС	Без регулирования
Присоединение СВ	Вне сети СО
⊟ Проектные температуры	
Тем-ра наружнего воздух	-46
Тем-ра в подающем тр-де,	115
Температура на входе СО	95
Температура на выходе С	70
Тем-ра внутреннего возду	20
⊟ Проектные теплонагрузки	
СО, Гкалл/ч	значение не определено
ГВС, Гкалл/ч	значение не определено
СВ, Гкалл/ч	значение не определено
Координаты узла (с.ш., в.д.),	52.25891, 76.96825

Figure 3.20. Example of displaying the passport data of a consumer node

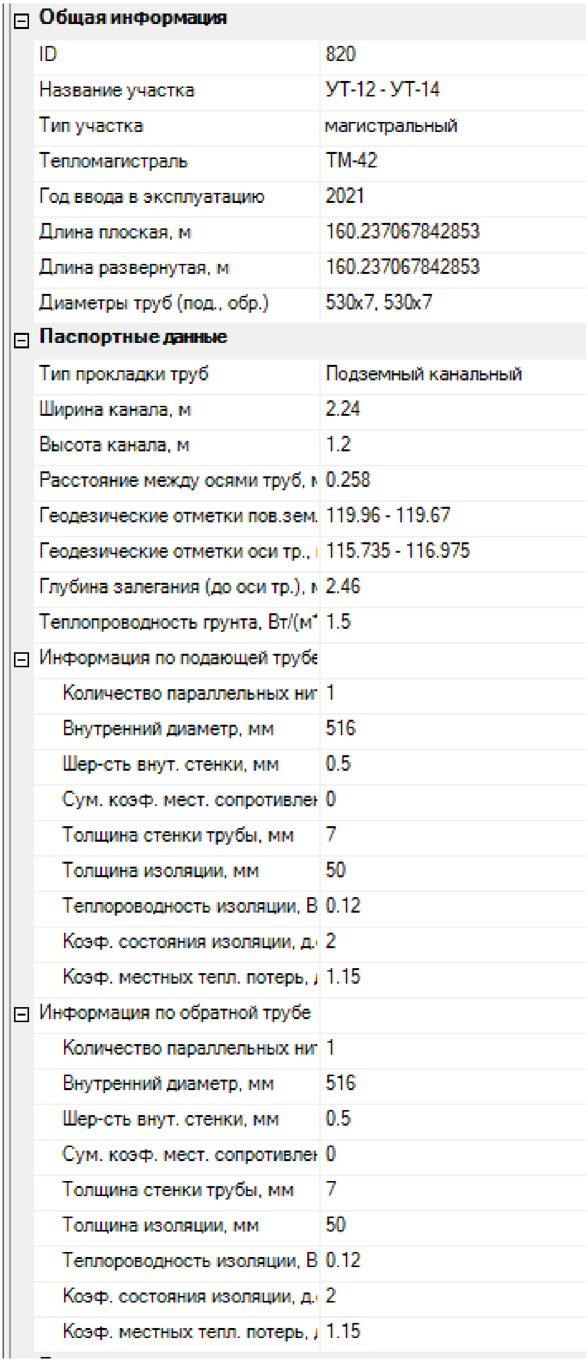

⊟ **Общая информация**	
ID	820
Название участка	УТ-12 - УТ-14
Тип участка	магистральный
Тепломагистраль	ТМ-42
Год ввода в эксплуатацию	2021
Длина плоская, м	160.237067842853
Длина развернутая, м	160.237067842853
Диаметры труб (под., обр.)	530x7, 530x7
⊟ **Паспортные данные**	
Тип прокладки труб	Подземный канальный
Ширина канала, м	2.24
Высота канала, м	1.2
Расстояние между осями труб,	0.258
Геодезические отметки пов.зем.	119.96 - 119.67
Геодезические отметки оси тр.,	115.735 - 116.975
Глубина залегания (до оси тр.),	2.46
Теплопроводность грунта, Вт/(м*	1.5
⊟ Информация по подающей трубе	
Количество параллельных ни	1
Внутренний диаметр, мм	516
Шер-сть внут. стенки, мм	0.5
Сум. коэф. мест. сопротивле	0
Толщина стенки трубы, мм	7
Толщина изоляции, мм	50
Теплороводность изоляции, В	0.12
Коэф. состояния изоляции, д	2
Коэф. местных тепл. потерь,	1.15
⊟ Информация по обратной трубе	
Количество параллельных ни	1
Внутренний диаметр, мм	516
Шер-сть внут. стенки, мм	0.5
Сум. коэф. мест. сопротивле	0
Толщина стенки трубы, мм	7
Толщина изоляции, мм	50
Теплороводность изоляции, В	0.12
Коэф. состояния изоляции, д	2
Коэф. местных тепл. потерь,	1.15

Figure 3.21. Example of displaying the passport data of the heating network pipe section

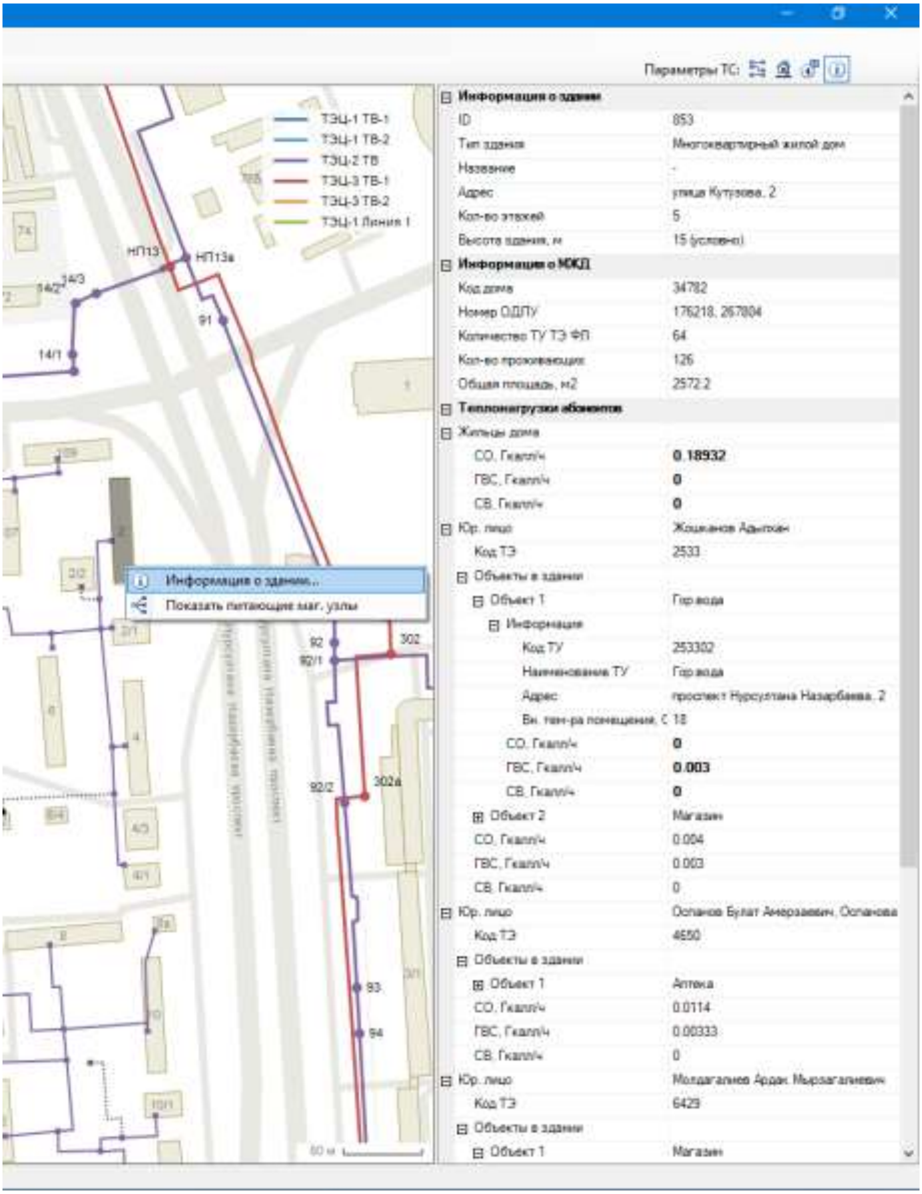

⊟ **Информация о здании**	
ID	853
Тип здания	Многоквартирный жилой дом
Название	-
Адрес	улица Кутузова, 2
Кол-во этажей	5
Высота здания, м	15 (условно)
⊟ **Информация о МКД**	
Код дома	34782
Номер ОДПУ	176218, 267804
Количество ТУ ТЭ ФП	64
Кол-во проживающих	126
Общая площадь, м2	2572.2
⊟ **Теплонагрузки абонентов**	
⊟ Жильцы дома	
СО, Гкал/ч	**0.18932**
ГВС, Гкал/ч	**0**
СВ, Гкал/ч	**0**
⊟ Юр. лицо	Жошканов Адылхан
Код ТЭ	2533
⊟ Объекты в здании	
⊟ Объект 1	Гор.вода
⊟ Информация	
Код ТУ	253302
Наименование ТУ	Гор.вода
Адрес	проспект Нурсултана Назарбаева, 2
Вн. тем-ра помещения, С	18
СО, Гкал/ч	**0**
ГВС, Гкал/ч	**0.003**
СВ, Гкал/ч	**0**
⊞ Объект 2	Магазин
СО, Гкал/ч	0.004
ГВС, Гкал/ч	0.003
СВ, Гкал/ч	0
⊟ Юр. лицо	Оспанов Булат Амерзаевич, Оспанова
Код ТЭ	4650
⊟ Объекты в здании	
⊞ Объект 1	Аптека
СО, Гкал/ч	0.0114
ГВС, Гкал/ч	0.00333
СВ, Гкал/ч	0
⊟ Юр. лицо	Молдагалиев Ардак Мырзагалиевич
Код ТЭ	6429
⊟ Объекты в здании	
⊟ Объект 1	Магазин

Figure 3.22. Example of displaying a city building passport

CHAPTER 4

DEVELOPMENT OF A GIS SYSTEM FOR A DIGITAL TWIN OF THE URBAN HEATING NETWORK

.

Uzak Zhapbasbayev

Timur Bekibayev

Gaukhar Ramazanova

4.1. Creating a tool for importing city object data (information and locations of buildings, streets, districts, water and forest objects) from web mapping services

The SP implemented the functionality of importing city object data from the OpenStreetMap web mapping service. The specified service contains city data obtained from personal GPS trackers, aerial photographs, videos, satellite images and street panoramas provided by various companies.

Reading city data

In order to use the OpenStreetMap data, the user needs to create a special osm file on the cartographic web service by selecting the territory of the entire city or individual districts of the city and clicking the "Export" button. The user can save multiple osm files for different cities or districts of the city. Then, to import the city object data into the SP, go to the "Data" menu and select "Import city data..." and specify the required osm file in the window that opens. After the completed actions, information on buildings, streets, districts, water and forest objects of the selected city area will be uploaded to the SP DB.

The osm file contains data in xml format (see Figure 4.1), which uses a topological data structure consisting of objects:

–*node* - a point with the specified coordinates;

–way - an ordered list of points that make up a line or polygon;

–relation - groups of points, lines, and other relationships to which certain properties are assigned;

–tag - key - value pairs, can be assigned to points, lines, and relationships.

A special parser for OpenStreetMap data script was developed. Due to the fact that, in the general case, the structure of the osm file has a nested tree topology, the program code for reading the osm file data was implemented using a recursive depth-first search algorithm.

For each geometric point of the object (node), its ID and its geographical coordinates (longitude/latitude) were read. For each list of *way* points, its type is determined by the following tags:

- building (*tag k="building"*);
- street (*tag k="highway"*);
- special zone (*tag k="landuse"* or *tag k="natural"*).

For each street or special zone object, only its identifier, geometry, and type are read. For each building object, its geometry and the following parameters are read:

- identifier *(id)*;
- building address (*tag k="addr:street"* and *tag k="addr:housenumber"*);
- destination (*tag k=“amenity”*);
- number of floors (*tag k="building:levels"*);
- height (*tag k="height"*);
- name (*tag k="name"*).

To correctly read objects with complex geometries (for example, branching streets, block houses with indoor areas), the following keywords were taken into account: *member*, *relation, inner*, *outer*, *outline*, *part*, *role*.

Figure 4.1. Example of the contents of an osm file for importing city data

Loading data into the DB

The program code was implemented using SQL queries to load the data read from the osm file into the SP DB. The osm file data is recorded in the tables described in paragraph 1.1 of the monograph.

The parameters of each imported object of buildings, streets, urban areas of the city and osm identifiers are recorded in the corresponding fields of the *Buildings, CityRoads, CityZones* tables of the SP DB. For residential imported apartment buildings in the city, separate records are also created in the *ApartmentBuildings* and *ApartmentBuildingsInModes* tables of the SP DB. The read coordinates of the points of the city objects are written to the rows of the *MapNodes* table. Based on the read order of traversal of points of city objects and using their identifiers in *MapNodes,* the necessary records are created in the *MapShapes* (for buildings and urban areas) and MapLines (for streets/roads) tables. Further, in the SP DB, the records in these tables are linked to the corresponding records in the *Buildings, CityRoads,* and *CityZones* tables.

Drawing city data

A program code was implemented to draw city objects on the HN map. The display of city elements on the map has been carefully worked out in order to conveniently perceive the objects of the HNs against the background of the city.

In order for the city objects not to contrast with the HN objects, which are colored in the color range "red - green - blue - purple", neutral colors were chosen to display the city: light shades of brown and gray.

In order to avoid visual clutter of urban objects, the SP provided for different rendering of the city map at different scales. Nine rendering scales were selected, where 10 screen pixels correspond to real-world lengths of 800, 400, 200, 100, 50, 25, 12, 6, and 3 m. The user has the option to zoom in or out of the display by using the mouse scroll wheel.

Tables 5 and 6 describe the differences in the display of common city elements at different map scales.

Table 5. Displaying common city elements at different map scales

Scale	Display of city elements		
	Streets, roads	Rails	Buildings
3 m : 10 px	All streets and their names	All rails	With boundaries and names
6 m : 10 px			
12 m : 10 px			
25 m : 10 px			With boundaries, but without names
50 m : 10 px			
100 m : 10 px	Drawing of all streets. Regular city streets without names.		Without boundaries and names
200 m : 10 px			Not displayed
400 m : 10 px	Drawing of all streets. Regular and inter-district city streets without names.	Only main rails	
800 m : 10 px	Regular city streets are not displayed. Names are only for roads that are not lower than regional significance.		

Table 6. Displaying different types of city roads at different map scales

Road type	Line thickness (px) at different scales									Line type
	53m: 10px	56m: 10px	512m: 10px	525m: 10px	550m: 10px	5100m: 10px	5200m: 10px	5400m: 10px	800m: 10px	
Interregional highways	27	21	18	10	10	6	6	4	2	Solid
Regional highways	27	21	18	10	10	5	5	4	2	
Roads of Regional Importance	27	21	18	10	9	5	5	4	1	
Interdistrict city roads	27	21	18	10	9	5	4	3	1	
Regular city streets	17	13	12	6	5	3	3	1	-	
Auxiliary streets	17	13	12	6	5	3	3	1	-	
Residential zone roads	17	13	12	6	5	3	3	1	-	
Driveways in Courtyards	11	9	7	4	2	2	-	-	-	

Pedestrian streets	17	13	12	6	5	3	3	1	-	
Unpaved roads	2	2	2	2	2	1	1	-	-	Dashed
Pedestrian sidewalks	2	2	2	2	2	1	-	-	-	Dotted
Stair roads	3	3	3	3	3	1	-	-	-	Dash
Paths	2	2	2	2	1	1	-	-	-	Dashed

Figure 4.2 shows an example of drawing the objects of the city of Pavlodar at different map scales. The font size of street and building names also depends on the scale of the map.

a) 800 m: 10 px

b) 400 m: 10 px

c) 200 m : 10 px


улица Мира
улица Торайгырова
улица Лермонтова
улица Академика Сатпаева
улица Каирбаева

d) 100 m : 10px

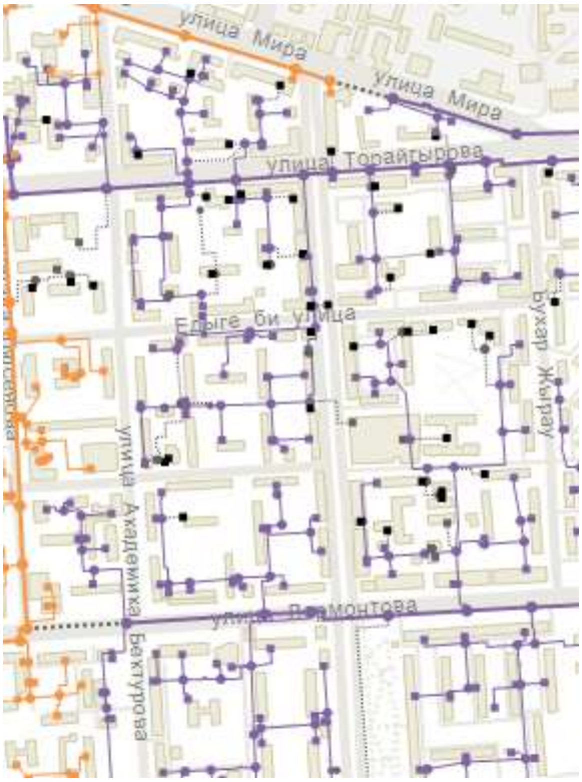
улица Мира
улица Мира
улица Торайгырова
Едыге би улица
Бухар Жырау
улица Академика Бектурова
улица Лермонтова

e) 50 m : 10 px

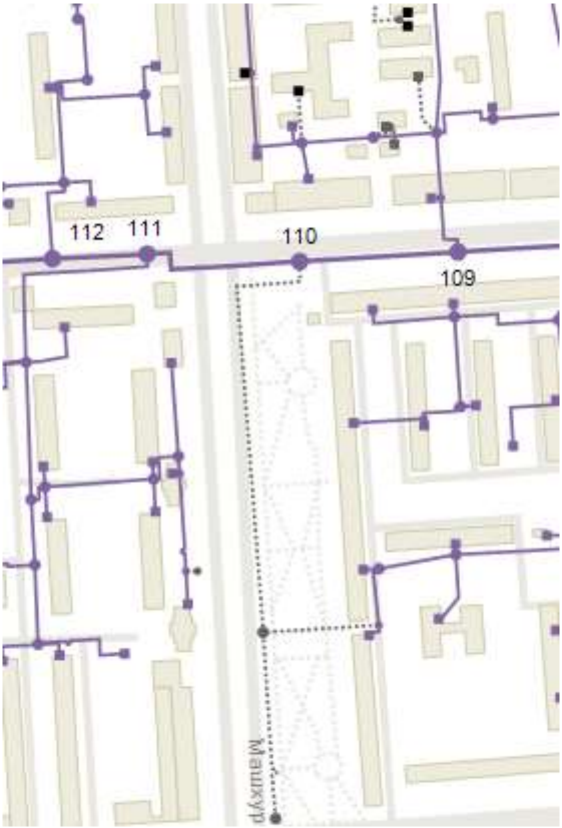

f) 25 m : 10 px

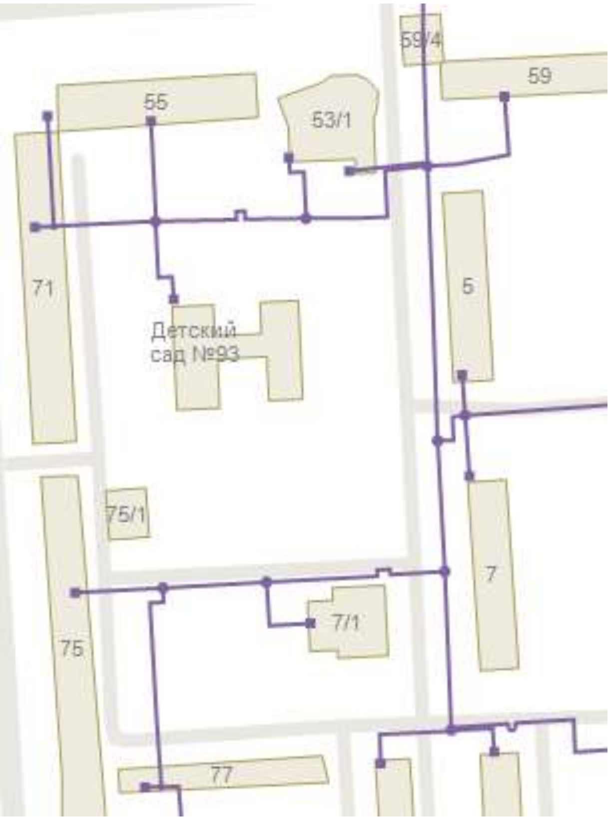

g) 12 m : 10 px

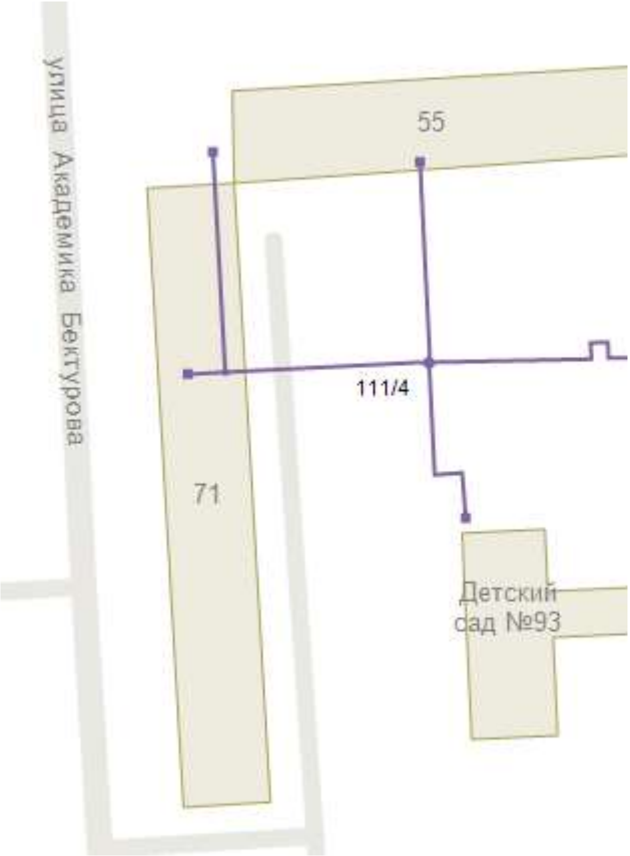

h) 6 m : 10 px

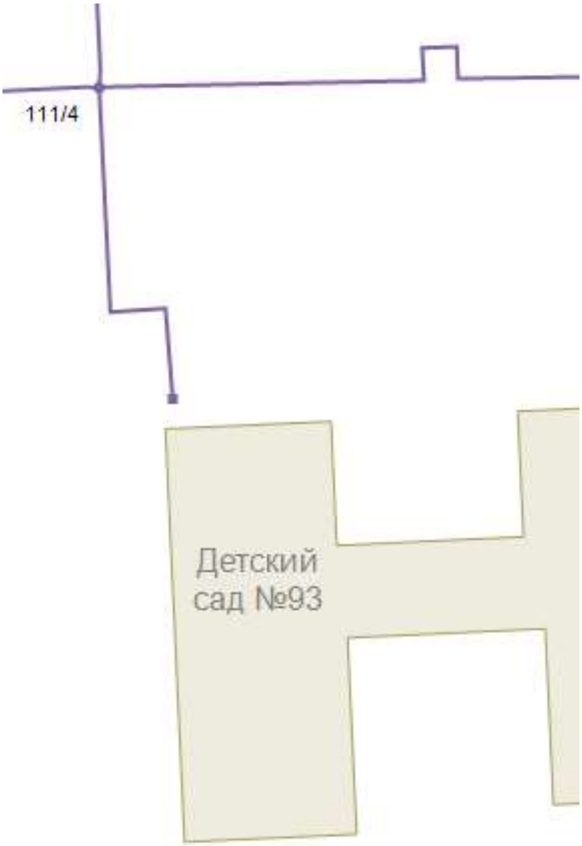

i) 3 m : 10 px

Figure 4.2. Fragments of the drawing of objects of the city of Pavlodar at different map scales

4.2 Creation of tools for linking to geographical coordinates and reorienting heating network facilities to city facilities

The SP implemented the functionality of linking to geographical coordinates and reorienting HN facilities to city facilities. Next, the mechanism for linking to geographic coordinates and the required actions of the SP user are described.

In order to tie objects to geographic coordinates, it is necessary to determine in advance the coordinate systems in which the HN facilities are located. For this purpose, an editable list of user coordinate systems was implemented. To access it, the user should select "Data" → "Coordinate systems of HN elements" from the top menu (see Figure 3.18), which opens the coordinate systems window (see Figure 4.3). In this window, the user can edit the list itself (add/delete coordinate systems) or modify a selected coordinate system. The list of coordinate systems is located on the right side of the window, while the parameters of the selected coordinate system are displayed on the left. The coordinate system parameters include the coordinates of three reference points and a brief description of files in which the HN facilities use the selected coordinate system. Each reference point with coordinates in the selected coordinate system is linked to the corresponding geographic coordinates (degrees north latitude and east longitude).

The SP function was implemented to convert the position of any point in the selected coordinate system into its geographic coordinates. This function consists of the following steps:

1. Conversion of the geographic coordinates of the reference points (latitude, longitude) into a planar metric projection.

2. Calculation of the affine transformation coefficients from the local coordinates of the selected coordinate system to the metric projection coordinates using three reference points.

3. Conversion of the geographic coordinates of the required point using the calculated affine transformation coefficients.

The conversion of geographic coordinates of reference points into a planar metric projection is performed using the Gauss–Krüger projection, which, as is well known, features small distortions of linear distances, angles, and areas: distortions usually do not exceed a few centimeters per 1 km within a single zone (3° in geographic longitude). In the CIS territory, the Gauss–Krüger projection has historically been the standard in geodesy. A large number of topographic maps, cadastral data, and engineering networks are created precisely in the Gauss–Krüger projection. Functions were implemented to convert point coordinates from geographic coordinates to the Gauss–Krüger projection and, conversely, from the Gauss–Krüger projection back to geographic coordinates.

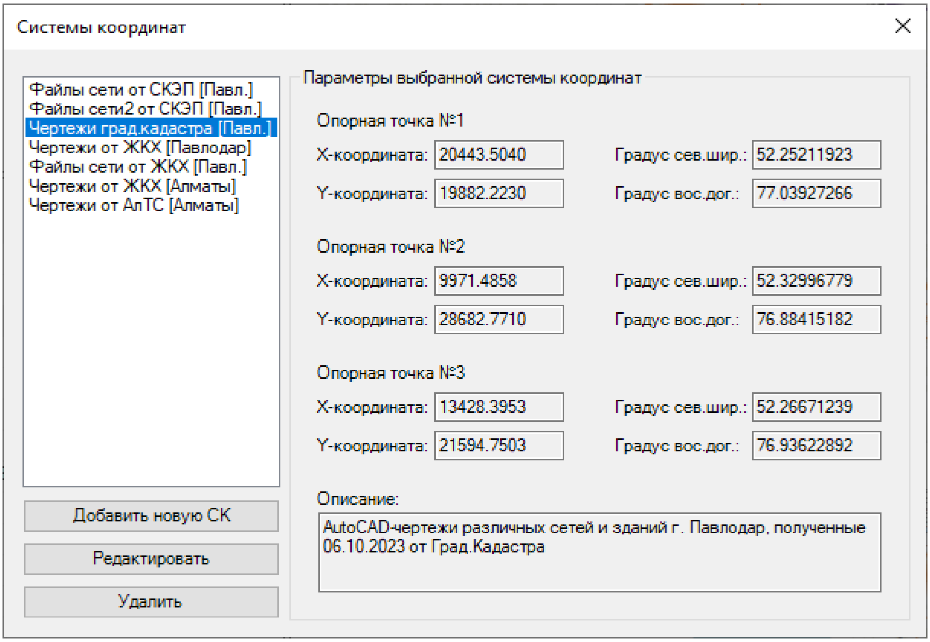

Системы координат

Файлы сети от СКЭП [Павл.]
Файлы сети2 от СКЭП [Павл.]
Чертежи град.кадастра [Павл.]
Чертежи от ЖКХ [Павлодар]
Файлы сети от ЖКХ [Павл.]
Чертежи от ЖКХ [Алматы]
Чертежи от АлТС [Алматы]

Параметры выбранной системы координат

Опорная точка №1
X-координата: 20443.5040
Y-координата: 19882.2230
Градус сев.шир.: 52.25211923
Градус вос.дог.: 77.03927266

Опорная точка №2
X-координата: 9971.4858
Y-координата: 28682.7710
Градус сев.шир.: 52.32996779
Градус вос.дог.: 76.88415182

Опорная точка №3
X-координата: 13428.3953
Y-координата: 21594.7503
Градус сев.шир.: 52.26671239
Градус вос.дог.: 76.93622892

Описание:
AutoCAD-чертежи различных сетей и зданий г. Павлодар, полученные 06.10.2023 от Град.Кадастра

Figure 4.3. Linking different coordinate systems to geographical coordinates

Let (x, y) be a point in the user-selected local coordinate system, and (X, Y) be the corresponding point in the Gauss–Krüger planar projection. The affine transformation of the point (x, y) to (X, Y) is carried out as follows:

$$a \cdot x + b \cdot y + t_x = X$$

$$c \cdot x + d \cdot y + t_y = Y$$

where a, b, c, d, t_x, t_y are the coefficients of the affine transformation, which are uniquely determined by solving the following system of linear equations:

$$\begin{cases} a \cdot x_1 + b \cdot y_1 + t_x = X_1 \\ c \cdot x_1 + d \cdot y_1 + t_y = Y_1 \\ a \cdot x_2 + b \cdot y_2 + t_x = X_2 \\ c \cdot x_2 + d \cdot y_2 + t_y = Y_2 \\ a \cdot x_3 + b \cdot y_3 + t_x = X_3 \\ c \cdot x_3 + d \cdot y_3 + t_y = Y_3 \end{cases}$$

where $x_1, y_1, x_2, y_2, x_3, y_3$ are the coordinates of three reference points in the selected coordinate system; $X_1, Y_1, X_2, Y_2, X_3, Y_3$ are the coordinates of the three reference points of the Gauss-Kruger plane projection, which are calculated using the geographical coordinates of the reference points. In fact, when the reference points of the coordinate system are entered or edited, the affine transformation coefficients are calculated once and stored in the system DB.

As described earlier, when adding a node or section of the HN with coordinates set to the user coordinate system, or when importing HN geometry from AutoCAD drawings, the user of the system specifies the used coordinate system (see Figures 3.12 and 3.19), which is stored in the system DB and automatically linked to geographical coordinates using the appropriate affine transformation coefficients and reorientation of the HN object to the city objects.

4.3 Data input of Almaty city objects into the database

Work was carried out to enter the section parameters of the HN of Almaty city, which is located in the Samal microdistrict, into the program DB. The specified section of the HN was divided into nodes (pipe branching points, pumping stations, consumer nodes) and pipeline sections connecting these nodes, which were then entered into the DB as objects of the corresponding tables. The geographical coordinates of the section objects of the HN and the objects of buildings in the specified area of the city were also entered into the DB. Figure 4.4 shows the objects of the specified section of the HN and the city buildings, which are entered into the SP DB.

The digitized sections of pipelines and HN nodes are attached to the corresponding nodes of the Nodes tables in the SP DB (see section 1). Next, objects were created in the *Segments, HeatPoints,* and *PumpStations* tables (see section 1) and were associated with the corresponding *Nodes* objects. Next, objects were created in the *Buildings* and *ApartmentBuilndings* tables (see section 1), which correspond to the city buildings. Then the objects of the city buildings were attached to the corresponding nodes of the HN. Some buildings are connected to several nodes of the HN, which can be CHS or an IHS. Moreover, some buildings are connected to 3-5 nodes of the HN.

Taking into account geographical coordinates, objects were created in the *MapPoints*, *MapLines*, and *MapShapes* tables, which are used to draw the SP map. The *MapPoints* objects were then attached to the corresponding *Nodes* objects, the *MapLines* objects to the *Segments* objects, and the *MapShapes* objects to the *Buildings* objects.

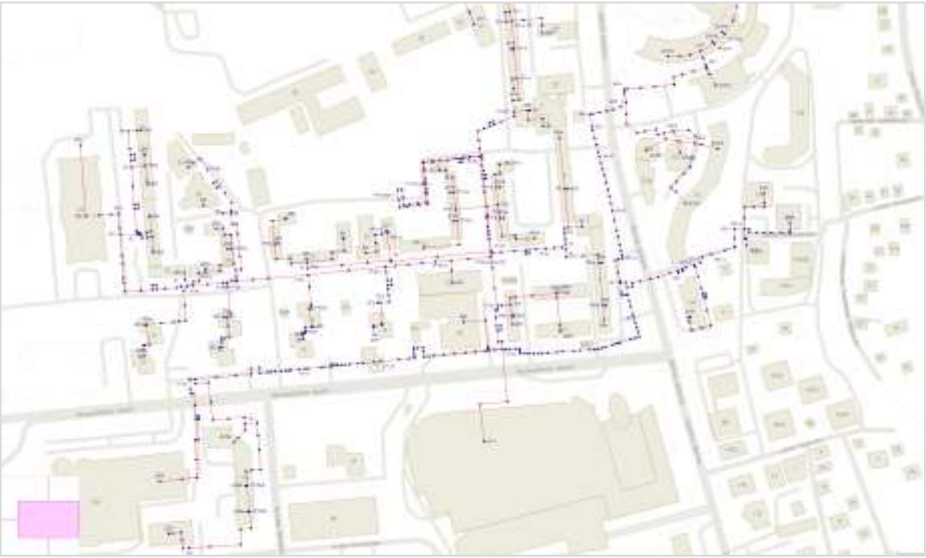

Figure 4.4. Display of a digitized section of the heating network of Almaty city on the SP map

4.4 Entering data on Pavlodar city objects into the database

The DB includes a geometric model of the routes of heating networks in Pavlodar city, covering both main and intra-block sections (Fig. 4.5). The system includes parameters of main and distribution pipelines, thermal chambers, central and individual heating points, pumping stations and other elements of the HN infrastructure of the city.

In addition, the DB contains information on 46,738 buildings of various types, including 1,275 multi-storey residential buildings, 3,073 legal entities (enterprises, institutions and organizations), 7,524 objects of legal entities, 1,132 nodes of the HN and 1,173 pipeline sections (Fig. 4.5).

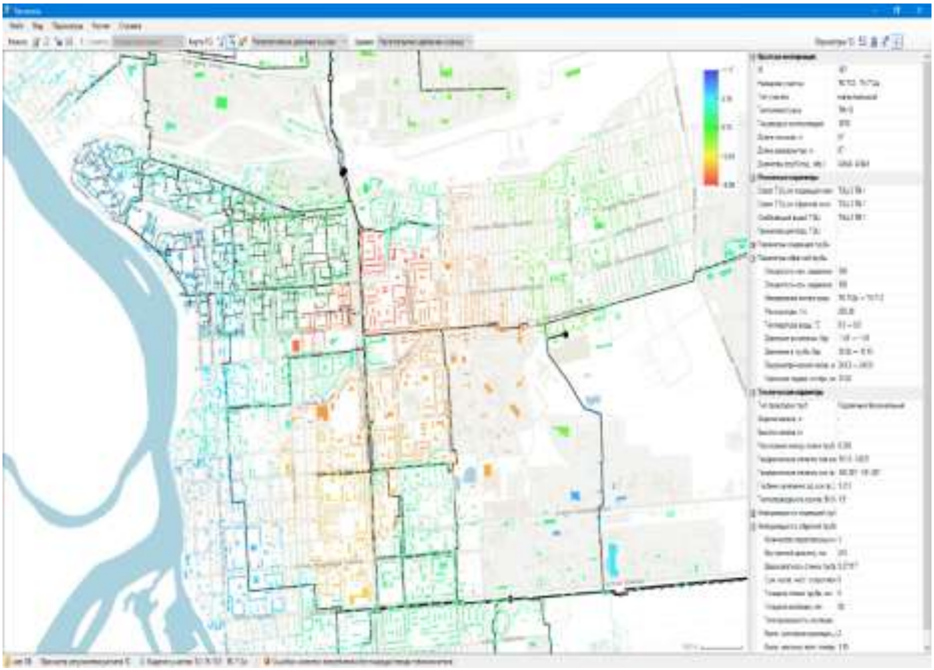

Figure 4.5. GIS system of the heating network of Pavlodar

In addition, the DB provides the possibility of parametric selection of linear sections of the HN for performing thermal and hydraulic calculations (Fig. 4.6).

As part of the calculation, the following types of data are generated:

- distribution of pressure in the network;
- distribution of heat carrier temperature;
- heat carrier flow rate in the network sections;
- pressure at the inlet and outlet of pumping stations and CHPs;
- heat carrier temperature at the inlet and outlet of the CHP;
- the amount of electricity consumed by pumping stations and CHP pumps;
- the amount of fuel burned at the CHP.

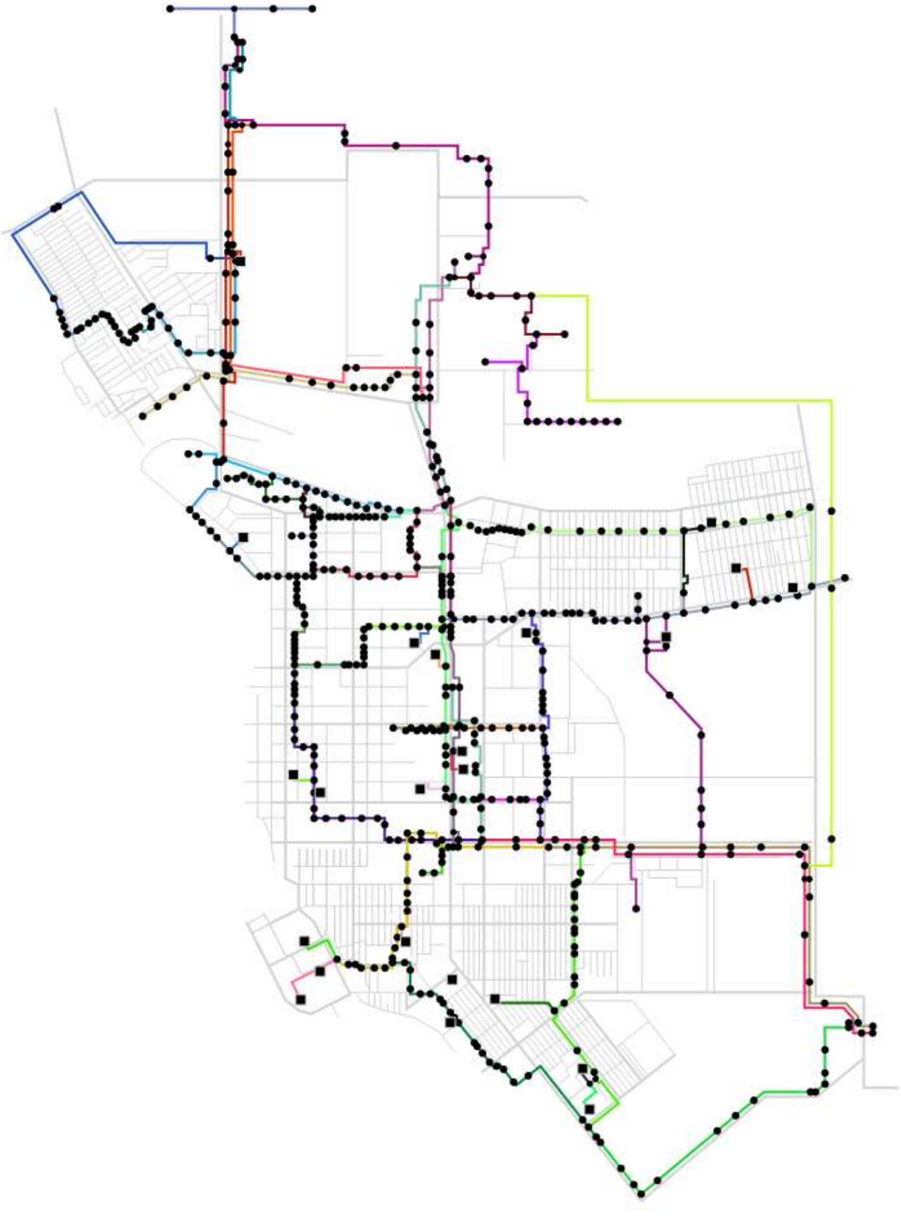

Figure 4.6. An example of a diagram of linear sections of a heating network

ACKNOWLEDGMENTS

This monograph was prepared based on the results of research work on the topic "Software development to digitalize and optimize heat supply system operation in Kazakhstan's cities" (BR24992907), funded by grants from the Science Committee of the Ministry of Science and Higher Education of the Republic of Kazakhstan for 2024–2026.

REFERENCES

1 Allegrini J., Orehounig K., Mavromatidis G., Ruesch F., Dorer V., Evins R. A review of modelling approaches and tools for the simulation of district-scale energy systems // Renewable and Sustainable Energy Reviews. 2015. Vol. 52. P. 1391-1404.

2 Vreenegoor R.C.P., Hensen J.L.M., Vries B. Review of existing energy performance calculation methods for district use // Proceedings of the Symposium Gebouwsimulatie: Ontmoeten & Ontdekken – IBPSA-NVL / EinHNoven, Netherlands (October 9, 2008). 2008. P. 1-8.

3 Crawley D.B., Hand J.W., Kummert M., Griffith B.T. Contrasting the capabilities of building energy performance simulation program // Building and Environment. 2008. Vol. 43. P. 661- 673

4 Ortiga J., Bruno J.C., Coronas A., Grossman I.E. Review of optimization models for the design of polygeneration systems in district heating and cooling networks // Computer Aided Chemical Engineering. 2007. Vol. 24. P 1121-1126

5 Ancona M.A., Branchini L., De Lorenzi A., De Pascale A., Gambarotta A., Melino F., Morini M. Application of Different Modeling Approaches to a District Heating Network // AIP Conf. Proc. 2019. Vol. 2191 (1). 020009. https://doi.org/10.1063/1.5138742

6 Gebremedhin A. Introducing District Heating in a Norwegian town – Potential for reduced Local and Global Emissions // Applied Energy. 2012. Vol. 95. P. 300-304.

7 Fan X., Sun L., Feng J. Calculation of pressure at pressurization points of heating system with multi-heat sources // Gas Heat. 2015. Vol. 35. P. 1–4.

8 Fang Z., Zhang X., Li F., Wu R. Case study on hydraulic condition of centralized heat network with multi-heat source // Dist. Heat. 2016. Vol. 2. P. 65–69.

9 Feng J., Xie M., Bu W., Jiang C. Research on secondary network backwater temperature forecast for centralized heat-supply

system based on neural network // Computer Simulation. 2014. Vol. 31. P. 351–354.

10 Gabrielaitiene, I., Bohm, B., Sunden, B. Modelling temperature dynamics of a district heating system in Naestved, Denmark-A case study // Energy Conversion and Management. 2007. Vol. 48. P. 78–86. http://dx.doi.org/10.1016/ j.enconman.2006.05. 011.

11 Zhong W., Chen J., Zhou Y. et al. Investigation of optimized network splitting of large-scale urban centralized heating system operation // Energy Reports. 2020. Vol. 6. P. 467–477.

12 Gao L., Cui X., Ni J., Lei W., Huang T., Bai C., Yang J. Technologies in smart district heating system // Energy Procedia. 2017. Vol. 142. P. 1829–1834. http: //dx.doi.org/10.1016/J.EGYPRO.2017.12.571.

13 Guelpa E., Sciacovelli A., Verda V. Thermo-fluid dynamic model of large district heating networks for the analysis of primary energy savings // Energy. 2019. Vol. 184. P. 34–44. http://dx.doi.org/10.1016/J.ENERGY.2017.07.177.

14 Hu J., Meng H., Li Z., Analysis on features and energy consumption of various heating source // Appl. Energy Technol. 2010. Vol. 4. P. 46–49.

15 Jiang Y. Problems in improvement of central heating systems in China and possible solutions // Heating, Ventilation and Air Conditioning. 2006. Vol. 36. P. 42–46.

16 Jiang Z., Meng J., Zhao X., Li J., Li L., Lin X. Research and application of optimized dispatch of smart steam heating system based on simulation model // Dist. Heat. 2018. Vol. 195. P. 83–88.

17 Köfinger M., Schmidt R.R., Basciotti D., Terreros O., Baldvinsson I., Mayrhofer J., Moser S., Tichler R., Pauli H. Simulation based evaluation of large-scale waste heat utilization in urban district heating networks: Optimized integration and operation of a seasonal storage // Energy. 2018. Vol. 159. P. 1161–1174. http://dx.doi.org/10.1016/J.ENERGY.2018.06.192.

18 Lei C., Zou P. Constant-variable flow control and energy consumption analysis of indirect connection heating systems //

Heating, Ventilation and Air Conditioning. 2008. Vol. 38. P.125–129.

19 Liu L. Major issues and solutions in the management system of space heating system in North China // Renewable and Sustainable Energy Reviews. 2015. Vol. 49. P. 221–231. http://dx.doi.org/10.1016/J.RSER.2015.04.116.

20 Liu Q. The Analysis of Multi Heat Source Network Operation in the Eastern Part of Jinan City. - Harbin Institute of Technology, 2016.

21 Pakere I., Romagnoli F., Blumberga D. Introduction of small-scale 4th generation district heating system. Methodology approach // Energy Procedia. 2018 Vol. 149. P. 549–554. http://dx.doi.org/10.1016/J.EGYPRO.2018.08.219.

22 Postnikov I., Stennikov V., Mednikova E., Penkovskii A. Methodology for optimization of component reliability of heat supply systems // Applied Energy. 2018. Vol. 227. P. 365-374. http://dx.doi.org/10.1016/J.APENERGY.2017. 11.073.

23 Qin X., Jiang Y. Accessibility analysis of district heating networks // Heating, Ventilation and Air Conditioning. 1999. Vol. 29. P. 2–7.

24 Qin X., Jiang Y. Hydraulic optimization of multi heat source heating networks // Heating, Ventilation and Air Conditioning. 2001. Vol. 31. P. 11-16.

25 Shan X., Wang P., Lu W. The reliability and availability evaluation of repairable district heating networks under changeable external conditions // Applied Energy. 2017. Vol. 203. P. 686–695. http://dx.doi.org/10.1016/J.APENERGY. 2017.06. 081.

26 Tol H.I., Svendsen S. Improving the dimensioning of piping networks and network layouts in low-energy district heating systems connected to lowenergy buildings: A case study in Roskilde, Denmark // Energy. 2012. Vol. 38. P. 276–290. http://dx.doi.org/10.1016/j.energy.2011.12.002.

27 Vigants G., Blumberga D. Modelling of the district heating system’s operation // Environ. Clim. Technol. 2011. Vol. 6. P. 132–137. http://dx.doi.org/ 10.2478/v10145-011-0019-x.

28 Wang P. Reliability of district heating system based on graph theory / PhD Thesis. Harbin Institute of Technology, 2010.

29 Wang Y., Zhang N., Zhuo Z., Kang C., Kirschen D. Mixed-integer linear programming-based optimal configuration planning for energy hub: Starting from scratch // Applied Energy. 2018. Vol. 210. P. 1141–1150. http://dx.doi.org/10.1016/J.APENERGY. 2017. 08. 114.

30 Zhang Y., Liu X., Qin B. Energy saving operation optimization in urban district heating system: A case study // Heat. Vent. Air Cond. 2015. Vol. 45. P. 97–100.

31 Zhong W., Chen J., Zhou Y., Li Z., Lin X. Network flexibility study of urban centralized heating system: Concept, modeling and evaluation // Energy. 2019. Vol. 177. P. 334–346. http://dx.doi.org/10.1016/j.energy.2019.04.081.

32 Zhong W., Feng H., Wang X., Wu D., Xue M., Wang J. Online hydraulic calculation and operation optimization of industrial steam heating networks considering heat dissipation in pipes // Energy. 2015. Vol. 87. P. 566–577. http://dx.doi.org/10.1016/J.ENERGY.2015.05. 024.

33 Zia M.F., Elbouchikhi E., Benbouzid M. Microgrids energy management systems: A critical review on methods, solutions, and prospects // Appl. Energy. 2018. Vol. 222. P. 1033–1055. http://dx.doi.org/10.1016/J.APENERGY. 2018.04.103

34 Zhong W., Chen J., Zhou Y., Li Zh., Yu Z., Lin X. Investigation of optimized network splitting of large-scale urban centralized heating system operation // Energy Reports. 2020. Vol. 6. P. 467-477.

35 Zheng X., Sun Q., Wang Y., Zheng L., Gao X. and et all. Thermo-hydraulic coupled simulation and analysis of a real large-scale complex district heating network in Tianjin // Energy. 2021. Vol. 236. 121389. https://doi.org/10.1016/j.energy.2021.121389

36 Hussein A., Klein A. Modelling and validation of district heating networks using an urban simulation platform // Applied Thermal Engineering. 2021. Vol. 187. 116529. https://doi.org/10.1016/j.applthermaleng.2020.116529

37 Pourbozorgi Langroudi O., Weidlich I., Hay S. Backward simulation of temperature changes of District Heating networks for enabling loading history in predictive maintenance // Energy Reports. 2021. Vol. 7. P.110-127. https://doi.org/10.1016/j.egyr.2021.09.031

38 Vandermeulen A., Van Oevelen T., der Heijde B., Helsen L. A simulation-based evaluation of substation models for network flexibility characterisation in district heating networks // Energy. 2020. Vol. 201, No. 15. 117650. https://doi.org/10.1016/j.energy.2020.117650

39 Korshak A.A. The versatility of the generalized formulas of L.S. Leibenson // Oil industry. 2019. № 5. P. 105-108 (in Russian).

40 Agapkin V.M. Thermal and hydraulic calculations of pipelines for oil and petroleum products. M.: Nedra, 1981. 256 p. (in Russian).

41 RD 153-34 RK.0-20.523-02. Guidelines for Compiling Energy Performance Characteristics for Thermal Energy Transport Systems (in three parts). Astana, 2002. (in Russian).

42 Vafin D.B. Heat supply and heating networks: a textbook. - Nizhnekamsk: Nizhnekamsk Chemical-Technological Institute (branch) of the Federal State Budgetary Educational Institution of Higher Professional Education "KNRTU", 2014. 228 p. (in Russian).